

2020

Investigating serviceability issues related to thermal movement accommodation in bridges

Conor Duffy
Iowa State University

Follow this and additional works at: <https://lib.dr.iastate.edu/etd>

Recommended Citation

Duffy, Conor, "Investigating serviceability issues related to thermal movement accommodation in bridges" (2020). *Graduate Theses and Dissertations*. 18121.
<https://lib.dr.iastate.edu/etd/18121>

This Thesis is brought to you for free and open access by the Iowa State University Capstones, Theses and Dissertations at Iowa State University Digital Repository. It has been accepted for inclusion in Graduate Theses and Dissertations by an authorized administrator of Iowa State University Digital Repository. For more information, please contact digirep@iastate.edu.

Investigating serviceability issues related to thermal movement accommodation in bridges

by

Conor Duffy

A thesis submitted to the graduate faculty
in partial fulfillment of the requirements for the degree of

MASTER OF SCIENCE

Major: Civil Engineering (Structural Engineering)

Program of Study Committee:
Brent Phares, Major Professor
Behrouz Shafei
Jennifer Shane

The student author, whose presentation of the scholarship herein was approved by the program of study committee, is solely responsible for the content of this thesis. The Graduate College will ensure this thesis is globally accessible and will not permit alterations after a degree is conferred.

Iowa State University

Ames, Iowa

2020

Copyright © Conor Duffy, 2020. All rights reserved.

TABLE OF CONTENTS

| | Page |
|---|-----------|
| LIST OF FIGURES | iv |
| LIST OF TABLES | viii |
| ACKNOWLEDGMENTS | ix |
| ABSTRACT..... | x |
| CHAPTER 1. INTRODUCTION | 1 |
| 1.1 Overview | 1 |
| 1.2 Research Needs and Motivations | 2 |
| 1.3 Research Objectives | 2 |
| 1.4 Thesis Outline..... | 3 |
| CHAPTER 2. EVALUATION OF D.S. BROWN STRIP SEAL EXPANSION JOINT SYSTEMS AT SKEW | 4 |
| 2.1 Background and Objectives..... | 4 |
| 2.2 Literature Review | 5 |
| 2.2.1 Michigan DOT Determination of Allowable Movement Ratings for Various Proprietary Bridge Deck Expansion Joint Devices at Various Skew Angles (1984) and Special Provision for Expansion Joint Device (2004)..... | 5 |
| 2.2.2 Iowa DOT Office of Bridges and Structures LRFD Bridge Design Manual 5.8.3: Expansion Joints..... | 7 |
| 2.2.3 D.S. Brown New Construction Expansion Joint Systems (2018)..... | 9 |
| 2.3 Methods and Procedures..... | 9 |
| 2.3.1 Specimen and Test Apparatus Design..... | 9 |
| 2.4 Standard Movement Tests | 13 |
| 2.4.1 Laboratory Testing Procedure | 13 |
| 2.4.2 Standard Movement Test Results..... | 15 |
| 2.4 Debris Testing..... | 25 |
| 2.4.1 Debris Testing Procedure | 25 |
| 2.4.2 Debris Test Results..... | 29 |
| 2.5 Recommendations and Design Table Recommendations | 32 |
| 2.5.1 BDM Table 5.8.3.2.1-1 | 32 |
| 2.5.2 BDM Table 5.8.3.2.1-2 | 35 |
| CHAPTER 3. MOVEABLE ABUTMENT RESEARCH AND INVESTIGATIONS | 36 |
| 3.1 Background..... | 36 |
| 3.2 Literature Review | 37 |
| 3.2.1 Overview | 37 |
| 3.2.2 Surveys and Field Observations | 37 |
| 3.2.3 Recommendations for Mitigating Approach Slab Failure | 45 |
| 3.3 Inventory of Iowa Approach Slab Performance | 50 |

| | |
|---|----|
| 3.3.1 Approach Slab Inventory Background and Process | 50 |
| 3.3.2 Sample Investigation | 52 |
| 3.3.3 Pilot Inventory Findings..... | 53 |
| CHAPTER 4. FINITE ELEMENT MODELING..... | 55 |
| 4.1 Jasper and Story County Finite Modeling Techniques..... | 56 |
| 4.1.1 Model Parts and Assembly | 56 |
| 4.1.2 Material Properties | 58 |
| 4.1.3 Boundary Conditions..... | 58 |
| 4.1.4 Springs and Model Calibration..... | 59 |
| 4.1.5 Loading..... | 61 |
| 4.2 Jasper and Story County Model Analyses | 62 |
| 4.2.1 Jasper FE Model Analysis | 63 |
| 4.2.2 Story FE Model Analysis | 67 |
| 4.2 Washington County Finite Model | 76 |
| 4.2.1 Purpose and Background..... | 76 |
| 4.2.2 Design Details | 77 |
| 4.2.3 Iowa DOT Field Investigation History..... | 81 |
| 4.2.4 Finite Modeling Procedure | 82 |
| 4.2.5 Finite Element Study and Results | 86 |
| CHAPTER 5. CONCLUSIONS AND RECOMMENDATIONS | 92 |
| 5.1 Strip Seal Recommendations | 92 |
| 5.2 Moveable Abutment Approach Slab Recommendations..... | 93 |
| 5.2.1 Literature Review and Slab Inventory Conclusions..... | 93 |
| 5.2.2 Jasper and Story Model Conclusions | 94 |
| 5.2.3 Washington Investigation Conclusions..... | 96 |
| 5.2.4 Future Approach Slab Research | 97 |
| REFERENCES | 99 |

LIST OF FIGURES

| | Page |
|--|------|
| Figure 1: Iowa DOT Skewed Strip Seal Detail..... | 8 |
| Figure 2: Iowa DOT Turned-Up Termination Detail | 8 |
| Figure 3: SSA2 Railing Detail | 9 |
| Figure 4: Upturned Specimen Prior to Assembly | 10 |
| Figure 5: Assembled Straight Strip Seal..... | 10 |
| Figure 6: Assembled Strip Seal Cross-Section | 11 |
| Figure 7: Test Frame Concept..... | 12 |
| Figure 8: Test Frame..... | 12 |
| Figure 9: Rotational Disk Close-Up | 13 |
| Figure 10: Typical Failure (Entrance into Roadway) | 14 |
| Figure 11: Typical Failure (Excessive Flexure)..... | 14 |
| Figure 12: Closure Limit Due to Sealant Bending..... | 15 |
| Figure 13: Image Demonstrating String Pot. Drift at 50-Degree Skew | 17 |
| Figure 14: Racking Displacement (WisDOT) | 18 |
| Figure 15: Typical A2R-400 Behavior in Extension | 18 |
| Figure 16: Typical Cycling Behavior | 19 |
| Figure 17: Rippling Effect in Extension (Front View) | 21 |
| Figure 18: Rippling Effect in Extension (Rear View) | 21 |
| Figure 19: Failure Due to Entrance into Roadway | 22 |
| Figure 20: Upturned Section Failing in Closure Following Extension | 22 |
| Figure 21: Upturned Section Unable to Completely Close | 23 |
| Figure 22: Horizontal Test Rig..... | 26 |

| | |
|--|----|
| Figure 23: Half-Full Condition | 27 |
| Figure 24: Half-Full Condition (Open)..... | 28 |
| Figure 25: Full Condition..... | 28 |
| Figure 26: Restricted Closure Due to Debris (Typ.)..... | 29 |
| Figure 27: Increased Racking Due to Debris | 30 |
| Figure 28: No Apparent Damage Following Testing | 30 |
| Figure 29: Zero-Degree Skew Full-Capacity Compression Data | 32 |
| Figure 30: Voiding Under Approach Slab (White, 2007)..... | 39 |
| Figure 31: Diagram Summarizing Frequent Problems at Several Bridge Sites (White, 2007) | 39 |
| Figure 32: Structural Movement Due to Thermal Effects (Griemann et al., 2008)..... | 40 |
| Figure 33: Problems Leading to the Formation of the Bump (Briaud et al., 1997)..... | 40 |
| Figure 34: Transverse Cracking of Approach (Krapf, 2019)..... | 42 |
| Figure 35: WJE GPR Voiding Sample (WJE, 2011)..... | 43 |
| Figure 36: Plan View of Severe Voiding (WJE, 2011) | 43 |
| Figure 37: Examples of Voiding at Integral Abutment Bridges (IDOT)..... | 44 |
| Figure 38: Approach Settlement Away from Abutment (Chen and Abu-Farsakh, 2016)..... | 47 |
| Figure 39: Effects of Increasing Slab Thickness and Reinforcement Ratio (Chen and Abu-Farsakh, 2016) | 49 |
| Figure 40: Cracking at Barrier Rail Indicating Settlement | 53 |
| Figure 41: Differences in Slab Height Indicating Settlement..... | 54 |
| Figure 42: Jasper FE Assembly | 57 |
| Figure 43: Story FE Assembly and Mesh..... | 57 |
| Figure 44: Jasper Boundary Conditions..... | 59 |
| Figure 45: Story FE Model Spring Layout | 60 |
| Figure 46: Jasper FE Model Loading..... | 61 |

| | |
|---|----|
| Figure 47: Jasper Base Displacement | 64 |
| Figure 48: Jasper Base Model Stress Distribution (Top)..... | 64 |
| Figure 49: Jasper Base Model Stress Distribution (Bottom) | 65 |
| Figure 50: Linearly-Elastic Jasper Model Stress Distribution..... | 67 |
| Figure 51: Initial Vertical Settlement for Story County Approach Slab | 68 |
| Figure 52: Initial Stress Values for Story Model (Top)..... | 69 |
| Figure 53: Initial Stress Values for Story Model (Bottom) | 69 |
| Figure 54: Stress Concentrations at Dowel Connection | 70 |
| Figure 55: Story County 8-Foot Void Scenario..... | 70 |
| Figure 56: Max Vertical Displacement vs. Void Length..... | 72 |
| Figure 57: Concrete Tensile Stress in Joint vs. Void Length | 73 |
| Figure 58: Tensile Stresses in Connection Joint (13-foot void) | 73 |
| Figure 59: Locations of Damage-Based Failure in 16-Foot Void Model..... | 74 |
| Figure 60: Max Tensile Stress in Bottom of Span vs. Void Length..... | 75 |
| Figure 61: Maximum Principle Stress in Each Model..... | 75 |
| Figure 62: South Approach Slab Spalling Location | 77 |
| Figure 63: Bridge 606890 Location Map..... | 78 |
| Figure 64: General Layout of Precast Panels..... | 79 |
| Figure 65: Layout of Precast Panels at Abutment | 79 |
| Figure 66: Longitudinal Section of Approach and Abutment | 80 |
| Figure 67: Rebar Layout for Panel 1A..... | 80 |
| Figure 68: Washington Rebar and Connection Dowels..... | 84 |
| Figure 69: 606890 Model Meshing..... | 85 |
| Figure 70: Washington County Loading Scenario..... | 86 |

| | |
|--|----|
| Figure 71: Stress Concentrations on Bottom of Slab..... | 87 |
| Figure 72: Areas of Tensile Stress on Top Surface of Approach Slab | 87 |
| Figure 73: Concrete Failure in Washington Connection Joint..... | 88 |
| Figure 74: Stress Concentrations at Connection Joint | 89 |
| Figure 75: Washington Approach Slab Settlement..... | 90 |
| Figure 76: Max Principle Stresses in Washington Slab (Top)..... | 91 |

LIST OF TABLES

| | Page |
|--|------|
| Table 1: Total Travel Measured Along Centerline of Bridge (in inches) (From Michigan DOT)..... | 6 |
| Table 2: Table 5.8.3.2.1-2 Allowable Movement Capacity (From Iowa DOT) | 7 |
| Table 3: A2R Cross-Section and Perpendicular Movement Range (Manufacturer) | 9 |
| Table 4: A2R-400 Movement Data (Straight Section) | 16 |
| Table 5: A2R-400 Movement Data (Upturned Section)..... | 16 |
| Table 6: A2R-XTRA Movement Data (Straight Section) | 24 |
| Table 7: A2R-XTRA Movement Data (Upturned Section)..... | 24 |
| Table 8: A2R-400 Debris Test Data | 31 |
| Table 9: Proposed Updates to BDM 5.8.3.2.1-1..... | 33 |
| Table 10: Proposed Updates to BDM 5.8.3.2.1-2..... | 35 |

ACKNOWLEDGMENTS

I would first like to thank my major professor, Dr. Brent Phares, and Dr. Behrouz Shafei for giving me the opportunity to continue my engineering education at Iowa State University. Their guidance and feedback have been incredibly valuable in the successful production and completion of my research. Additionally, I would like to thank Dr. Jennifer Shane for serving as a member of my graduation committee.

I would also like to thank Douglas Wood and Owen Steffens for their assistance in the Structures Lab. Their knowhow and expertise in fabricating and conducting research made a large portion of the work I performed possible.

I would like to thank Iowa State University, The Iowa Department of Transportation, and the ISU Bridge Engineering Center for allowing me to continue my education at the graduate level. The time I have spent in Ames has been wonderful and fulfilling.

Finally, I would like to extend a special thank you to my friends and family for their continued love and support during my entire education.

ABSTRACT

Throughout the year, seasonal and daily temperature fluctuations cause the materials within a bridge to shrink and swell, resulting in the expansion and contraction of the entire superstructure. If left unaccounted for, these movements result in structural damage to the bridge. Thus, implementing ways to safely accommodate this movement is a crucial part of ensuring a serviceable, long-term structure is designed and built. The most traditional approach to accommodating this movement involves the use of movement joints placed at the ends of the bridge deck. These movement joints are often fitted with a rubber device to prevent excess drainage from eroding key structural members underneath the deck. However, these movement joints create several additional issues, including a high risk for premature failure due to environmental factors. As a result, “moveable” jointless integral or semi-integral abutment, which directly connects the abutment to the bridge deck. In this case, the abutment rotates inward and outward with the deck’s expansion and contraction and moves the expansion joints farther away from the bridge deck, limiting the potential issues associated with movement joints.

The first part of this thesis investigates a common issue with strip seal expansion joints—their somewhat problematic performance on skewed bridges. A literature review and laboratory testing series were conducted to quantify and recommend appropriate movement ranges for the A2R-400 and A2R-XTRA expansion joint systems for use by the Iowa Department of Transportation (IDOT). In addition, tests were performed simulating issues related to debris-entrance into the rubber expansion joint material. The conclusion of this research presents a series of acceptable movement guidelines, updated design table recommendations, and a sample set of design calculations.

The second part of this thesis investigates settlement issues resulting from the use of jointless “moveable abutment” bridges connected to approach slabs via steel connection dowels. As the Iowa DOT prefers the use of this type of design detail over movement joints when possible, it is important to monitor and optimize their performance for long-term serviceability. The research performed for this thesis involves a literature review investigating best practices for moveable abutment design, the outline for a state-wide inventory of Iowa approach slabs, and three Finite Element investigations of different Iowa DOT bridges. Through in-situ observations and computational computer models, the goal of this project is to present a clearer understanding of the structural behavior of integrally-tied approach slabs when used as an alternative to expansion joints. Areas of emphasis focus on the effect of field conditions that result in premature serviceability issues in approach slabs: settlement, voiding, and erosion of the subbase beneath the approach slab.

CHAPTER 1. INTRODUCTION

1.1 Overview

A key aspect of a successful bridge is a long-term, dependable service-life. Aside from the importance of constructing a structurally sufficient design, a cost-effect and serviceable structure free of frequent maintenance is often a chief concern. Unfortunately, serviceability issues are often not discovered until months or even years after initial construction. Although not critical to the safety concerns of the overall structure, these small failures are typically expensive to repair once identified in the field. As such, it is an important part of the bridge design process to constantly monitor and observe failures of field bridges to mitigate these serviceability issues in future designs. Areas of concern for the bridge design community are key components related to the accommodation of thermal movement, as these components tend to fail prematurely. Two common methods of accommodating this thermal movement are expansion joints and moveable abutments.

As the bridge superstructure expands and contracts throughout the year due to temperature fluctuations, these two methods allow for movements to ensure that excessive internal forces do not cause structural failures to other bridge components. While both expansion joints and moveable abutments are effective at accommodating this movement, they tend to create additional concerns. For strip seals, premature failure, whether due to incorrect design assumptions or improper maintenance, can create excessive drainage and harmful erosion of crucial bridge parts. For moveable abutments, thermal movement increases the likelihood of excessive soil erosion, soil settlement, and cracking in the approach slab. Regardless of the thermal accommodation technique, these concerns must be addressed and accounted for during the design process to ensure that they are mitigated under field conditions. Thus, the purpose of

this thesis is to address issues caused by expansion joints and moveable abutments and propose solutions to mitigate their negative impacts on future bridges' long-term performance.

1.2 Research Needs and Motivations

In the last few decades, research has been conducted both by universities, state Departments of Transportation, and private companies to quantify, explain, and determine solutions to the serviceability issues outlined in the previous section. During this period, the Iowa Department of Transportation (IDOT) and Iowa State University have closely collaborated to monitor and improve the performance of both expansion joints and approach slabs. Recently, IDOT has focused its attention on the issues associated with two specific forms of temperature-accommodating structure—the Steelflex Strip Seal Expansion Joint System, produced by the D.S. Brown Company; and the tied integral/semi-integral abutment bridge design. While both typically perform as intended from a movement managing standpoint and have been utilized by IDOT for several years, each comes with potential drawbacks that must be anticipated and accounted for. IDOT has observed that strip seals used in bridges with higher skews are at a greater risk for failure due to pullout, puncturing, and tearing. For tied integral/semi-integral abutment bridges, excessive cracking and excessive erosion, among other issues, are often observed. This thesis serves to investigate the issues noted above and provide insight into potential causes and solutions to these common problems.

1.3 Research Objectives

General research objectives for each of the two projects in this thesis are similar; however, differing techniques were employed to adequately capture and present the problems and subsequent recommendations for each movement device. For both the strip seal and the moveable abutment projects, a literature review of previous research was the initial step. By investigating the motivations, testing, and conclusions from previous researchers, a set of test

variables and research needs was determined for each study. Following the literature review, tests were performed and analyzed, and a set of recommendations or conclusions was offered. The testing procedure for each project, one for each of the two movement-accommodation methods, differed and is explained in further detail in subsequent chapters.

1.4 Thesis Outline

This thesis is organized into a series of chapters to convey the general processes, methods, findings, and conclusions for each of the two projects. The following chapter encompasses the body of work relating to strip seal expansion joints, including a literature review, a set of methods and testing procedures, and the presentation and discussion of results from those tests. Chapter 3 introduces prior research performed on approach slabs with moveable abutments, and includes a literature review, a compilation of previous studies performed on Iowa bridges, and a brief inventory of Iowa approach slab performance completed as a part of this thesis. Chapter 4 focuses on a set of finite element models generated to further explore and investigate the issues discussed in Chapter 3. Finally, Chapter 5, split into two categories, presents the overall conclusions and recommendations for each of the two thermal movement accommodating strategies.

CHAPTER 2. EVALUATION OF D.S. BROWN STRIP SEAL EXPANSION JOINT SYSTEMS AT SKEW

2.1 Background and Objectives

Throughout the year, as temperatures increase and decrease, the movement of the internal components of a bridge cause the structure to expand and contract. To alleviate the increased internal stress that these movements cause to a bridge, expansion joints are often installed. Typically, the type of expansion joint used for a project is determined by the expected amount of movement. Due to IDOT's preference for using integral abutments for smaller movement ranges, commonly used expansion devices are strip seals (for a movement of 4 to 5 inches) and finger joints (for a movement exceeding that allowed for a strip seal).

Strip seals are comprised of two metal railings embedded in the concrete and connected by a neoprene sealing gland. Compared to other forms of expansion device, strip seals are preferred for their durability, watertight seal, and efficient performance in the field. However, a high bridge skew can cause issues with strip seal performance due to the non-perpendicular loading conditions this angle forces on the sealing material. As a bridge's design skew increases, the strip seal begins to experience a larger amount of lateral movement for which the seal may not be designed to resist. Thus, higher skew angles increase the likelihood that a strip seal will experience premature failure via tear-out or issues caused by unusual torsion.

The Iowa DOT LRFD Manual currently specifies lower movement capacity as the skew increases and that strip seals may not be practical for skew values greater than 30-degrees. This study seeks to test and verify these requirements for the D.S. Brown A2R-400 and A2R-XTRA strip seals installed with D.S. Brown's SSA2 Railing. The A2R-400 version of this strip seal is rated at a total perpendicular movement of 4 inches, and the A2R-XTRA is rated for 7 total inches of movement. Currently, the IDOT LRFD Manual supplies acceptable movement ranges

for the A2R-400 strip seal at increasing skew angles, but similar guidelines for the A2R-XTRA do not exist. In addition, these acceptable movement ranges do not consider the strip seal's performance at their upturned terminations, which may present a higher susceptibility to premature failure.

The objectives for this phase of the project are as follows:

- Verify the manufacturer's claims of total perpendicular movement for both the A2R-400 and A2R-XTRA strip seals at a zero-degree skew for both the straight sections and the upturned sections
- Provide experimentally obtained movement ranges for the A2R-400 strip seal for skew angles from 0°-60° considering both the straight and upturned sections
- Document the A2R-XTRA strip seal's performance and appropriate movement ranges for skew angles from 0°-60° for both the straight and upturned sections
- Determine whether or not the upturned termination sections presented a higher risk for failure and controlled the movement ranges for each strip seal
- Document and quantify any range of movement restrictions on the A2R-400 due to foreign debris that may obstruct the strip seal in the field

2.2 Literature Review

2.2.1 Michigan DOT Determination of Allowable Movement Ratings for Various Proprietary Bridge Deck Expansion Joint Devices at Various Skew Angles (1984) and Special Provision for Expansion Joint Device (2004)

Since 1980, the Michigan Department of Transportation has run three separate tests (1980, 1984, and 2004) for several expansion joint devices to evaluate their acceptable movement ranges in skewed bridges. The most recent of these tests includes data and recommendations for the A2R-400 strip seal with the SSA2 railing, SSCM2 railing, and SSE2 railing. The ranges for the SSA2 railing are highlighted in Table 1. This series of testing provides the main source of data on this subject and the conclusions from this study are the basis for the Iowa DOT's design guidance for strip seal implementation at skew angles. These tests

determined that, as the skew angle value was increased, the maximum opening range for the strip seal was reduced. The movement ranges from the most recent update of this study are presented in the chart below and records the maximum movement range for each expansion joint in relation to the centerline of bridge. These tests were performed on straight strip seal specimens ranging from 4' to 6' in length and do not consider the behavior of the strip seal at an upturned termination point. In addition, these tests were performed starting from the manufacturer's reported "midpoint," a position halfway between the minimum closure limit and the maximum closure limit. These movement ranges are reported in relation "Angle of Crossing," which is defined as 90-degrees minus the skew angle.

Table 1: Total Travel Measured Along Centerline of Bridge (in inches) (From Michigan DOT)

| Expansion Joint Device | Angle of Crossing (in degrees) | | | | | | |
|--|--------------------------------|-----|-----|-----|-----|-----|-----|
| | 90 | 80 | 70 | 60 | 50 | 40 | 30 |
| Watson-Bowman & Acme SE-300 (Type E, A, & M extrusion) | 3.0 | 3.0 | 3.1 | 3.5 | 3.7 | 3.3 | 2.8 |
| D.S. Brown Steelflex SSA2-300A2R | 3.0 | 3.0 | 3.0 | 3.3 | 3.5 | 3.5 | 4.5 |
| D.S. Brown Steelflex SSE2-300A2R | 3.0 | 3.0 | 3.1 | 3.5 | 3.0 | 2.1 | 2.0 |
| Watson-Bowman & Acme SE-400 (Type E, A, & M extrusions) | 4.0 | 4.1 | 4.3 | 4.3 | 3.7 | 2.7 | 2.6 |
| D.S. Brown Steelflex SSA2-400A2R | 4.0 | 4.1 | 3.7 | 3.5 | 2.4 | 2.0 | 1.2 |
| D.S. Brown Steelflex SSCM2-400A2R | 4.0 | 4.1 | 4.3 | 4.0 | 4.3 | 5.1 | 4.0 |
| D.S. Brown Steelflex SSE2-400A2R | 4.0 | 4.1 | 4.3 | 3.1 | 2.0 | 2.0 | 1.6 |
| Structural Rubber Products Company Onflex 40SS | 4.0 | 4.1 | 4.3 | 4.5 | 2.8 | 2.8 | 2.0 |

The testing for these strip seals utilized a specially fabricated frame that expanded and contracted each specimen via a hydraulic ram operated by an MTS (Material Test System). The authors of this study utilized the following testing procedure:

- Each specimen was assembled and mounted in the frame to model the installation that would be experienced in the field.

- Prior to each test, the joint was readjusted to ensure a relaxed position at the midpoint of the manufacturer's recorded total perpendicular opening width.
- The joint was slowly expanded until it either a) showed signs of failure (physical distortion, buckling, or excessive shear) or b) reached the manufacturer's maximum recommended opening. This distance from the midpoint was recorded.
- The joint was slowly contracted until it either a) showed signs of failure (physical distortion, buckling, or excessive shear) or b) reached the manufacturer's minimum recommended opening. This distance from the midpoint was recorded.
- The smaller of the two perpendicular measurements was assumed to be one-half of the total perpendicular movement range.
- The joint was then cycled five times at a rate of two cycles per minute, and the forces applied to the joint at its two limit points were recorded.

2.2.2 Iowa DOT Office of Bridges and Structures LRFD Bridge Design Manual 5.8.3: Expansion Joints

Based on the data and design considerations recommended by the 2004 MDOT Special Provision, the following chart constitutes the design ranges for approved strip seals for usage in Iowa Department of Transportation projects. In addition, this chart specifies the minimum installation width, minimum opening width, and the allowable movement range data from the Michigan DOT Special Provision. The D.S. Brown A2R-400 with SSA2 railing is highlighted.

Table 2: Table 5.8.3.2.1-2 Allowable Movement Capacity (From Iowa DOT)

Table 5.8.3.2.1-2. Allowable movement capacity, minimum installation width, and minimum opening width for approved strip seals

| Seal type/steel extrusion type | Minimum installation width, inches ⁽¹⁾ | Minimum opening width, inches ⁽¹⁾ | Allowable movement capacity parallel with centerline of roadway in inches ⁽²⁾ for skew angle in degrees | | | | | | |
|--------------------------------|---|--|--|-----|-----|-----|-----|-----|-----|
| | | | 0 | 10 | 20 | 30 | 40 | 50 | 60 |
| Wabo SE-300/A | 1.5 | 0 | 3.0 | 3.0 | 3.1 | 3.5 | 3.7 | 3.3 | 2.8 |
| Wabo SE-400/A | 1.5 | 0 | 4.0 | 4.1 | 4.3 | 4.3 | 3.7 | 2.7 | 2.6 |
| Wabo SE-500/A | 2.0 | 0 | 5.0 | --- | --- | --- | --- | --- | --- |
| D.S. Brown A2R-400/SSA2 | 2.0 | 0.5 | 4.0 | 4.1 | 3.7 | 3.5 | 2.4 | 2.0 | 1.2 |

Table notes:

- (1) This dimension is measured perpendicular to the joint.
- (2) In 1980 the Michigan DOT determined allowable capacities and published them in *Determination of Allowable Movement Ratings for Various Proprietary Bridge Deck Expansion Joint Devices at Various Skew Angles, Final Report* [BDM 5.8.3.1.5]. Recently the Michigan DOT has updated the capacities in Special Provision – Frequently Used 03SP706(A), "Special Provision for Expansion Joint Device," 06-24-04.
- (3) No data is available.

Currently, the Iowa DOT terminates their strip seals with two successive 30-degree bends on either side of the bridge/railing cross-section (Figures 1 & 2); this design allows the edges of the strip seal to turn up into the barrier rail, allowing water to flow past the strip seal.

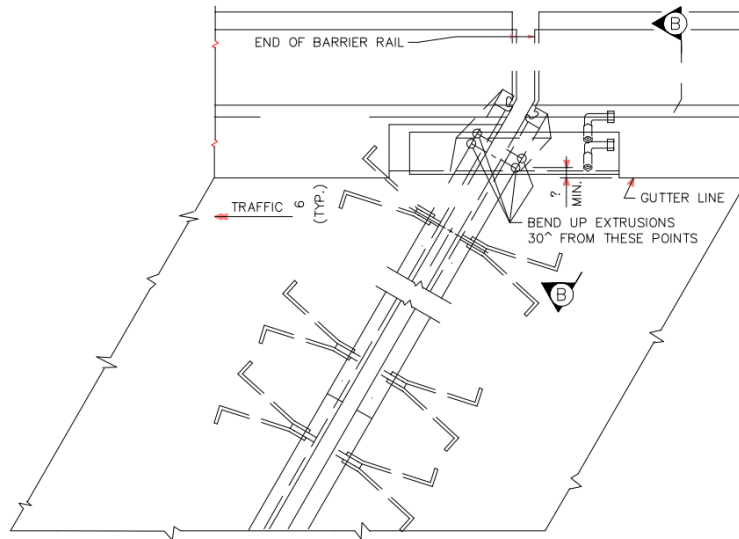


Figure 1: Iowa DOT Skewed Strip Seal Detail

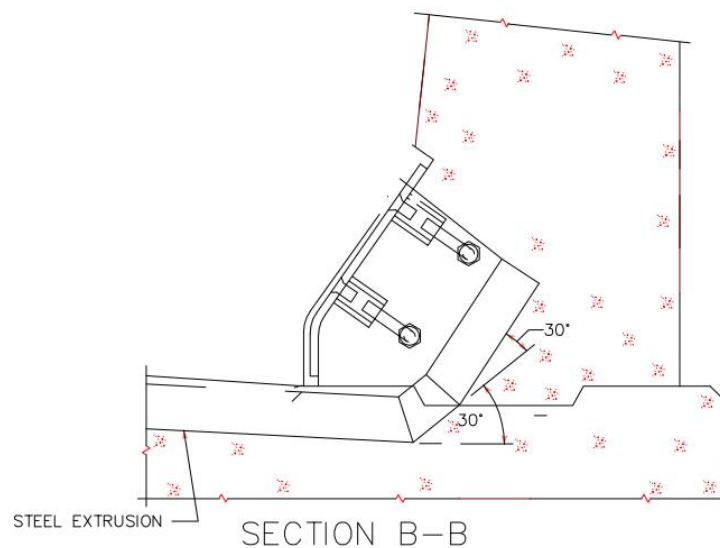



Figure 2: Iowa DOT Turned-Up Termination Detail

2.2.3 D.S. Brown New Construction Expansion Joint Systems (2018)

This document, produced by the manufacturer for these specimens, provides general details, schematics, and perpendicular movement ranges for both the A2R-400 and A2R-XTRA.

Table 3: A2R Cross-Section and Perpendicular Movement Range (Manufacturer)

| Sealing Element Cross-Section | Sealing Element Type | Lateral Movement Range (in.) | Transverse Movement Range (in.) | Joint Opening Range |
|--|----------------------|------------------------------|---------------------------------|---------------------|
|  A2R | A2R-400 | 4.0 | ±2.0 | 0.5-4.5 |
| | A2R-XTRA | 7.0 | ±2.0 | 0.5-7.5 |

Adapted from D.S. Brown's *New Construction Expansion Joint Systems*

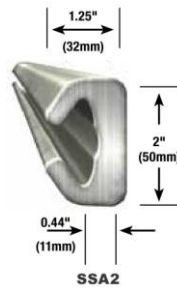


Figure 3: SSA2 Railing Detail

2.3 Methods and Procedures

2.3.1 Specimen and Test Apparatus Design

For this series of testing, four total test specimens were utilized. For each of the two A2R sealing elements (400 and XTRA), a straight section and an upturned section were fabricated for testing. In addition, a testing apparatus was fabricated to accomplish the goals of this study.

The fabrication of each strip seal specimen was as follows:

- Two matching 3-foot sections of SSA2 railing were cut from a larger section of railing for testing.
- Each railing piece was drilled with a series of holes to allow the section to be rigidly connected to the testing apparatus via screws.
- A segment of A2R sealing material was cut to the required length for installation

- Each railing and sealing material was sufficiently cleaned of debris and dried
- Per the installation instructions, a liberal amount of DSB 1520 Adhesive Lubricant was applied to the sealing element and was installed into each railing
- Each specimen was allowed to cure overnight



Figure 4: Upturned Specimen Prior to Assembly



Figure 5: Assembled Straight Strip Seal



Figure 6: Assembled Strip Seal Cross-Section

In order to simulate the behavior of a strip seal throughout a range of skew angles, a testing frame was designed and fabricated to allow each specimen to be both expanded and contracted via a continuously braced load applied along each railing. This load was provided from the top of the testing frame, and a load cell was connected to the bottom railing to monitor the applied load. A rotational disk with a semi-circle bolt pattern was utilized to allow the test specimen to rotate in 10° increments while maintaining a load in the direction of the theoretical “centerline” of the bridge. Two string potentiometers were used to measure both the perpendicular displacement and the displacement in the direction of loading (the theoretical “centerline of bridge” in the direction of traffic).

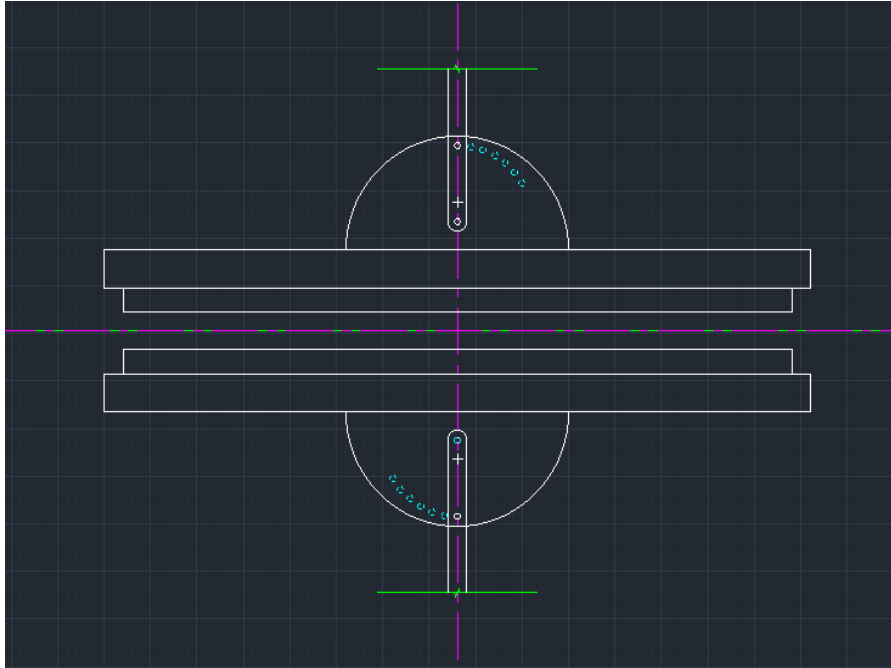


Figure 7: Test Frame Concept



Figure 8: Test Frame



Figure 9: Rotational Disk Close-Up

2.4 Standard Movement Tests

2.4.1 Laboratory Testing Procedure

The testing procedure for each specimen was as follows:

- The specimen was screwed into the testing apparatus and set at the required skew angle.
- The specimen was then adequately braced to prevent rotation out-of-plane.
- A load was applied until the width between each railing was 2.0" (manufacturer's recommended installation width) to ensure testing began from a relaxed position.
- The specimen was compressed until it either a) reached the manufacturer's recommended minimum opening distance or b) showed obvious signs of failure (excessive flexure, excessive load, torsional bending, or entrance into the path of traffic). This distance was recorded, and pictures were taken to document strip seal behavior.
- After this minimum limit was established, the specimen was extended until a) it reached the manufacturer's recommended maximum opening width or b) showed obvious signs of failure (excessive flexure, excessive load, torsional bending, or entrance into the path

of traffic). This distance was recorded, and pictures were taken to document strip seal behavior.

- Once this theoretical range was established, the specimen was cycled five (5) times to observe any issues due to repeated cycling.

For each test, string potentiometers and load cell were used to continuously monitor the load vs. displacement behavior of the strip seal as it was expanded and contracted.

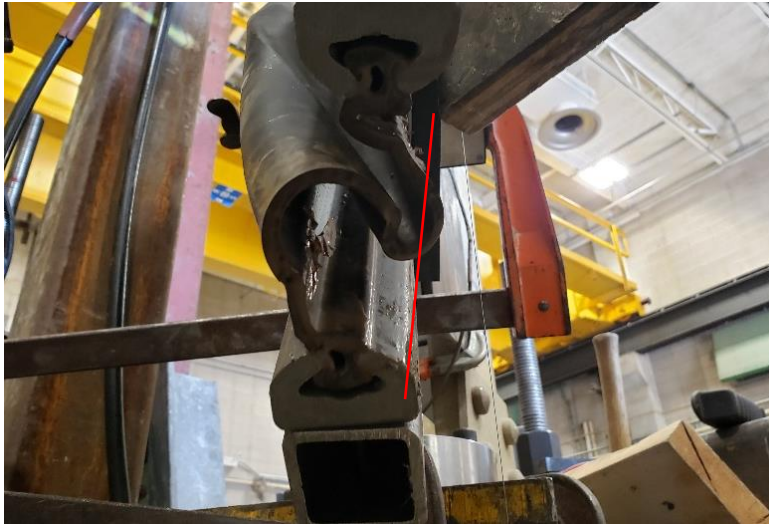


Figure 10: Typical Failure (Entrance into Roadway)

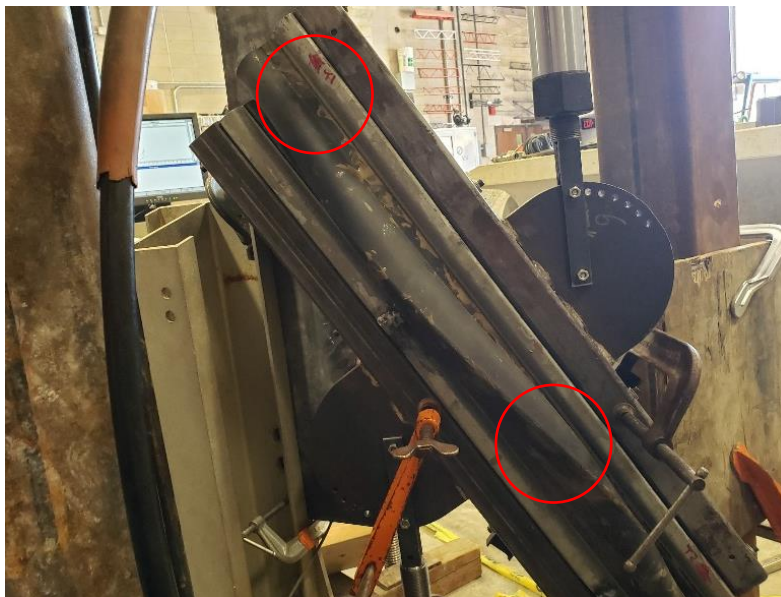


Figure 11: Typical Failure (Excessive Flexure)

2.4.2 Standard Movement Test Results

Throughout the series of testing for the A2R-400 sealing material, it was noted that, regardless of the skew angle, the expansion device comfortably moved throughout the entirety of the manufacturer's reported extension range for both the straight and upturned test specimens. The only limitation this joint experienced came during compression for the upturned section at the two highest skews; this restriction was a result of the rubber sealant bending into the underside of the railing in the upturned section of the specimen (Figure 12). It is likely that this limitation would not exist in a field bridge, as the forces presented in that environment would be sufficient to completely close the joint. However, it is likely that movement past the points defined in Table 5 would drastically increase the likelihood of the strip seal's failure.



Figure 12: Closure Limit Due to Sealant Bending

In addition, it was noted that the two 30-degree bends in the railing termination create this bending behavior regardless of skew, although this behavior is increased as the skew angle is increased. It was possible to reduce this behavior's impact on the joint's performance by

adjusting the two railings to make sure they were perfectly in line, although this adjustment would be impossible to perform in a finished bridge deck. Prior to fabrication, it was also observed that the two sets of matching SSA2 railing were not perfectly identical at this upturned section. This slight variation in the two 30-degree angles between the two rails increased the likelihood that the final product would not be perfectly aligned.

A complete summary of movement ranges for both the straight and upturned is located below in Tables 4 and 5 and notes the minimum and maximum perpendicular movement ranges, the total perpendicular movement, the minimum and maximum movement in relation to the centerline of the bridge (taken from the installation width of 2 inches), and the total centerline movement range.

Table 4: A2R-400 Movement Data (Straight Section)

| Skew | Perpendicular Movement Range (in.) | | | Movement Parallel to Centerline of Roadway (in.)* | | |
|------|------------------------------------|------|------------------|---|------|-----------------------|
| | Min. | Max. | Δ Perp. Movement | Min. | Max. | Δ Centerline Movement |
| 0° | 0.50 | 4.50 | 4.00 | -1.50 | 2.50 | 4.00 |
| 10° | 0.50 | 4.50 | 4.00 | -1.43 | 2.43 | 3.86 |
| 20° | 0.50 | 4.50 | 4.00 | -1.43 | 2.46 | 3.89 |
| 30° | 0.50 | 4.50 | 4.00 | -1.43 | 2.49 | 3.92 |
| 40° | 0.50 | 4.50 | 4.00 | -1.40 | 2.52 | 3.92 |
| 50° | 0.50 | 4.50 | 4.00 | -1.42 | 2.61 | 4.03 |
| 60° | 0.50 | 4.50 | 4.00 | -2.00 | 2.80 | 4.80 |

*Measured in relation to 2-inch installation width

Table 5: A2R-400 Movement Data (Upturned Section)

| Skew | Perpendicular Movement Range (in.) | | | Movement Parallel to Centerline of Roadway (in.)* | | |
|------|------------------------------------|------|------------------|---|------|-----------------------|
| | Min. | Max. | Δ Perp. Movement | Min. | Max. | Δ Centerline Movement |
| 0° | 0.50 | 4.50 | 4.00 | -1.50 | 2.50 | 4.00 |
| 10° | 0.50 | 4.50 | 4.00 | -1.41 | 2.44 | 3.85 |
| 20° | 0.50 | 4.50 | 4.00 | -1.39 | 2.47 | 3.86 |
| 30° | 0.50 | 4.50 | 4.00 | -1.45 | 2.44 | 3.89 |
| 40° | 0.50 | 4.50 | 4.00 | -1.70 | 2.62 | 4.32 |
| 50° | 0.77 | 4.50 | 3.73 | -1.40 | 2.82 | 4.22 |
| 60° | 0.70 | 4.50 | 3.80 | -1.63 | 2.86 | 4.49 |

*Measured in relation to 2-inch installation width

It is important to note that, as the skew angle increased, a correlating increase in lateral movement occurred. This behavior, known as “racking,” distorted the neoprene gland along its centerline as the skew angle increased, causing the perpendicular string potentiometer to drift in a second direction. Because string potentiometers were only placed in relation to the joint’s perpendicular movement and movement parallel to the centerline of the roadway, the movement parallel to the joint was not continuously monitored for these tests and slightly offset the measured perpendicular movement. However, a caliper was used at the end of each test to measure and verify that the correct perpendicular range was reflected in the final data tables (Tables 4 & 5).



Figure 13: Image Demonstrating String Pot. Drift at 50-Degree Skew

That being stated, a trigonometric calculation for design purposes would still be the appropriate way to account for this behavior; this calculation is modeled below in a figure provided in the Wisconsin Department of Transportation’s Bridge Manual (Figure 14):

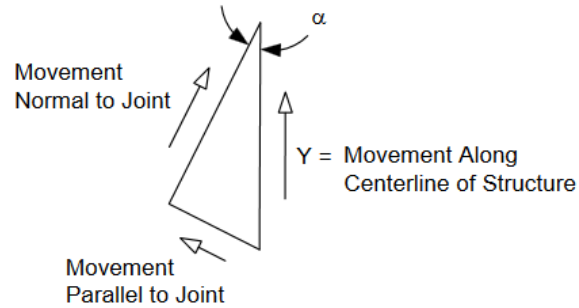


Figure 28.3-1
Racking Displacement

$$Y = (350')(12'')*(6 \times 10^{-6})(80) + (350')(12'')(0.0003) = 2'' + 1.26'' = 3.26''$$

$$Y(\text{normal}) = Y(\cos \alpha) = 3.26 \cos 33^\circ = 2.73''$$

Figure 14: Racking Displacement (WisDOT)

In general, both specimens demonstrated a slight drop-off in total centerline movement for lower skew angles, but this value increased as the skew angle was raised. Even at the highest skew angles, there appeared to be no signs of pull-out or unusual entrance into the vehicle pathway (Figure 15).



Figure 15: Typical A2R-400 Behavior in Extension

Throughout the cycling process for each specimen at each of the seven test angles, the behavior was noted to be completely elastic, showing no signs of sustained deformation. This behavior is demonstrated below in Figure 17. As the expansion device reached the maximum range of its motion, whether in extension or compression, a correlating increase in load was noted. Upon relaxing the joint back to its initial position, this load decreased back to its installation value. Each cycle followed a similar load pattern, with no observable change in required load at the maximum movement range.

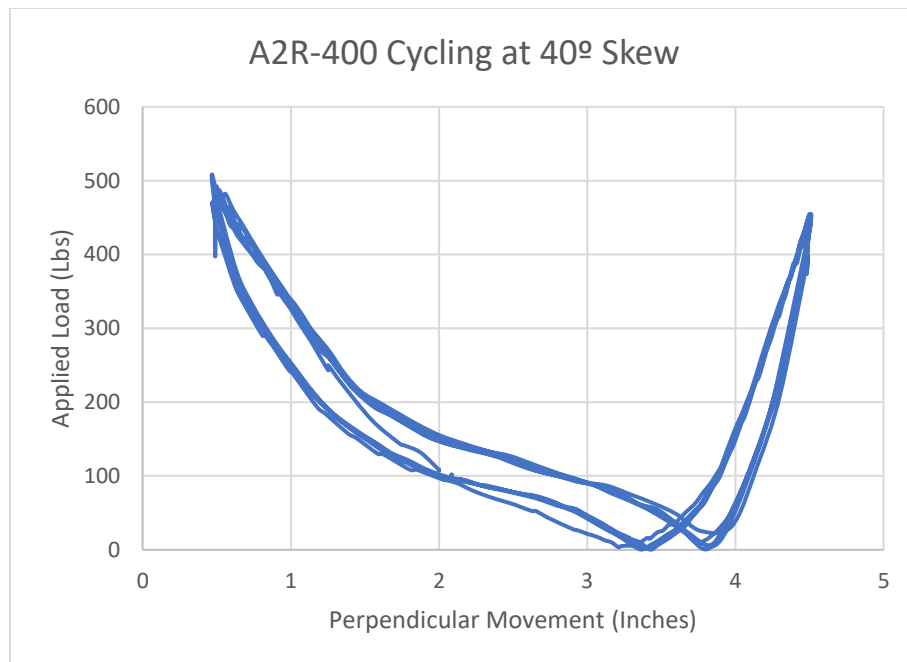


Figure 16: Typical Cycling Behavior

For the A2R-400 test sections, it was determined that they will comfortably move throughout their full range of motion for all tested skews given high quality installation conditions. The only shortcoming of this specimen came in compression at the upturned sections, which were unable to completely close due to the significant amount of bending in the neoprene sealing material underneath the railing.

As stated above, the only difference in total appropriate movement for these joints came in compression at the two highest skew angles. However, these tests were run in near-ideal conditions with nearly-perfectly aligned railings. In a field bridge, it is unlikely that these railings would be similarly aligned following concrete pouring and curing; these slight misalignments could potentially create additional stresses within the strip seal, leading to failures not exhibited in these laboratory tests.

Based on these tests, it appears that the A2R-400 strip seal, when properly installed with the SSA2 railing, performs well at each skew. However, these tests were conducted under laboratory conditions following the manufacturer's exact methods of installation, and no external field factors were considered. The performance of these joints may be impeded by the addition of foreign particles or materials, as these additions may put additional stress on the neoprene sealant's connection to the railing. Should a material become lodged in the seal while extended, there is an increased likelihood that the joint would fail upon closure.

Compared to the A2R-400, the A2R-XTRA exhibited more obvious signs of failure prior to reaching the manufacturer's purported perpendicular movement range. Premature failures occurred in both extension and compression, and clearly became more pronounced as the skew angle was increased. In extension, the joints exhibited a clear amount of rippling and unusual bending (Figures 18 & 19). This movement above the railing would position the joint in the path of traffic, drastically increasing the likelihood that the seal would fail prematurely (Figure 20). This behavior ceased for the straight specimen once the joint was subsequently closed.



Figure 17: Rippling Effect in Extension (Front View)



Figure 18: Rippling Effect in Extension (Rear View)



Figure 19: Failure Due to Entrance into Roadway

However, it was noted that, for the upturned specimen, this rippling effect did not dissipate upon closure, causing the seal to bend up and above the railing when closed (Figure 21). This behavior became worse as the joint was cycled and the only way to remove this failure was to manually force the joint back below the railing.



Figure 20: Upturned Section Failing in Closure Following Extension

In compression, particularly for the upturned specimen, the joint repeatedly suffered from the same bending issue mentioned for the A2R-400, often not being able to completely close (Figure 22); this behavior is mostly exacerbated by the excess amount of rubber being forced together below the railing. Again, it is likely that the joint would close completely in a field bridge due to the increased forces at play. However, this movement would likely cause significant damage to the strip seal.



Figure 21: Upturned Section Unable to Completely Close

A complete set of movement ranges for the A2R-XTRA Expansion Device are provided below (Tables 6 & 7). Again, it is important to note that increased lateral movement occurred as the skew angle was increased, leading to a discrepancy between the perpendicular movement and the centerline movement values.

Table 6: A2R-XTRA Movement Data (Straight Section)

| Skew | Perpendicular Movement Range (in.) | | | Movement Parallel to Centerline of Roadway (in.)* | | |
|------|------------------------------------|------|-------------------------|---|------|------------------------------|
| | Min. | Max. | Δ Perp. Movement | Min. | Max. | Δ Centerline Movement |
| 0° | 0.50 | 7.50 | 7.00 | -1.50 | 5.50 | 7.00 |
| 10° | 0.50 | 7.50 | 7.00 | -1.43 | 5.34 | 6.77 |
| 20° | 0.50 | 7.00 | 6.50 | -1.44 | 4.93 | 6.37 |
| 30° | 0.50 | 5.00 | 4.50 | -1.51 | 3.04 | 4.55 |
| 40° | 0.50 | 4.52 | 4.02 | -1.61 | 2.70 | 4.31 |
| 50° | 0.50 | 3.83 | 3.33 | -1.80 | 2.19 | 3.99 |
| 60° | 0.68 | 3.50 | 2.82 | -2.06 | 1.90 | 3.96 |

*Measured in relation to 2-inch installation width

Table 7: A2R-XTRA Movement Data (Upturned Section)

| Skew | Perpendicular Movement Range (in.) | | | Movement Parallel to Centerline of Roadway (in.)* | | |
|------|------------------------------------|------|-------------------------|---|------|------------------------------|
| | Min. | Max. | Δ Perp. Movement | Min. | Max. | Δ Centerline Movement |
| 0° | 0.70 | 7.50 | 6.80 | -1.50 | 5.50 | 7.00 |
| 10° | 0.76 | 7.50 | 6.74 | -1.18 | 5.40 | 6.58 |
| 20° | 0.68 | 6.46 | 5.78 | -1.28 | 4.37 | 5.65 |
| 30° | 0.70 | 6.07 | 5.37 | -1.36 | 4.14 | 5.50 |
| 40° | 0.90 | 5.18 | 4.28 | -1.26 | 3.42 | 4.68 |
| 50° | 1.10 | 5.01 | 3.91 | -1.20 | 3.31 | 4.54 |
| 60° | 1.03 | 4.38 | 3.35 | -1.54 | 3.00 | 4.54 |

*Measured in relation to 2-inch installation width

The upturned A2R-XTRA specimen exhibited a larger movement range compared to its straight counterpart. The research team determined that this behavior is likely due to the increased resistance to bending offered by the curve in the rubber at the two 30-degree upturns in the railing. Due to this extra rigidity, the upturned specimen extended more completely prior to the rubber sealant entering the path of traffic compared to the straight section.

Compared to the A2R-400 strip seal, the A2R-XTRA showed a marked decrease in movement as the skew angle was increased. The most common cause for failure came in extension for both the straight and upturned sections when the sealing material became warped and pushed above the railing. The upturned A2R-XTRA section also exhibited a consistent

limitation in compression due to the excess material forced between the two railings at the 30-degree bends. Further, the failure the upturned section experienced in extension did not dissipate upon closure at any skew higher than 10-degrees, and this limitation would likely be problematic in the field.

For these sections, it again follows that the introduction of foreign materials and environmental factors would likely limit the performance of these joints. It is likely that these larger seals would be more susceptible to these foreign entrants as, when extended, these seals would provide a larger opening for the entrance of these materials. In addition, the A2R-XTRA exhibited a larger dependence on skew angle and would likely perform poorly given less-than-ideal conditions. The A2R-XTRA joints would be most useful in low-skew situations where movement would exceed the limits of the A2R-400

2.4 Debris Testing

It was determined that the nature of the vertical test setup did not take into account the potential for debris entrance into the strip seal. To determine whether the strip seal's movement range would be inhibited by the inclusion of debris or create a situation resulting in premature failure, a second set of tests was run with a horizontal test configuration. In order to model the conditions present in the field, a mixture of limestone ($\frac{3}{4}$ " nominal) and sand was created to act as "debris" in these tests.

2.4.1 Debris Testing Procedure

For the debris testing, a modified version of the vertical test setup was used. In order to allow loose debris to easily stay within the confines of the railing, the test setup was reset horizontally (Figure 23). Three skews (0° , 30° , 60°) of A2R-400 strip seal were tested to model a broad range of skew situations. In addition, three levels of debris amount (no fill, half-full, and completely full) were used to note any differences in behavior.



Figure 22: Horizontal Test Rig

The testing procedure for each skew was as follows:

- The specimen was positioned at a relaxed position with a 2.0” opening between rails
- To establish a baseline, the joint was expanded to a perpendicular opening width of 4.5” and subsequently contracted to an opening width of 0.5”
- The specimen was then reset at a 2.0” perpendicular opening width and filled with debris until flush with the top of the railing; this represented the “half-full” condition (Figure 24)
- The specimen was then opened to a 4.5” perpendicular width to allow the debris to settle into the fully exposed gland (Figure 25)
- The strip seal was contracted until it reached an opening of 0.5” or was inhibited by the material present in the specimen, which caused a load spike when further loading was applied
- The specimen was then expanded to the maximum perpendicular opening of 4.5” and filled with additional debris until flush with the top of each railing; this represented the “completely-full” condition (Figure 26)

- The strip seal was contracted until it reached a perpendicular opening of 0.5” or was inhibited by the material present in the specimen*, which caused a load spike when further loading was applied
- Finally, the specimen was full opened and cleared of debris to inspect any damage inflicted upon the neoprene gland

*With the exception of the completely full zero-degree skew test, which was run until the specimen reached an opening of 0.5”, regardless of inhibition. The 30-degree and 60-degree tests were not overloaded due to the eccentricity present in the test setup and the potential for damage to the setup.



Figure 23: Half-Full Condition



Figure 24: Half-Full Condition (Open)



Figure 25: Full Condition

2.4.2 Debris Test Results

The following conclusions can be drawn from this debris testing:

- There is a clear limitation in the minimum opening range of the strip seal once debris is introduced (Figure 27)
- As skew angle increased, the required compression load increased. In a field application such force would be transferred to the bridge
- As the amount of debris increased, the amount of joint racking increased (Figure 28)
- Following each set of tests, there was no observable puncturing or damage present in the neoprene gland (Figure 29)
- A 0.5" closure is possible given a large enough load (which would be present in an actual bridge)



Figure 26: Restricted Closure Due to Debris (Typ.)



Figure 27: Increased Racking Due to Debris



Figure 28: No Apparent Damage Following Testing

As with the vertical tests, it is important to note that, although this particular test aims to recreate field conditions, there are some variables not accounted for. For example, given that the zero-degree, full-capacity test was able to close to an opening of 0.5” following a large application of load (Figure 30), it is clear that the other tests would likely have met this closure should a higher load been applied. However, this required load is roughly ten times higher than that required for an empty strip seal. Given that the forces at play in a field bridge would be much higher and more gradual than the forces present in this testing series, it is likely that these joints would be able to reach the minimum compression value provided by the manufacturer (0.5”). However, these increased forces could potentially overload the seal and push it out of the railing. That being said, as shown in Figure 29, none of the tests to complete closure in this series led to damage or puncturing of the neoprene gland. A list of movement ranges and the associated compression load required are provided in Table 8, and a graph of the loading pattern for the zero-degree, full-capacity test is shown in Figure 30.

Table 8: A2R-400 Debris Test Data

| Skew | Debris Condition | Perpendicular Movement Range (in.) | | | Max Load (lb) |
|------|------------------|------------------------------------|------|-------------------------|---------------|
| | | Min. | Max. | Δ Perp. Movement | Compression |
| 0° | None | 0.50 | 4.50 | 4.00 | 334 |
| | Half | 0.96 | 4.50 | 4.00 | 525 |
| | Full | 0.50 | 4.50 | 4.00 | 3436 |
| 30° | None | 0.50 | 4.50 | 4.00 | 405 |
| | Half | 0.78 | 4.50 | 3.72 | 578 |
| | Full | 0.91 | 4.50 | 3.59 | 637 |
| 60° | None | 0.50 | 4.50 | 4.00 | 316 |
| | Half | 0.76 | 4.50 | 3.74 | 404 |
| | Full | 0.81 | 4.50 | 3.69 | 517 |

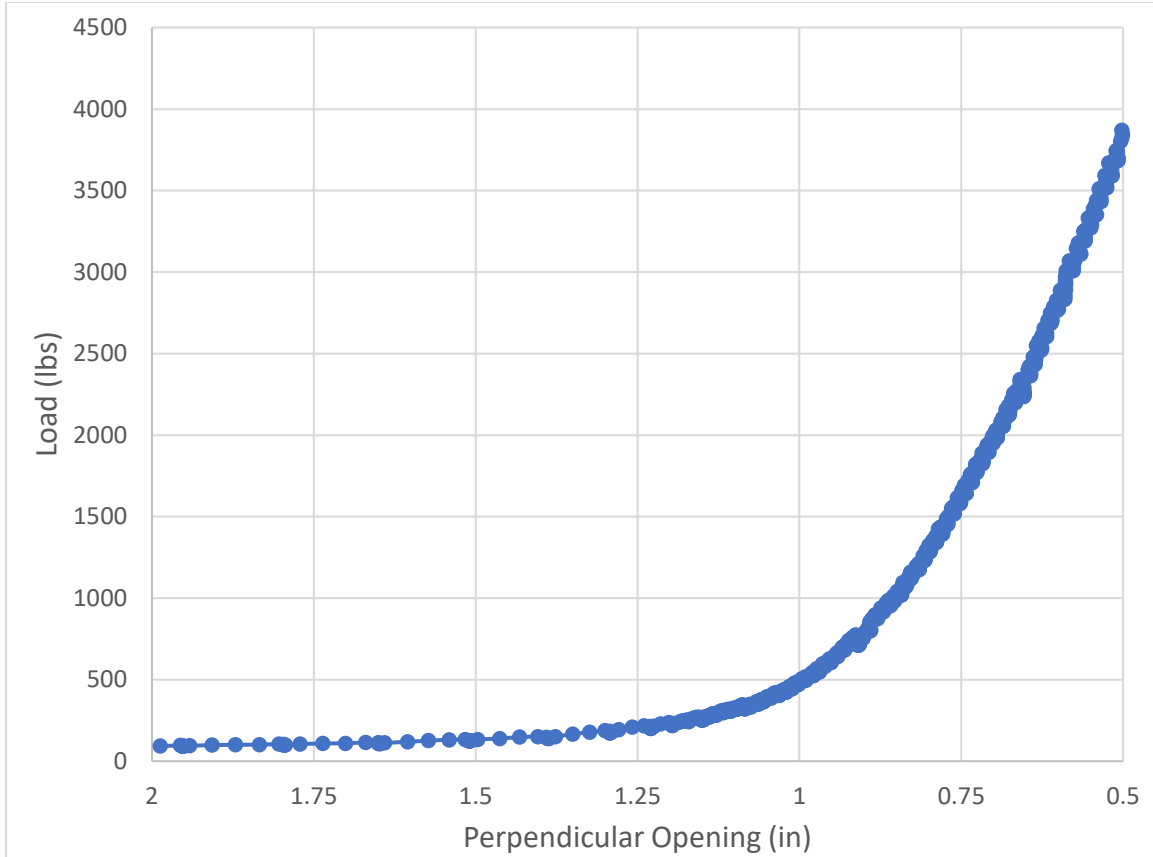


Figure 29: Zero-Degree Skew Full-Capacity Compression Data

2.5 Recommendations and Design Table Recommendations

2.5.1 BDM Table 5.8.3.2.1-1

Based off the Iowa DOT Strip Seal Expansion Joint Design Spreadsheet, the following amendments and additions are proposed for BDM Table 5.8.3.2.1-1. A comparison between current BDM standards, the results of this testing series, and a recommended design length is included.

Table 9: Proposed Updates to BDM 5.8.3.2.1-1

| Seal Type, Steel (S) or Concrete (C) | | Max. Gland Installation Temp. (F) | Minimum Install Width, inches | Approximate Maximum Allowable Expansion Length in Feet for Skew in Degrees | | | | | | |
|--|---------|---|-------------------------------------|---|-------|-------|-------|-------|-------|----|
| | | | | 0 | 10 | 20 | 30 | 40 | 50 | 60 |
| A2R-400, S | Current | 60.0 | 2.0 | 295.0 | 300.0 | 235.0 | 175.0 | -- | -- | -- |
| | Ideal | 60.0 | 2.0 | 295.0 | 300.0 | 265.0 | 235.0 | 190.0 | 130.0 | -- |
| | Field | 60.0 | 2.0 | 295.0 | 300.0 | 265.0 | 160.0 | 115.0 | 55.0 | -- |
| A2R-400, C | Current | 60.0 | 2.0 | 295.0 | 300.0 | 230.0 | 175.0 | -- | -- | -- |
| | Ideal | 60.0 | 2.0 | 295.0 | 300.0 | 260.0 | 235.0 | 190.0 | 130.0 | -- |
| | Field | 60.0 | 2.0 | 295.0 | 300.0 | 260.0 | 160.0 | 115.0 | 55.0 | -- |
| A2R-XTRA, S | Ideal | 60.0 | 2.0 | 295.0 | 300.0 | 310.0 | 340.0 | 250.0 | 130.0 | -- |
| | Field | 60.0 | 2.0 | 295.0 | 300.0 | -- | -- | -- | -- | -- |
| A2R-XTRA, C | Ideal | 60.0 | 2.0 | 520.0 | 525.0 | 530.0 | 340.0 | 250.0 | 130.0 | -- |
| | Field | 60.0 | 2.0 | 520.0 | 525.0 | -- | -- | -- | -- | -- |

Given the nature of these devices discussed above, it is noted that they may be subject to premature failure in less-than-ideal conditions, namely due to the entrance of debris or foreign substances. Because these conditions are highly variable and case-dependent, it is difficult to anticipate the allowable movement capacity for field conditions. To apply a factor of safety, based on the BDM's current standard that strip seals experience a performance drop-off at skews greater than 30-degrees, each movement capacity has been reduced by ½" for the A2R-400 for each skew greater than 30-degrees. Further, based on the test results for the A2R-XTRA, it is not recommended that these joints be used at a skew greater than 10-degrees. These updated movement ranges account for the reduction in appropriate maximum length for each expansion device.

The above table's values are based on the set of design calculations and considerations proposed in BDM 5.8.3 for the following design conditions:

- Long-term movement capacity parallel with centerline of roadway including shrinkage if applicable,
- Long-term maximum opening at minimum deck temperature after shrinkage,
- Short-term minimum opening at maximum deck temperature before shrinkage, and

- Manufacturer's minimum installation width, which will determine the maximum gland installation temperature.

An example set of design calculations as prescribed in BDM C5.8.3.2.1 is provided below.

These calculations show the design of a 40-degree skewed bridge not passing current specifications but passing those proposed recommendations based on this study.

Current Guidelines

Given: Steel bridge, 200 feet long, 100-foot expansion length, 40-degree skew.

Make preliminary selection.

For 40-degree skew, Table 5.8.3.2.1-1 lists maximum expansion length of 260 feet for Wabo SE-300 and 235 feet for Wabo SE-400. D.S. Brown A2R-400 is not acceptable. Try Wabo SE-300.

Proposed Guidelines

Given: Steel bridge, 200 feet long, 100-foot expansion length, 40-degree skew.

Make preliminary selection.

For 40-degree skew, Table 5.8.3.2.1-1* lists maximum expansion length of 260 feet for Wabo SE-300 and 115 feet for D.S. Brown A2R-400. Try A2R-400.

Check allowable movement capacity parallel with centerline of roadway for A2R-400.

$$(\Delta L)_{\text{thermal}} = \alpha L \Delta T = (0.0000065)(100)(12)(150) = 1.17 \text{ inches}$$

$$(\Delta L)_{\text{shrink}} = k L = (0)(100)(12) = 0 \text{ inches}$$

$$(\Delta L)_{\text{total}} = 2.106 + 0 = 1.17 \text{ inches } [< 3.4 \text{ inches from Table 5.8.3.2.1-2, OK}]$$

Check long-term maximum joint opening. [Numerical subscripts refer to temperatures in degrees Fahrenheit. Shrinkage is zero and not shown.]

Try 2 inch at 90 °F joint setting for best installation options.

$$\text{Width}_{25} = \text{Setting}_{90} + (\Delta L)_{115} = 2.0 + (0.0000065)(100)(12)(115)(\cos 40) = 2.69 \text{ inches } [< 3 \text{ inches } \{\text{minimum of seal size and } (4)(\cos 40) = 3.06 \text{ inches, Table 5.8.3.2.1-2**}\}, \text{ OK}]$$

Check short-term minimum joint opening.

$$\text{Width}_{125} = \text{Setting}_{90} - (\Delta L)_{35} = 2.0 - (0.0000065)(100)(12)(35)(\cos 40) = 1.79 \text{ inches } [> 0.5 \text{ inches, Table 5.8.3.2.1-2, OK}]$$

Determine joint settings for plans

$$\text{Setting}_{50} = \text{Setting}_{90} + (\Delta L)_{40} = 2.0 + (0.0000065)(100)(12)(40)(\cos 40) = 2.24 \text{ inches}$$

$$(\Delta L)_{40} = \alpha L \Delta T = (0.0000065)(100)(12)(40)(\cos 40) = 0.24 \text{ inches}$$

$$\text{Setting}_{10} = \text{Setting}_{50} + (\Delta L)_{40} = 2.24 + 0.24 = 2.53$$

$$\text{Setting}_{90} = \text{Setting}_{50} - (\Delta L)_{40} = 2.24 - 0.24 = 2.00$$

Determine maximum gland installation temperature.

Maximum installation temperature if 60 °F from joint setting trial above.

Specify only one strip seal: D.S. Brown A2R-400 with joint settings of 2 inches at 90 °F, 2 1/4 inches at 50 °F, and 2 ½ inches at 10 °F. Specify that maximum gland temperature is 60 °F.

*Table 5.8.3.2.1-1 for the purposes of this example are from Table 8 of this report

** Table 5.8.3.2.1-2 for the purposes of this example are from Table 9 of this report

2.5.2 BDM Table 5.8.3.2.1-2

Based on the ideal test conditions performed in this series, the following is a proposed set of movement range updates and additions for both the A2R-400 and A2R-XTRA.

Table 10: Proposed Updates to BDM 5.8.3.2.1-2

| Seal Type | Specimen Type | Minimum Installation | Minimum Opening | Allowable Movement Capacity Parallel with Centerline of Roadway in | | | | | | |
|-----------|---------------|----------------------|-----------------|--|-----|-----|-----|-----|-----|-----|
| | | | | 0 | 10 | 20 | 30 | 40 | 50 | 60 |
| A2R-400 | Current | 2.0 | 0.5 | 4.0 | 4.1 | 3.7 | 3.5 | 2.4 | 2.0 | 1.2 |
| | Ideal | 2.0 | 0.5 | 4.0 | 4.1 | 3.9 | 3.9 | 3.9 | 4.0 | 3.8 |
| | Field | 2.0 | 0.5 | 4.0 | 4.1 | 3.9 | 3.4 | 3.4 | 3.5 | 3.3 |
| A2R-XTRA | Current | 2.0 | 0.5 | -- | -- | -- | -- | -- | -- | -- |
| | Ideal | 2.0 | 0.5 | 7.0 | 6.6 | 5.7 | 4.6 | 4.3 | 4.0 | 4.0 |
| | Field | 2.0 | 0.5 | 7.0 | 6.6 | -- | -- | -- | -- | -- |

Given the nature of these devices discussed above, it is noted that they may be subject to premature failure in less-than-ideal conditions, namely due to the entrance of debris. Because these conditions are highly variable and case-dependent, it is difficult to anticipate the allowable movement capacity for field conditions. To apply a factor of safety, based on the BDM's current standard that strip seals experience a performance drop-off at skews greater than 30-degrees, each movement capacity has been reduced by ½" for the A2R-400 for each skew greater than 30-degrees. Further, based on the test results for the A2R-XTRA, it is not recommended that these joints be used at a skew greater than 10-degrees.

CHAPTER 3. MOVEABLE ABUTMENT RESEARCH AND INVESTIGATIONS

3.1 Background

The previous chapter explored and sought to mitigate premature failure related to expansion joint usage as a means of accommodating thermal movement in bridges. It was noted that strip seals present severe drainage and potential erosion of critical elements should they fail. It is for this reason that alternatives for thermal movement accommodation are also often utilized in lieu of expansion devices. One common method includes the use of integral or semi-integral moveable abutments, which allow the expansion joints to be moved further away from the abutment. Among the benefits to using a moveable abutment are increased structural rigidity a lower maintenance demand. Unfortunately, a new host of problems is likely to occur with the presence of a moveable abutment, the most prevalent of them being the “bump at the end of the bridge,” a side-effect of excessive settlement in the connected approach slab. Typically, this settlement is accompanied by large amounts of voiding at the abutment, improper drainage to the base of the abutment, and cracking within the approach slab. The last twenty years has seen the Iowa DOT prefer the use of moveable abutments over expansion devices for bridges with a relatively small amount of expected thermal movement (less than 3 inches). While these designs often work as intended, correspondence with IDOT indicates that they are still experiencing issues related to moveable abutment usage most notably with their approach slabs. As such, Iowa State University’s Bridge Engineering Center has worked with IDOT on several occasions to provide insight into how the state’s moveable abutment bridges are performing. Currently, ISU is a part of a multi-year project that seeks to observe the performance of changes made to the state’s standard moveable abutment design in the last decade.

The previous phase of this project, performed by Douglas Krapf in 2019, provided an in-depth literature review of previous research on the subject, instrumented two bridges in the state to monitor their performance, performed several field investigations of IDOT bridges, and originated two finite element models of the two instrumented bridges. The current phase of this project seeks to expand upon these measures by starting a statewide inventory of IDOT approach slab performance, adding additional investigations and refinement into the previously-generated Finite Element models, and investigating the failure mode of an integral abutment connection in Washington County. It is through these additions that this project will expand upon the research previously performed in this area.

3.2 Literature Review

3.2.1 Overview

As previously noted, there are several key approach slab issues that are exacerbated by utilizing a jointless, moveable abutment bridge. The culmination of these negative side-effects manifest in the “bump at the end of the bridge,” an issue which several DOTs and previous authors have investigated numerous times via field investigations, instrumented monitoring of field bridges, literature reviews, and finite element analysis. This literature review serves to provide context for previous research in the area, emphasizing common issues with moveable abutments, the reasons for these issues, and recommendations for mitigating them in future designs.

3.2.2 Surveys and Field Observations

An effective way of determining required areas of improvement for a future moveable abutment designs is to take stock of how the approach slabs on previous projects are performing under field conditions. In a comprehensive review performed by Yasrobi et al. (2015), it was concluded that 46% of the 28 reviewed states were not satisfied with their current approach slab

design. It was noted that the most common cause for this failure was inappropriate approach slab settlement, which many DOTs mainly attributed to poor construction practices. Further, this excessive settlement was often accompanied by poor drainage, which led to erosion and void occurrence underneath the approach slab. As this runoff continues to make its way underneath the slab, the presence of the void continues to worsen, increasing the likelihood of structural issues with the slab. Based on their findings, it was determined that backfill design and construction were the most important factors leading to approach slab settlement and failure. However, it was noted that properly designed backfill is not enough to eliminate approach slab issues on its own.

The findings presented above by Yasrobi et al. (2015) have been echoed by previous research. In a series of studies performed by White et al. (2005 & 2007) that investigated 74 Iowa bridges to quantify common issues with failed approach slabs, it was determined that severe voids had developed under 25% of the inspected bridge approaches. In addition, severe erosion was present at 40% of the bridges and 60% of the bridges had ineffective runoff. Majority of the bridges exceeded the recommended 1/200 slope proposed by Wahls (1990) and Long et al. (1998), and differential settlement of 2 to 6 inches was common at the end of the abutment wingwall. Runoff and erosion often accompany one another, as excess runoff typically leads to increased erosion underneath the approach slab. The erosion was found to typically leave a void ranging 6 inches to 12 inches between the base of the slab and the geotextile reinforced subbase (Figure 31).



Figure 30: Voiding Under Approach Slab (White, 2007)

While this voiding does not lead to immediate failure of the connection joint or approach slab, it does present other issues that may develop over time, including connection joint shearing, settlement and transverse cracking of the approach slab, and erosion and fracturing of the slope, embankment, and piles (Figure 2). Typically, this void development was observed within the first year of service, and grouting underneath the slab to mitigate these issues was found to not necessarily prevent further settlement.

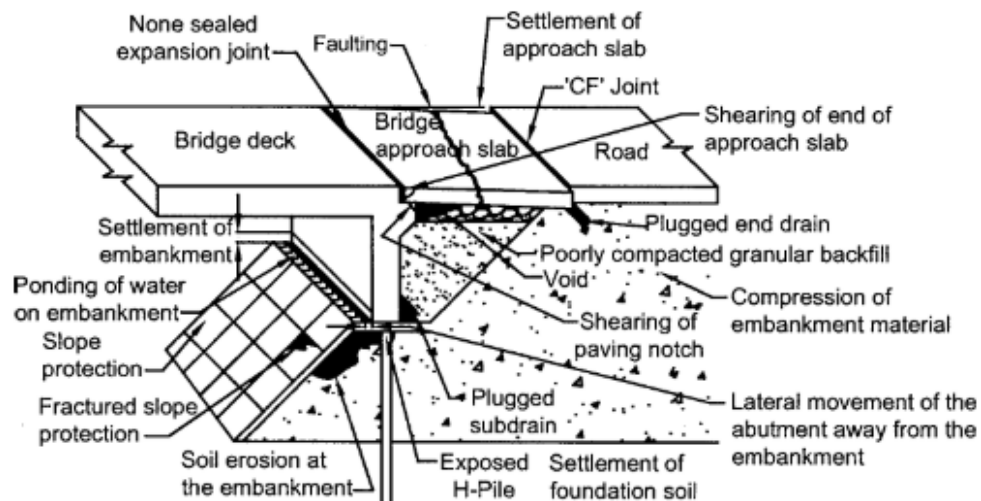


Figure 31: Diagram Summarizing Frequent Problems at Several Bridge Sites (White, 2007)

The prevalence of the void directly adjacent to the abutment is further aggravated by the introduction of integral abutments, which push and pull the backfill as the bridge structure expands and contracts with thermal effects. These thermal movements, reported by Schaefer and Koch (1992), create a compaction in the soil as the bridge expands. However, once the bridge contracts and pulls away from the embankment, a void is left.

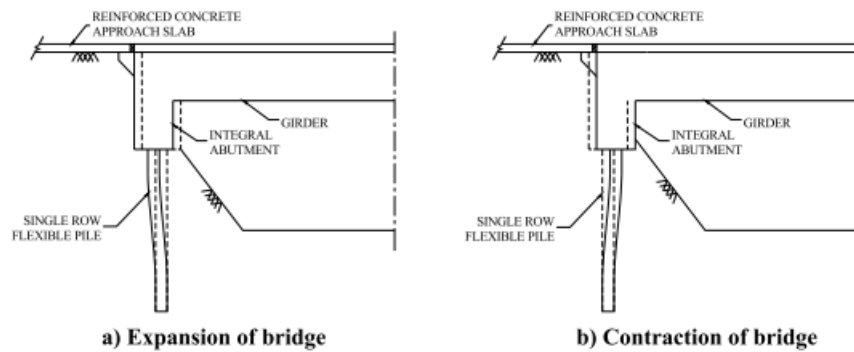


Figure 32: Structural Movement Due to Thermal Effects (Griemann et al., 2008)

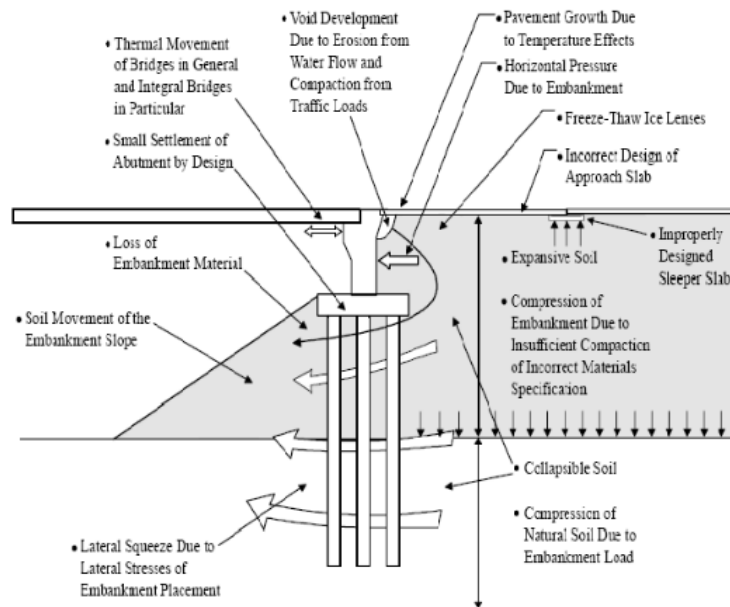


Figure 33: Problems Leading to the Formation of the Bump (Briaud et al., 1997)

Once this initial void is formed, the integral abutment is at a much higher risk for further erosion and voiding due to excess, mismanaged runoff. This cyclical nature of this movement has been verified by several subsequent studies via field inspection and approach slab instrumentation. In a project that monitored the temperature and displacement of two integral abutment connections, one with a precast slab and one with a cast-in-place slab, “strain ratcheting” was observed (Greimann et al., 2008). This ratcheting effect, which progressively worsens the voiding condition underneath the slab with time, provides an area where additional runoff may erode the subbase. Additionally, while the vertical reinforcing bar connection initially worked as intended, an opening in the joint formed over time. A 22” void was also documented underneath the doubly-reinforced south approach slab, and transverse cracking of the slab was reported. A similar study was performed by Nadermann et al. (2010), where it was observed that this temperature movement took the form of two patterns: a long-term cycle encompassing the general temperature movement throughout the year and a repeated short-term cycle as the temperature fluctuated throughout the course of each day. Again, while this tied connection initially performed well, it was later shown by Krapf (2019) to age poorly, excessively opening as time went on. Majority of the vertical tie bar connections investigated had not performed well long-term, often opening more than twice their initial design width due to thermal movement. In addition, several of these bridges displayed transverse cracking, and it was hypothesized that this cracking and voiding would lead to inadequate drainage and further problems.



Figure 34: Transverse Cracking of Approach (Krapf, 2019)

In an effort to determine how widespread the settlement and voiding situation in Iowa approach slabs was, the Iowa DOT contracted Wiss Janney Elstner Associates to perform two empirical surveys of slab performance in the state (Rende and Donnelly, 2011). The first study, performed in 2011 in the wake of a large amount of Missouri River flooding in western Iowa, utilized ground penetrating radar (GPR) and impulse-response (IR). In addition to these two forms of non-destructive evaluation, coring was performed to verify the accuracy of the acquired data. In total, 22 bridges (44 individual reinforced approach slabs) were investigated for voiding and vertical settlement, and the coring verification determined that GPR was a reliable way to scan and detect deficiencies in the soil beneath the approach slab.

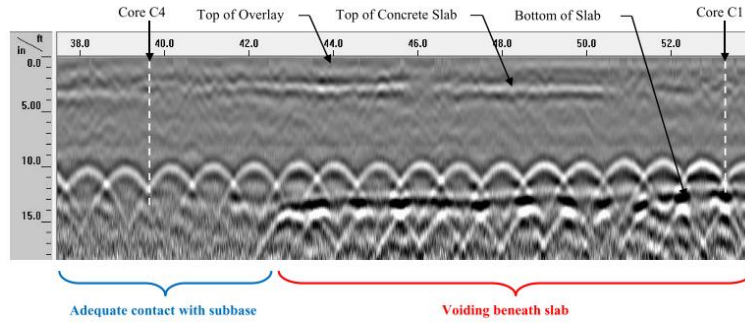


Figure 35: WJE GPR Voiding Sample (WJE, 2011)

Of the 44 slabs investigated, 3 experienced severe voiding ranging between 10 to 20 feet in length and 2 to 5 feet inches depth. Soil tests conducted beneath these slabs indicated that none of the original subbase remained. However, none of these slabs displayed any visible signs of structural impairment to the approach slab. Of the remaining 41 approach slabs, 28 exhibited voiding, although it typically spanned less than 10 feet from the face of the abutments with a depth less than 2 inches; the original subbase, consisting of compacted sand or gravel, was typically present at these locations.

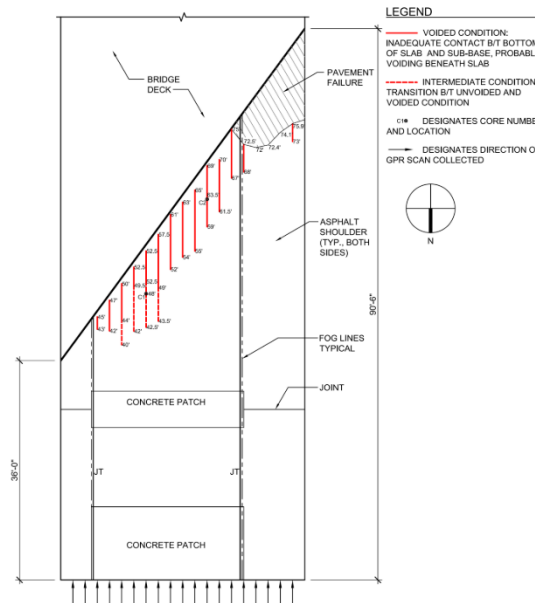


Figure 36: Plan View of Severe Voiding (WJE, 2011)

A second study with a similar intent was again conducted by WJE in 2018. In this case, the goal was to investigate the performance of 12 Iowa approach slabs with stub and integral abutments constructed between 2006 and 2015 following the implementation of design recommendations proposed by White et al. (2005). This second survey consisted of visual inspections and GPR and was supplemented by coring and borescope investigations to confirm the presence and extent of voiding. Similar to the visual inspections later performed by Krapf in 2019, a large majority of the connection joints and expansion joints had fared poorly, differing from the design plans in opening width by as much as 3 inches. The GPR and borescope inspections revealed similar performance of that observed in the 2011 report—the bridges with integral abutments displayed large voids adjacent to the abutment, likely from repeated thermal expansion and contraction. The approach slabs on these bridges are likely more susceptible to further erosion and damage as a result of these movement voids. However, it was recorded that many of these bridges were performing well structurally, although several did show signs of transverse cracking and pavement spalling. The maximum settlement and differential settlement were recorded as 1 inch and 0.4 inch, respectively. Investigation of the stub abutment bridges displayed a stark contrast to the performance of the integrally connected bridges, showing much less voiding in general.



Figure 37: Examples of Voiding at Integral Abutment Bridges (IDOT)

3.2.3 Recommendations for Mitigating Approach Slab Failure

Given the nature of the failures described in the section above, the main factors contributing to approach slab/connection joint failure in moveable abutment bridges stem from geotechnical problems related to soil settlement and erosion. Typically, design techniques to anticipate and prepare for these failures are split between two overarching categories: soil preparation and structural design considerations.

Standard design recommendations for the subbase beneath approach slabs is centered around limiting settlement and limiting loss of the original subbase. Exact recommendations vary, but most researchers agree that a stiff, well-drained soil condition performs best. According to the study performed by Yasrobi et al. (2015), backfill should consist of a well-graded pervious material with a minimum 95% compacted Standard Proctor Density. It was also recommended that in-situ density tests are performed on the proposed soil in order to gauge the possibility of future settlement. In a finite element analysis run as a part of an approach slab performance study at the University of Wisconsin, Madison, it was found that soil stiffness had a notable impact on concrete cracking (Oliva, 2011). As soil stiffness decreased, the amount of settlement and slab rotation at the abutment both increased; these responses were followed by a higher likelihood for transverse cracking. The same was true for void occurrence. As the length of the void increased, the likelihood of structural failure increased as the slab was required to span the longer settlement trenches. A similar study was conducted by Nassif (2002), and determined that edge settlement led to tensile stress concentrations in the top of the slab, whereas settlement in the middle of the slab led to tensile stress concentration in the bottom of the slab. In order to improve subgrade performance and ensure an optimal stiffness, Phares et al. (2011) recommended improving compaction effort via a light vibratory compactor on granular backfill

to mitigate settlement. By providing a sufficiently stiff soil, the entire length of the approach slab is consistently supported and deflection is limited.

Should soil with an appropriate stiffness be used, it is also important to prevent future erosion due to poor drainage. It is often recommended that proper water drainage be an integral part of design (Phares and Dahlberg, 2015; White et al., 2007). It has also been emphasized that increasing routine inspections and maintenance to ensure that designed drains and expansion devices are clear of debris, which can prove detrimental to proper drainage (WJE, 2018). To reduce the overall forces present within the slab due to thermal movement, steps should also be taken to lower the friction factor between the base of the slab and the subgrade underneath. The most common recommendation is the use of polyethylene sheeting between these two components (Mistry, 2005; Aktan and Attanayake, 2011; Phares and Dahlberg, 2015). By lowering the amount of friction force required for the approach slab to slide across the underlying subbase, the amount of force transferred through the abutment connection is reduced, lowering the likelihood of a connection failure.

The inclusion of a sleeper slab has also been suggested to overcome settlement at the far end of an approach slab (Phares et al., 2011; Yasrobi et al., 2015). Unlike side of the slab adjacent to the bridge, which rests on a seat provided by the abutment, majority of the slab is supported only by the soil underneath. Thus, areas farther from the abutment are at a higher risk for settlement, as shown in Figure 39.

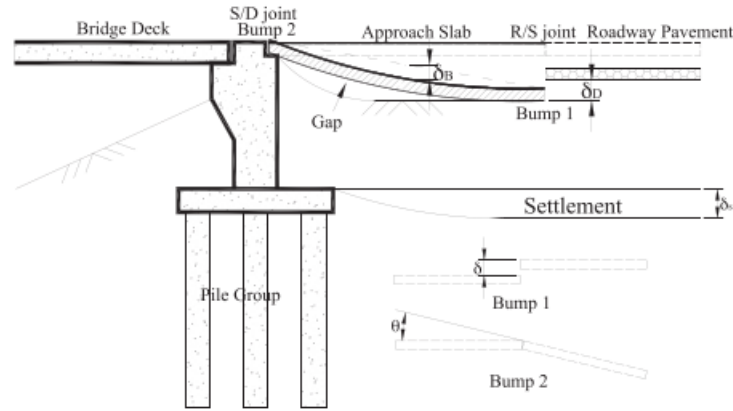


Figure 38: Approach Settlement Away from Abutment (Chen and Abu-Farsakh, 2016)

The inclusion of a sleeper slab provides an additional concrete support condition in the area most likely to experience higher total settlement. If the approach slab is designed with enough structural rigidity to span any voids or settlement that may occur between the abutment and the sleeper slab, then deflection and transverse cracking will theoretically be mitigated. However, in their field study of several approach slab panels in Wisconsin, Phares and Dahlberg (2015) hypothesized that not all slabs were being adequately designed to span this settlement ditch between the sleeper slab and abutment. However, the inclusion of a sleeper slab does not always perform as intended. Should the approach slab be built on weak, settlement-prone soil, then it will vertically displace along with the rest of the approach slab system. Recommendations typically include proper compaction and use of geogrid layers for reinforcement beneath the sleeper slab (Chen and Abu-Farsakh, 2016).

While increasing soil stiffness and insuring proper drainage are key factors in a successful tied moveable abutment design, several of these soil considerations are difficult to guarantee, and it is for that reason that many researchers recommend designing the slab with enough stiffness to span any voiding or settlement that may occur (Phares and Dahlberg, 2015).

The factors generally studied regarding structural rigidity for approach slabs are slab thickness, reinforcement ratio, slab length, and concrete strength.

In a study performed by the New Jersey DOT (Nassif, 2002) to improve approach slab design details, a finite element model was originated utilizing ABAQUS modeling software. The goal of the study was to correlate the failure patterns of the computer model with those observed in the investigated field bridges. The computer models featured a series of springs to represent the subgrade beneath the approach slab, and these springs were added and removed at various points to simulate voiding conditions. These conditions were coupled with a standard HS-20 service truck load to simulate likely field loading. As noted by earlier field investigations above, results indicated that an increase in soil settlement led to a higher likelihood of premature slab failure in the form of transverse cracking. The model displayed a similar cracking pattern to that observed with the field bridge, showing cracks near the entrance and exit of the slab. A parametric analysis was performed on the computer model to investigate how possible design detail modifications could improve the performance in future designs. The most significant factor for mitigating transverse cracking and slab settlement was determined to be slab thickness; as the slab depth was increased, the forces present in the extreme tensile regions of the slab were reduced. Further study revealed that a higher concrete strength had a positive effect on tension reduction, although it was much less effective than increasing slab depth. An increased steel reinforcement ratio and a higher steel yield strength had little to no impact limiting failure. The results of this study are substantiated by a field study performed on behalf of the Louisiana DOT (Chen and Abu-Farsakh, 2016), which monitored two similar approach slabs with different design details based on previous research (Cai et al., 2005; Chen, 2007; Abu-Farsakh et al.,

2008). It was clearly observed that an increased slab thickness and higher reinforcement ratio in the West approach slab led to significantly less cracking and reduced tensile strain values.

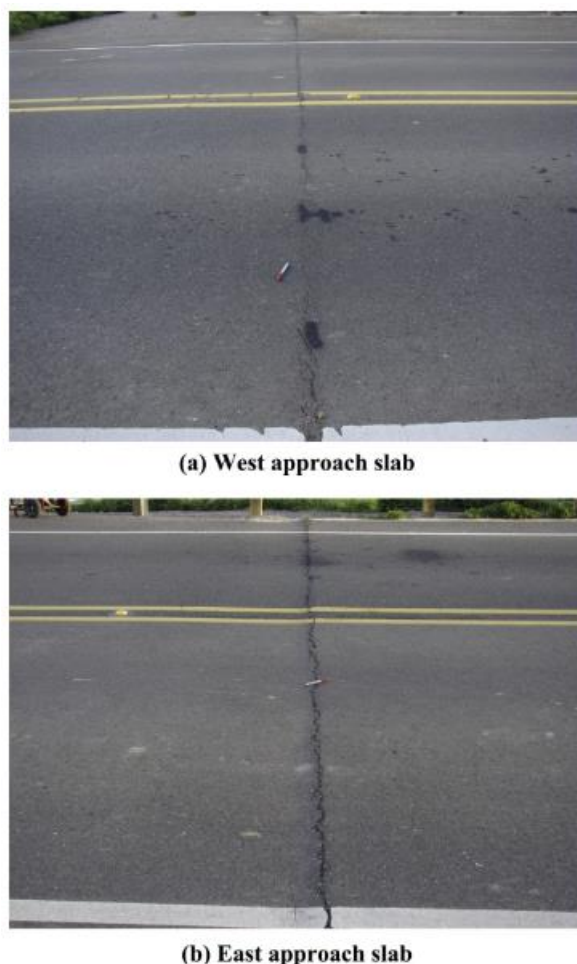


Figure 39: Effects of Increasing Slab Thickness and Reinforcement Ratio (Chen and Abu-Farsakh, 2016)

A similar finite approach was taken by Oliva (2011). In this case, the goal was to quantify the amount of rotation that could be present at the connection between the approach slab and the abutment. It was observed that decreased soil stiffness led to higher amounts of settlement, connection rotation, and risk of transverse cracking. The transverse cracking observed on “loose” soil conditions with standard strength (4 ksi) concrete was mitigated by utilizing concrete with a higher compressive strength (8 ksi). It was also noted that, based on the standard amount of

rotation observed, the expansion joint or ductile concrete between the abutment and approach slab should be designed for a rotation of 0.002 radians. Further, voiding conditions adjacent to the abutment were modeled, and it was determined that slab performance was affected for voids greater than 4 feet in length with much higher levels of tensile forces becoming present once the void became 6 feet or longer. Slab length was determined to have little effect on reducing transverse cracking beyond 10 feet.

3.3 Inventory of Iowa Approach Slab Performance

3.3.1 Approach Slab Inventory Background and Process

As a supplement to the studies performed above, the Iowa Department of Transportation, through the Iowa State University Bridge Engineering Center, has decided to perform an inventory quantifying the performance of IDOT approach slabs constructed since 2009, as a number of design changes were made during that time. The motivation behind this review of state slab performance is to verify whether or not these design updates are working to mitigate common approach slab issues. It is the goal of this venture to gain a more complete idea of approach slab performance throughout the state to identify which design details and methods produce the best performance during field operation. Because there have been over 450 approach slabs constructed within the state between 2009 and 2020, it is anticipated that this study will take a fair amount of time to complete. As this investigation directly relates to the content and scope of the research presented in this thesis, it was determined that a brief pilot version of this venture would be beneficial to determining typical approach slab performance throughout the state. It is anticipated that the remainder of this phased investigation will continue based on the methods outlined and explained in this section.

As stated above, the goal of this inventory is to investigate and compare the performance of different approach slab details and conditions throughout the state of Iowa. Per IDOT, the key

areas of concern for this review have been identified as “bump” presence, slab settlement, slab cracking, joint issues, and paving notch issues. For each approach slab, these performance indicators can be correlated based on their prevalence among bridges with similar designs, including bridge type, abutment type, approach type, and traffic data. By noting which bridges are susceptible to higher amount of performance issues, these designs can be investigated in more detail.

For the purposes of this pilot study, one bridge from each year between 2009 and 2018 were selected and inspected, as inspection records were not yet available for bridges built in 2019 and 2020. In most cases, the performance and design details of each approach slab was determined via Iowa’s Structure Inventory and Inspection Management Systems (SIIMS), which contains original design documents and a record of all routine state inspections. It is anticipated that future analysis will utilize IRI data and Roadview to gain more quantitative data.

To compare bridges with similar design expectations, only interstate bridges were used for this brief investigation, and included bridges on I-80, I-35, and I-29 throughout the state. Generally, a bridge with one of the highest Annual Average Daily Travel (AADT) values was chosen from each year. All bridges selected during this phase of study were prestressed concrete bridges with beams or girders. It was noted that images of approach slab performance were often difficult to ascertain from the inspection reports and images, and Google Earth was utilized when necessary. Unfortunately, due to this lack of notable information for a large number of the approach slabs, it was often surmised that a given issue was non-existent for the approach slab if it was not explicitly stated in the inspection report and not clearly seen from the available images. In addition, a several of the plan sets did not include the exact type of approach slab

used. This was again surmised based on the thickness of the bridge, the type of the bridge, and the approach slab type used on similar structures.

3.3.2 Sample Investigation

A sample of the process is provided below for bridge FHWA 42021 located on I-80 EB:

Year Constructed: 2012

AADT: 23950

Design Number: 1010

Bridge Type: 5 - Prestressed Concrete 02 - Stringer/Multi-beam or Girder

Abutment Type: Integral (from plan sheets)

Approach Type: Not in plans — Assumed as 12” double reinforced

Bump Presence: Likely — Panel 1 shows cracking and depressions in first two panels

Settlement: Yes — Clear settlement cracks and differential settlement between panels

Cracking: Yes

Paving Notch Issues: Likely — Erosion noted under slab adjacent to abutment

Joint Issues: Openings noted as greater than 2”

Images:



Far Approach Panel 1 Cracking



Near Approach Panel 2 Cracking



Barrier Diff Settlement/Cause of Drainage



Erosion, thickness = 2 ft.

3.3.3 Pilot Inventory Findings

Of the ten approach slabs investigated as a part of this brief study, settlement appeared to likely be present in eight of the subjects. The most obvious sign of this settlement was the presence of cracking between the barrier rail and the approach slab shoulder, indicating that the slab had displaced vertically downward from its original position. This displacement is believed to create tensile cracking between the railing and the shoulder surface. Another obvious sign of differential settlement was the distinct difference in the height of adjacent approach slabs. Settlement appeared to be more prevalent and obvious in the approach slabs constructed prior to 2014.



Figure 40: Cracking at Barrier Rail Indicating Settlement



Figure 41: Differences in Slab Height Indicating Settlement

Four of the approach slabs investigated exhibited cracking of the approach slab surface, and there was no clear correlation relating construction year to crack presence. Erosion was noted in two of the inspection reports, and erosion paving notch issues were difficult to determine as most of the pictures were taken of the approach surface unless an explicit picture was taken to highlight an issue at these locations. Several of the expansion joints were filled with growth and noted as being own greater than the recommended 2 inches, indicating that the bridges were possibly improperly accommodating thermal movement.

CHAPTER 4. FINITE ELEMENT MODELING

Following the research conducted by Krapf (2019), the finite element (FE) models utilized for this project series were made utilizing ABAQUS/CAE software. Acting as an extension of this previous research, the analyses run on the three models included in this paper are intended to refine and expand upon those initially observed to account for settlement and erosion. Each of these models was originally constructed to model the effects of thermal movement on the tied connection joint between the approach slab and the moveable abutment connected to the bridge superstructure. However, given the additional issues with settlement and voiding erosion noted in the inspections of approach slabs throughout the state, it was determined additional parameters should be added to these models to gain a more accurate picture of their behavior. The first two of these models were originated to investigate the impact of thermal movement on two moveable abutment bridges located in Jasper County and Story County in Iowa. Additionally, of these bridges were instrumented to correlate the FE models' behavior to that observed in the field bridges. The previous simulations run on these models sought to investigate how friction force from the slab was carried by the tied bars connecting the approach slab to the abutment. As such, the Story and Jasper County models have been calibrated based on the data observed from their field bridge counterpart, respectively; background and discussion on the instrumentation and monitoring processes are provided in earlier research performed by Krapf (2019). The third model was originated to investigate the observed failure of a set of approach slabs in Washington County, Iowa; this bridge was not instrumented but relies on the modeling techniques and correlations provided by the other two models. The investigations put forth in this chapter focus on the effects of settlement on the approach slab in a tied moveable abutment configuration. By applying the settlement and voiding

conditions observed in field bridges to these previously established models, an understanding of their structural response to these conditions is observed.

4.1 Jasper and Story County Finite Modeling Techniques

As indicated above, the Jasper and Story County bridges were originated in a previous phase of this study that focused on thermal movement force transfer through the tied connection joint. As these bridges were recreations of instrumented field bridges, a known correlation of their accuracy and behavior has been established. The current phase of this research, presented in the remainder of this chapter, expands upon the analyses run on these models to capture the effects of settlement and voiding. While previous research analyzed the structural consequences of horizontal movement of the approach slab, this project seeks to investigate the structural consequences of vertical displacement of the approach slab due to settlement and voiding.

4.1.1 Model Parts and Assembly

Several of the model components remained the same or similar to the original models provided in the previous study, including the abutment section, the approach slab adjacent to the abutment, the tied connection dowels, the slab rebar, and, in the case of the Story model, the sleeper slab. However, due to this study's focus on the concrete behavior when subjected to soil settlement and voiding, it was important to determine an appropriate way of modeling soil-structure interaction. A set of linear springs was used to model the settlement of the soil beneath the approach slab as it was loaded. As it was deemed important to maintain the soil-to-concrete interaction present in the previous study, the set of soil springs was set beneath a modified version of the soil block previously present. In order to minimize the impact that this added soil weight would provide, the thickness of the soil block was adjusted to be as thin as possible without creating convergence issues with each model—the final thickness used was one half inch thick. For these two models, longitudinal and transverse rebar were modeled as planar shell

elements with spacing and bar orientation taken from the plan sets for each bridge. Paving notch connection dowel placement and angle were taken from a combination of plan sets and IDOT design standards.

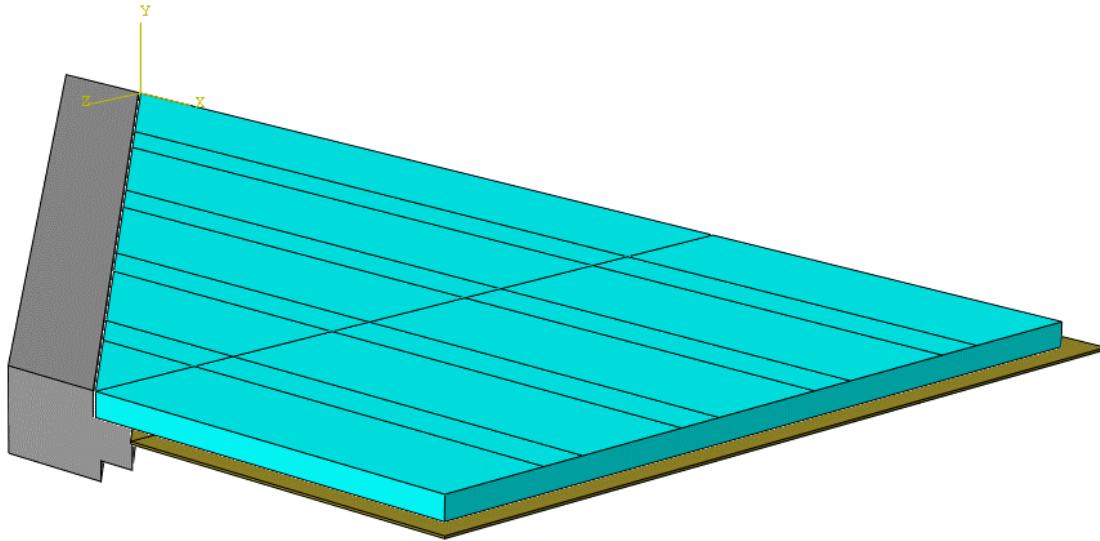


Figure 42: Jasper FE Assembly

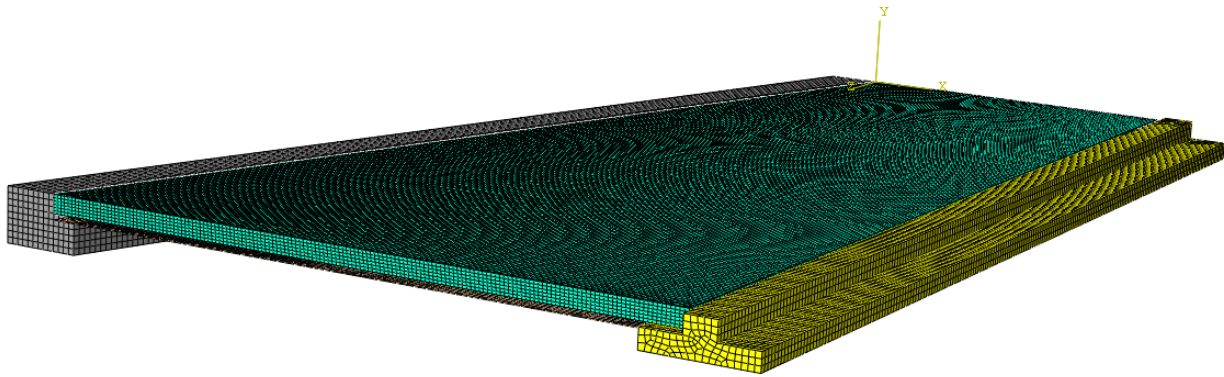


Figure 43: Story FE Assembly and Mesh

4.1.2 Material Properties

Material properties for these models were generally kept similar to those utilized in the previous study. While Taking the values from the Jasper and Story bridge plan sets, a Young's Modulus of 3605 ksi and Poisson's Ratio of 0.3 were used for the elastic concrete range. Because this study is also concerned with cracking and failure of the concrete in the approach slab as settlement and voiding was applied, Concrete Damaged Plasticity and Concrete Compression Damage settings in ABAQUS were also applied to each model to investigate concrete failure behavior. Concrete strength for each model was set as 4 ksi per the plan sets. Soil properties were taken from correspondence with the Iowa DOT and intended to act as a shear layer between the approach slab and springs; this layer ties the springs together, preventing them from acting as completely independent elements. Steel properties for the longitudinal and transverse rebar, in addition to the tied dowels, were taken from the respective plan sets.

4.1.3 Boundary Conditions

Boundary conditions for these models were modified from earlier research to allow for accurate representation of approach slab settlement. The entirety of the abutment was not modeled as it would needlessly increase the complexity and runtime of the models. Instead, the top portion of the abutment was modeled to provide support for the approach slab as it would in the field bridge. The portion of the abutment that was removed was replaced with a roller to represent the "moveable" abutment condition. Non-vertical movement of the soil condition was restricted to represent soil support surrounding the modeled soil block. No explicit boundary conditions were placed on the approach slab, but it was supported by the abutment, soil and springs, and sleeper slab in the case of the Story County bridge.

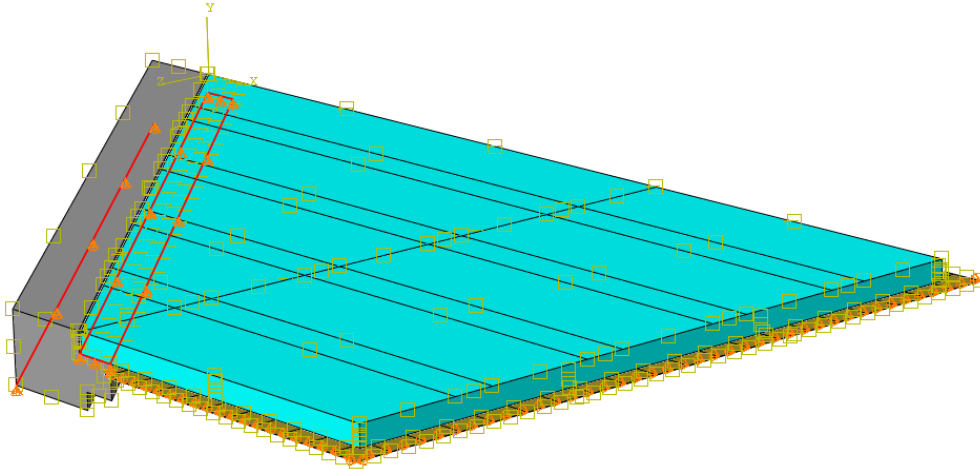


Figure 44: Jasper Boundary Conditions

4.1.4 Springs and Model Calibration

To model the void and settlement conditions present in these models, a series of linear-elastic springs coupled with a thin shear layer of soil were used to represent different soil scenarios. Several different modeling techniques were considered to model soil conditions. Initial models used a displacement-based approach where the soil block beneath the approach slab was moved a specified distance as a boundary condition. However, it was noted that this produced settlement patterns that were not indicative of situations observed in the field. A literature review of similar approach slab FE models led to the decision to use a layer of linear springs (Oliva, 2011). Initially, springs were arranged on the bottom of the soil layer in a grid with 2 foot spacing. Uneven settlement patterns and convergence issues were eventually resolved via a finer spring grid with a higher number of spring elements. As the spring elements were linearly elastic, a spring stiffness constant, K , was required. The initial stiffness value for each spring was calculated by multiplying the anticipated modulus of subgrade reaction, K_s , for the soil by the tributary area acting on each spring.

To ensure that the loading and spring scenarios in each of the two models were accurate and would appropriately model the anticipated settlement once loading was applied, a calibration model was also originated. Set in a simpler configuration than the two models mentioned previously, the parts for the test model consisted of a 10-foot by 10-foot by 10-inch concrete slab resting on a thin of soil and a linear spring grid. As this model was to verify the effects of gravity and settlement, no additional support conditions were applied, and no abutments or sleeper slabs were added. Accounting for the volume of concrete and the load applied to the slab, hand-calculations were performed to and a theoretical settlement of one inch was calculated. The model analysis was run and correctly displaced one inch vertically in the negative Y direction, indicating that the slab had settled as expected. This verified that the material properties, load application, and spring linear springs were performing as intended with no unusual irregularities.

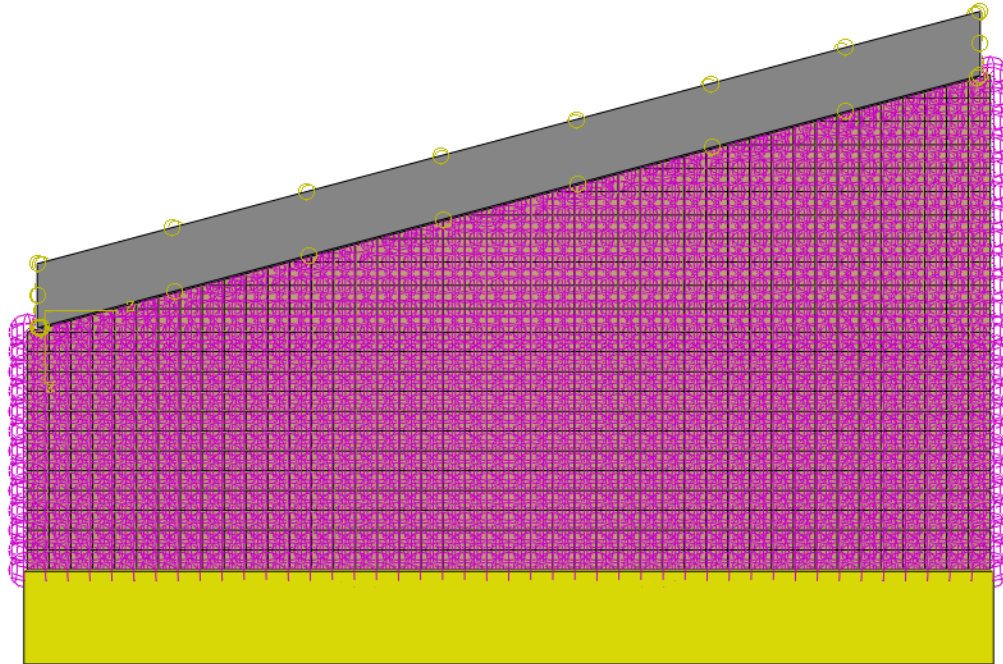


Figure 45: Story FE Model Spring Layout

4.1.5 Loading

Loading for the model consisted of the self-weight of the slab coupled with expected loading from truck traffic. Per the normal strength concrete used in these approach slabs, the material density for the slab concrete was set as 0.087 with the gravity set to -1; this produced an end weight of 150 pounds per cubic foot of self-weight. The weight of HL-93 design trucks was used to simulate field loading, and the number of trucks simulated on each approach slab was determined by the number of available lanes. As the purpose of this study was to determine the effects of gradual settlement of the slab, it was deemed reasonable to model the total load of each truck as two distributed tire loads running in the direction of traffic. One truck's worth of load was applied for each traffic lane present on the approach slab. In the case of the Jasper model, a maximum loading scenario consisted of two trucks crossing the bridge simultaneously. As the Story County bridge is expected to accommodate three traffic lanes in the future, it was modeled with the weight of three truck paths.

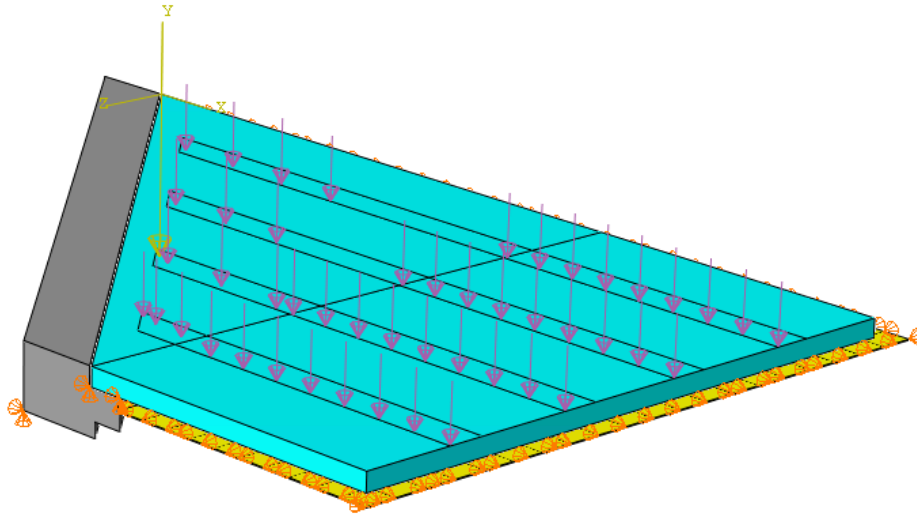


Figure 46: Jasper FE Model Loading

4.2 Jasper and Story County Model Analyses

The simulations performed on the Jasper and Story County Finite Element models are meant to investigate the structural impact of common approach slab issues related to the underlying soil. As observed in the field inspections and literature review, there are two main soil-related issues that result in approach slab cracking. The first type of failure is related to general settlement, which occurs when soil with a less-than-optimal stiffness is utilized, results in vertical displacement of the entire approach slab. Because the slab is supported on one end by the abutment seat and connection joint, excessive rotation of the entire slab system about the abutment connection occurs, creating a higher-than-anticipated tensile stress in the top of the approach slab. The second type of failure occurs when the soil erodes and a void forms underneath the approach slab, typically beginning adjacent to the abutment. In this case, the approach slab is required to span this void, as it is still supported on each end by the abutment and remaining soil. This second scenario introduces tensile stresses in the bottom of the approach slab. In each case, if the approach slab has not been designed to adequately resist these tensile forces, the slab is liable to crack and create an uneven riding surface.

The focus of the Jasper FE analysis was to investigate the impact of general settlement and rotation on an approach slab designed without a sleeper slab. Upon establishing the expected structural response of the original field structure, the model was modified to feature a standard dowel-tied connection joint. By comparing these two analyses, the differences in their structural response to a settlement scenario will be compared. In the case of the Story model, the inclusion of the sleeper slab would likely provide additional support against complete settlement of the slab. Based on the prevalence of voiding and erosion noted in Iowa approach slabs, the Story FE analysis focuses on determining whether the current approach slab is sufficiently rigid enough to span a standard settlement trench.

4.2.1 Jasper FE Model Analysis

The purpose of FE analysis of the Jasper model was to investigate the impact of tied connection dowels on the stress distribution within an approach slab as it settles over time. The Jasper models provided in previous research offer an ideal opportunity for investigating this effect, as two previously-existing versions of the same slab exist. The first version—the base model that replicates the current field bridge—features a “standard” approach slab design without a tied connection. This model will be used to investigate the initial stress distributions expected in the field bridge. After establishing these values, a similar set of conditions will be applied to the modified version of the approach slab to investigate how the addition of the connection dowels impact the stresses within the slab.

The base model for this study was adapted from the previous research conducted by Krapf in 2019. However, as noted earlier in the modeling techniques, it was modified to create a settlement condition as opposed to a thermal movement condition. This was accomplished by resting a thin layer of soil atop a grid of linear-elastic springs calibrated with the loading condition to approximate one half-inch of settlement. The Jasper County approach slab is 28' wide and 10" thick with a 45° skew and supports two traffic lanes. Therefore, loading consisted of two HL-93 truckloads placed as a total of four strip-loads of 36 kips each, approximating the load that would be applied by each wheel path. Meshing for the Jasper model proved to be incredibly difficult given the combination of a high skew angle and the geometric issues required to partition surfaces for the wheel loads. Attempts were made to refine the mesh to prevent issues due to meshing.

The initial Jasper model yielded expected results. Following approximately 0.47 inches of maximum settlement, the slab itself did not show any signs of concrete failure. Maximum stress values of 287 psi occurred at the obtuse corner of the approach slab roughly above the

edge of the paving notch. These high tensile stress values likely occur due to the rotation occurring on either side of this point, creating an area of high flexure in the top of the slab. High tensile stresses were also noted on the underside of the approach slab due to the abutment supporting on end of the slab while the other end displaces vertically, creating flexure in the bottom of the slab. The highest of these stresses was recorded as 230 psi.

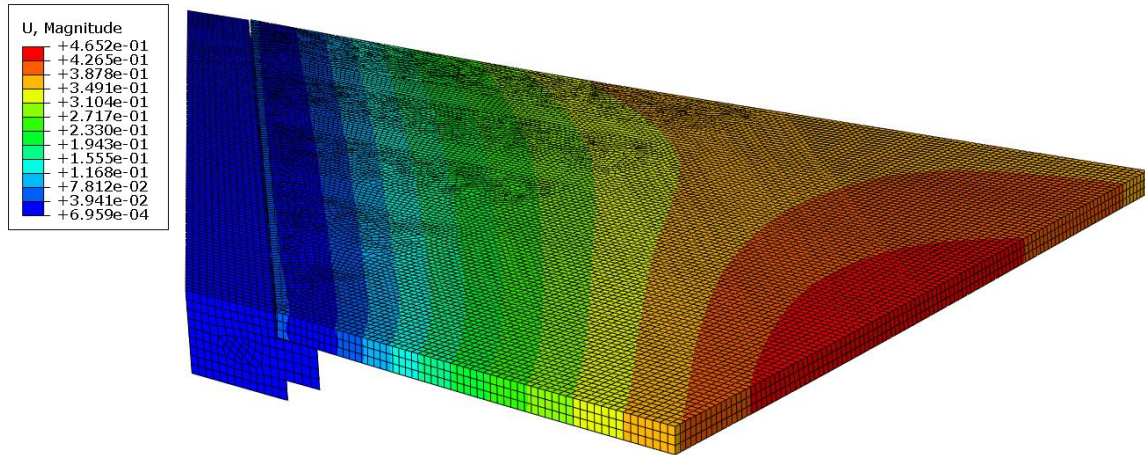


Figure 47: Jasper Base Displacement

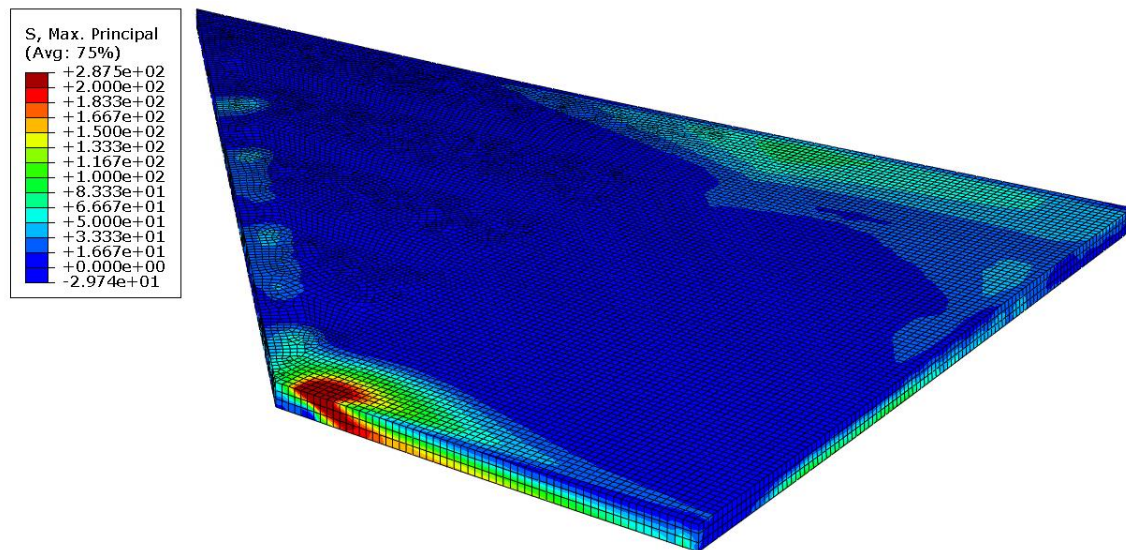


Figure 48: Jasper Base Model Stress Distribution (Top)

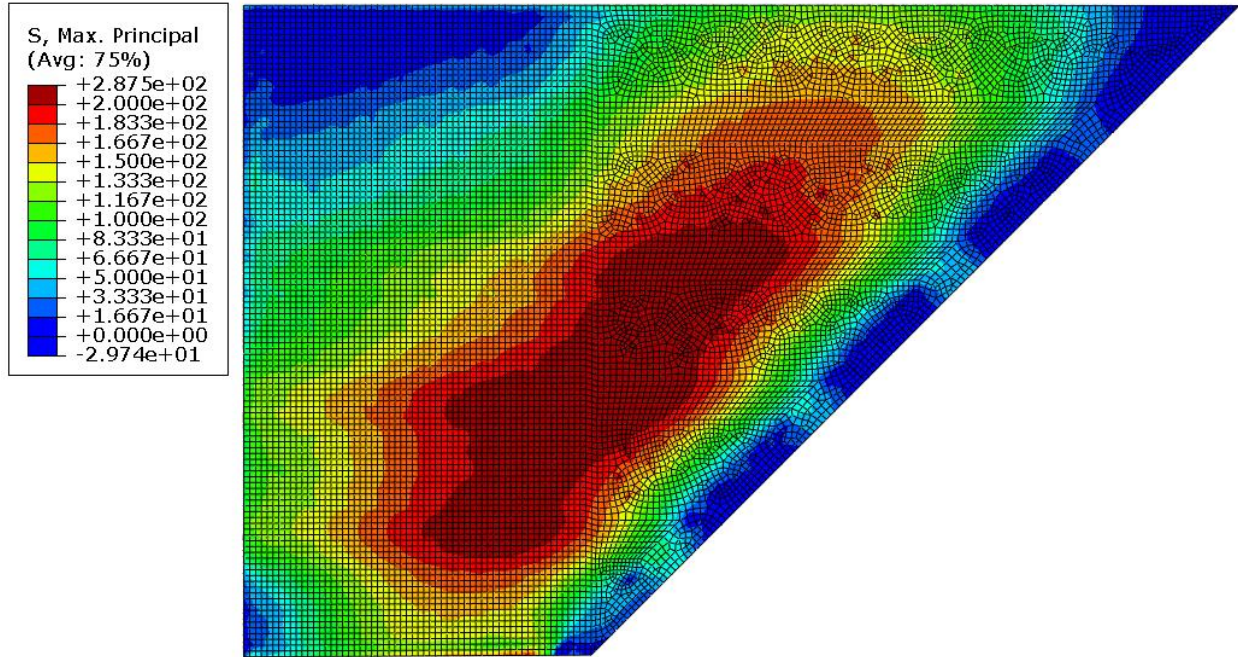


Figure 49: Jasper Base Model Stress Distribution (Bottom)

Following the tests run on the base model, the same loading scenario was run on the modified Jasper model, which features the addition of 23 #8 bars spaced 14.8 inches apart tying the approach slab to the abutment. Compared to the original model, significant issues arose with establishing convergence as the modified model attempted to run. Further investigation into this issue revealed that the concrete in the connection joint was experiencing material failure at a very low level of settlement. Tensile forces in the connection reached the limit to induce cracking and this led to premature model failure as the stiffness matrix was unable to establish stability. The peak stresses observed in the original model, the maximum stresses observed in the model occurred at the dowel connection points between the approach slab base and the abutment seat. These stress concentrations make sense given that the steel dowels are embedded in both the approach slab and the abutment; as the slab settles and begins to rotate about the abutment, the dowels are pulled from both ends and put in tension. This behavior also creates additional tension in the concrete in the top of the slab directly above the edge of the abutment seat. It is

likely that, as the general settlement of the approach slab increases, these areas of initial stress concentration will be the first to fail. It is important to note, however, that this approach slab was not originally designed to accommodate the forces created by this type of connection joint. The purpose of this investigation is to theoretically investigate how the stresses within the slab are impacted by the addition of a tied connection condition. As a result, continuing to run the model utilized damage parameters was unrealistic for the scope of this project. In order to allow the model to continue running past the point of theoretical concrete failure, the material properties for the concrete were adjusted to assume a linear-elastic model, ensuring that the stress concentrations would not lead to model instability prior to reaching the desired settlement. Due to the fact that the embedded tie bars in the FE model do not allow rotation of the approach slab at the connection joint, these forces result in high stress concentrations that may be unrealistic representations of what would occur in the field. As such, it is important to investigate other potential areas of failure.

Removing the damage parameters removed any convergence issues, and the model completed running without any additional errors. While this is a less-accurate view of determining how and when the model would fail, it does provide a general view of how the stresses in the model would develop past the point of initial failure in the connection joint. Similar to the original Jasper model, the area with the highest stress values occurs at the obtuse corner in the top of the slab. However, the stress value in this area at one half inch of settlement was now recorded as 440 psi, as opposed to the 287 psi noted in the original model. This indicates that the rotation restriction introduced by the connection dowels results in increased amounts of tensile stress along the top portion of the slab about the connection joint.

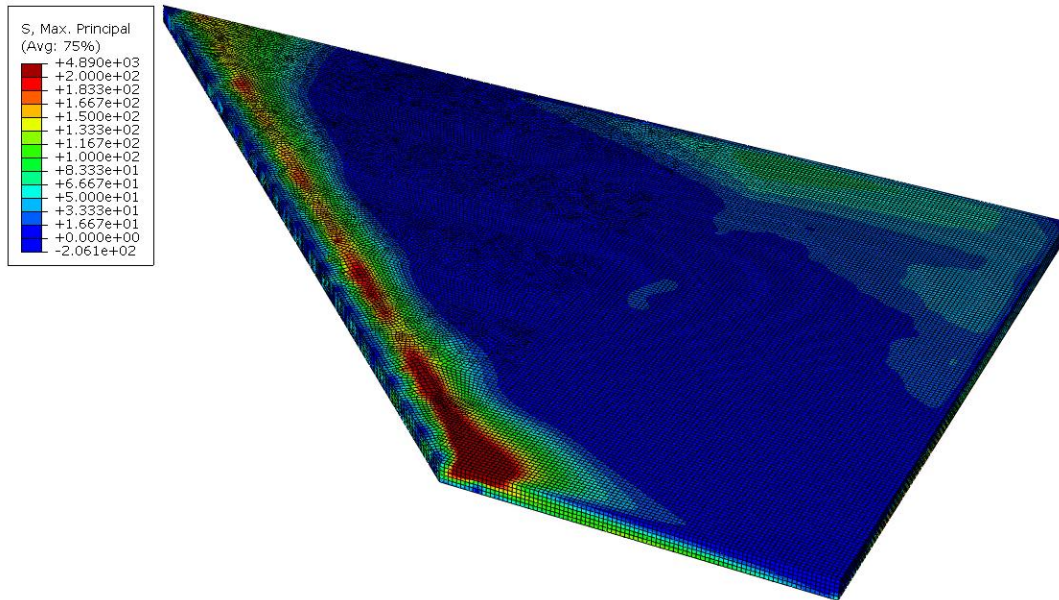


Figure 50: Linearly-Elastic Jasper Model Stress Distribution

These results indicate that a consequence of utilizing tied connection dowels to accommodate thermal movement results in additional stresses should the slab begin to settle over time. Due to the fact that settlement is not an uncommon occurrence in many of Iowa's approach slabs, it follows that approach slabs designed with tied approach slab connections should factor in the increased stress values that come with restricting the rotation of the approach slab about the abutment.

4.2.2 Story FE Model Analysis

The analyses performed on the Story approach slab models were performed to model the results observed from the WJE inspections from 2011 and 2018, which indicated that a fair amount of IDOT approach slabs suffered from erosion of the original subbase. However, this report also noted that majority of the approach slabs suffering from voiding were adequately performing with little structural damage. Following these conclusions, the FE models used in this study seek to investigate how the Story County approach slab would perform should it experience voiding and erosion in the future.

An initial model with no erosion or voiding was run to gain insight into how the approach slab would behave in a best-case scenario. Again, this version adapted the thermal movement models from previous research to account vertical displacement due to settlement. Initially, adequately stiff soil was used to create a base model with a minor amount of settlement. As expected, the slab was supported on each end by the abutment seat and sleeper slab, resulting in a max displacement 0.0673 inches roughly near the middle of the slab. Based on this flexural behavior, it follows that the tensile stresses in the bottom of the slab were much higher than those in the top—161 psi compared to 27 psi, respectively. The highest stress values were observed in the concrete surrounding the embedded connection dowels with a peak value of 270 psi. This is likely a result of the dowel being pulled away from the abutment as the approach slab attempts to rotate at the abutment seat due to settlement. It is important to note that the boundary conditions of this model operate under the assumption that the sleeper slab undergoes no settlement. This is to ensure that the model focus is on whether the approach slab has been designed to adequately span the distance between the abutment and sleeper slab should a full loss of soil support occur.

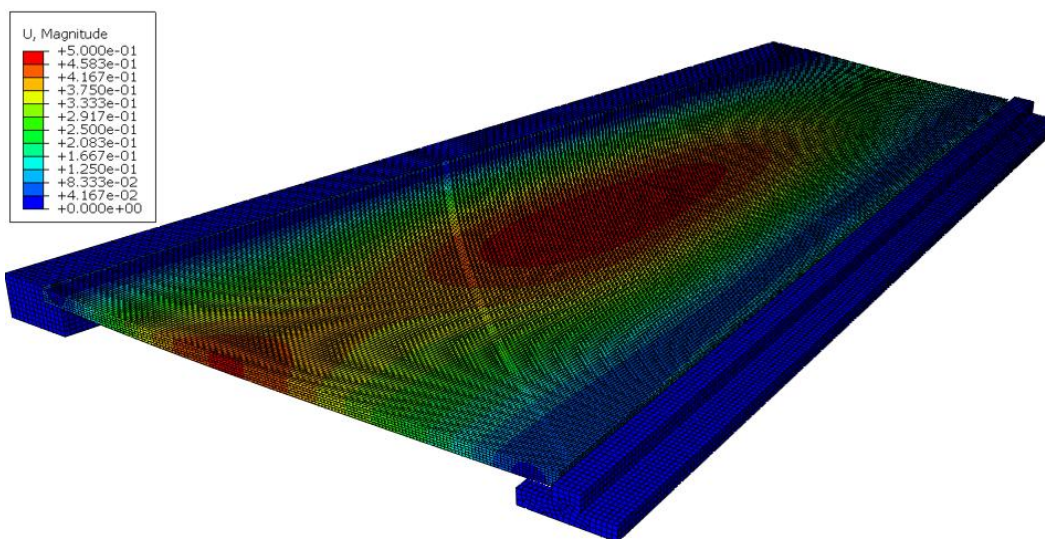


Figure 51: Initial Vertical Settlement for Story County Approach Slab

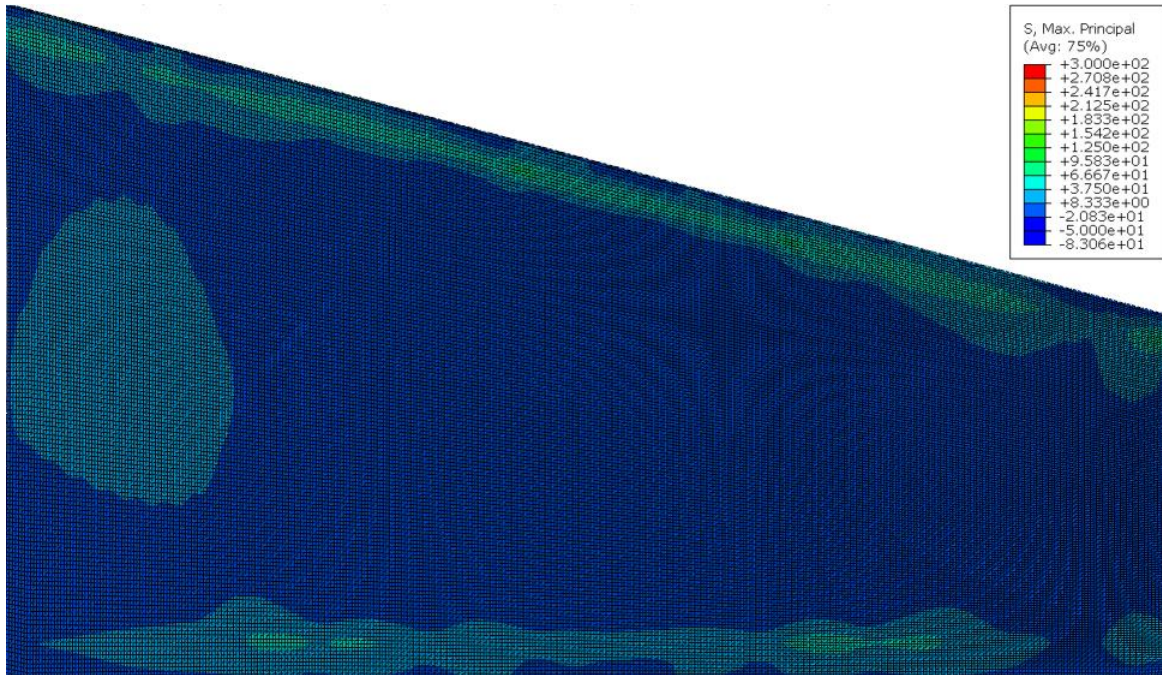


Figure 52: Initial Stress Values for Story Model (Top)

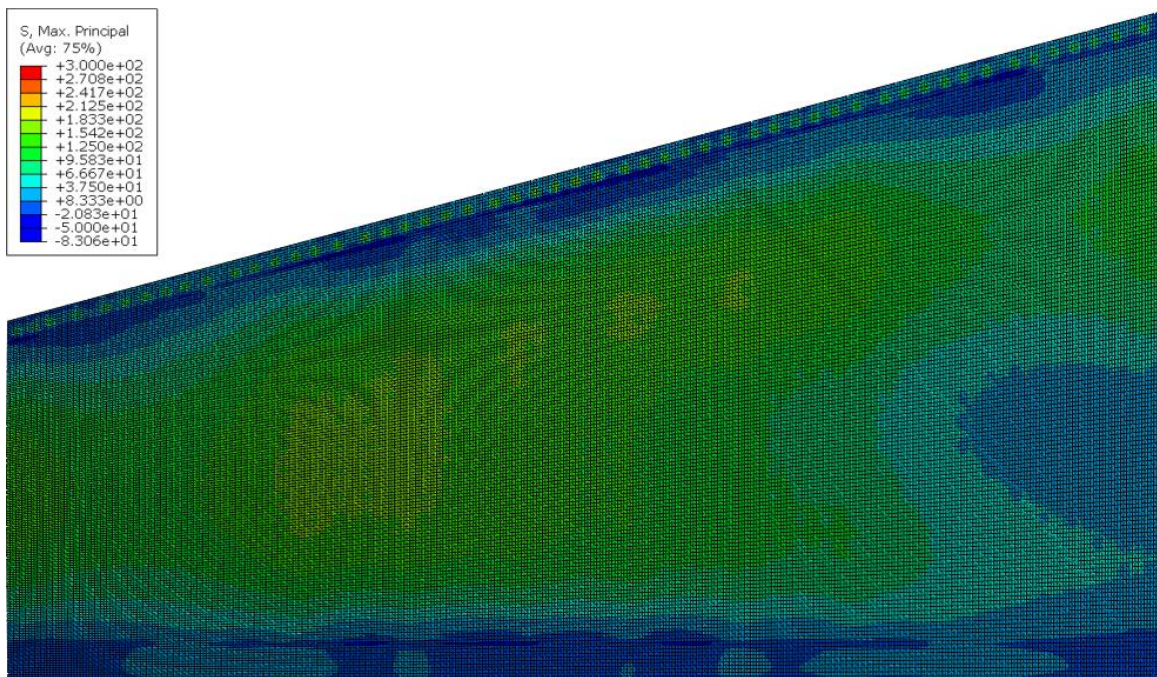


Figure 53: Initial Stress Values for Story Model (Bottom)

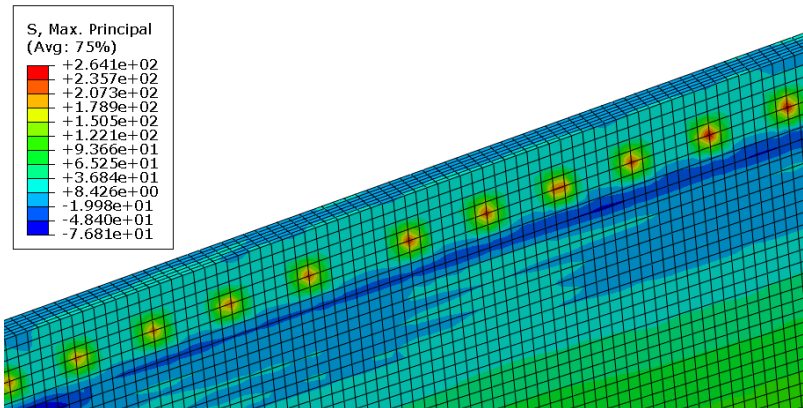


Figure 54: Stress Concentrations at Dowel Connection

Following a similar approach to those performed by Nassif (2002) and Oliva (2011) on similar projects, voids due to erosion were modeled by removing the soil springs directly adjacent to the abutment in varying lengths. The lengths and patterns of voiding scenarios were modeled based on those observed in the two WJE research reports (2011, 2018), which indicated that voiding generally follows the same skew angle as the abutment. An example of the spring layout for an 8-foot simulated void is given in Figure 53. Test models were run for voids of 5, 8, 10, 13, and 16-feet to determine the point where the structural rigidity of the approach slab would be compromised begin to excessively deflect and show signs of cracking.

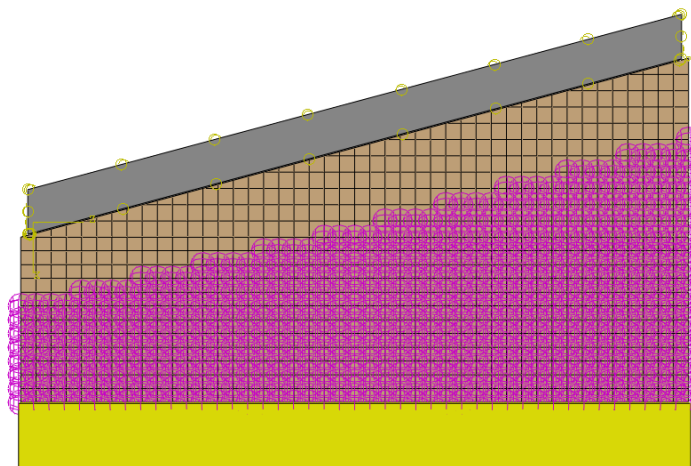


Figure 55: Story County 8-Foot Void Scenario

The models exhibited expected behaviors. An increased void length resulted in higher peak deflections, stress concentrations at the tied connections, and tensile stresses in the bottom of the slab. Stresses did not begin to drastically increase until voiding reached roughly six feet in length from the abutment. At this point, displacement began to increase more rapidly, indicating that the stiffness of the slab was being impacted by the loss of soil support underneath the slab. As the maximum displacement of the slab increases, the areas of extreme flexure within the slab begin to experience much higher levels of tensile stress. Additionally, this settlement introduced rotation at the connection joint, increasing the tensile forces transferred through the steel dowels. In this case, due to the embedded nature of the tied connection bars in the joint, rotation is restricted, creating areas of high stress concentration. These forces are similar to those noted in the Jasper model, although manifest with a much lower magnitude as the voiding condition creates less rotation compared to a uniform settlement condition. Areas of notable stress increase were in the concrete at the dowel connections and in the bottom of the slab at the midpoint of the void.

Maximum stresses and peak displacement remained similar between the first two models, indicating that there is little increase in stresses in the slab for shorter voiding lengths. However, a clear increase in stresses in the connection joint begins to occur between the 5-foot and 8-foot models, and peak stresses in the connection joint increased from 285 psi to 331 psi. However, the maximum vertical slab displacement in this range remains fairly similar to the base model, indicating that the slab is remaining structurally stiff and adequately spanning the erosion void.

The first major stress increase occurs between the 8-foot and 10-foot models. The tensile stress in the connection joint increased drastically from 331 psi to 447 psi, and it is at this point that the slab begins to become at risk for early signs of concrete failure in the connection joint, as

the tensile cracking stress for 4 ksi concrete is roughly 474 psi. It is in this range that the concrete at the connection joint begins to fail, beginning to crack around 474 psi at a deflection of 0.13 inches. The peak stress observed in the connection joint was recorded at 461 psi prior to the failure of the concrete in the joint for both the 13-foot and 16-foot models, and it appears that the concrete in the connection joint may be susceptible cracking at a void length of around 11 feet. Once the concrete in the connection joint begins to fail, it is anticipated that the displacement of the slab will become more drastic as the dowels will no longer be able to transfer force through the broken concrete in the slab. Once this occurs, the slab will begin to sink into the erosion void below, creating a “bump” between the approach slab and the abutment.

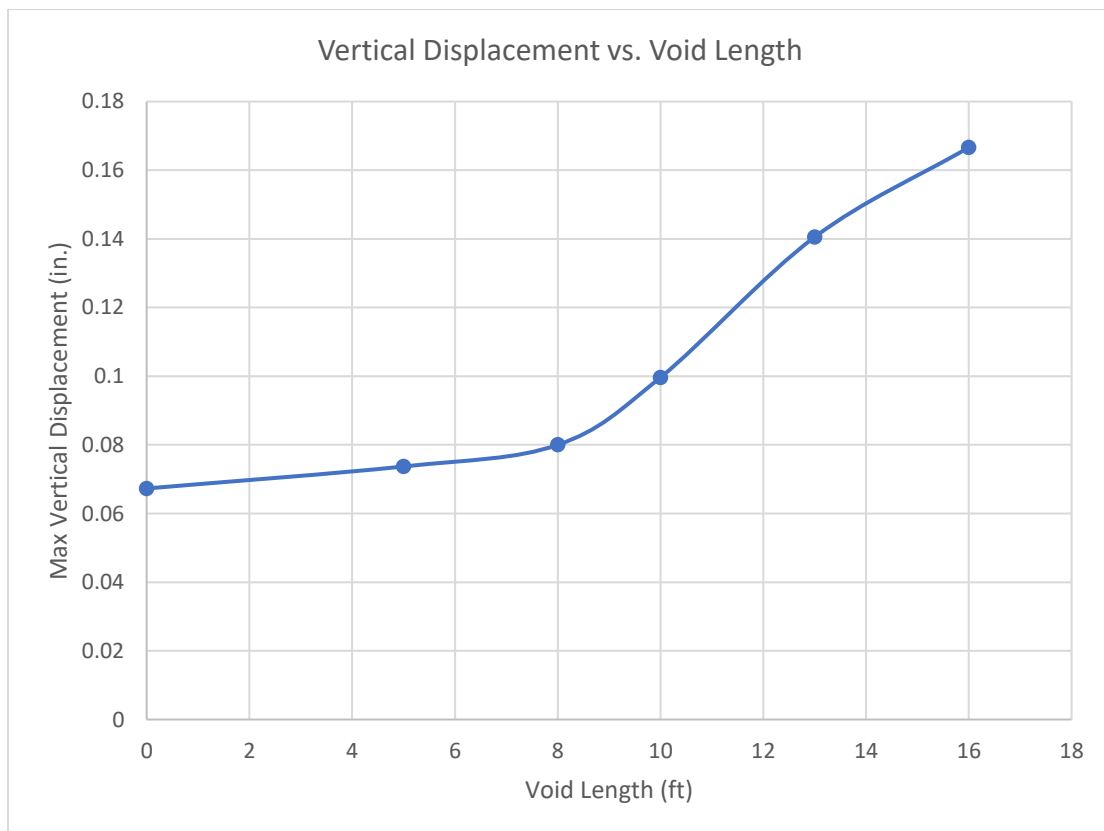


Figure 56: Max Vertical Displacement vs. Void Length

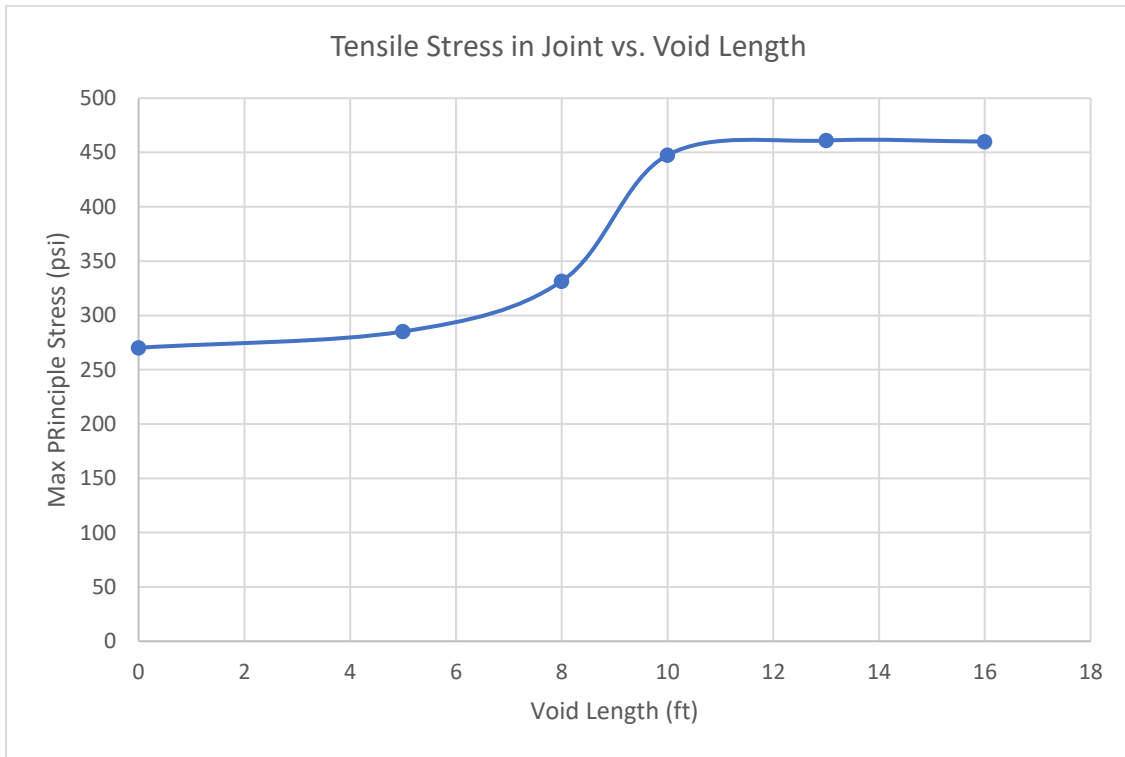


Figure 57: Concrete Tensile Stress in Joint vs. Void Length

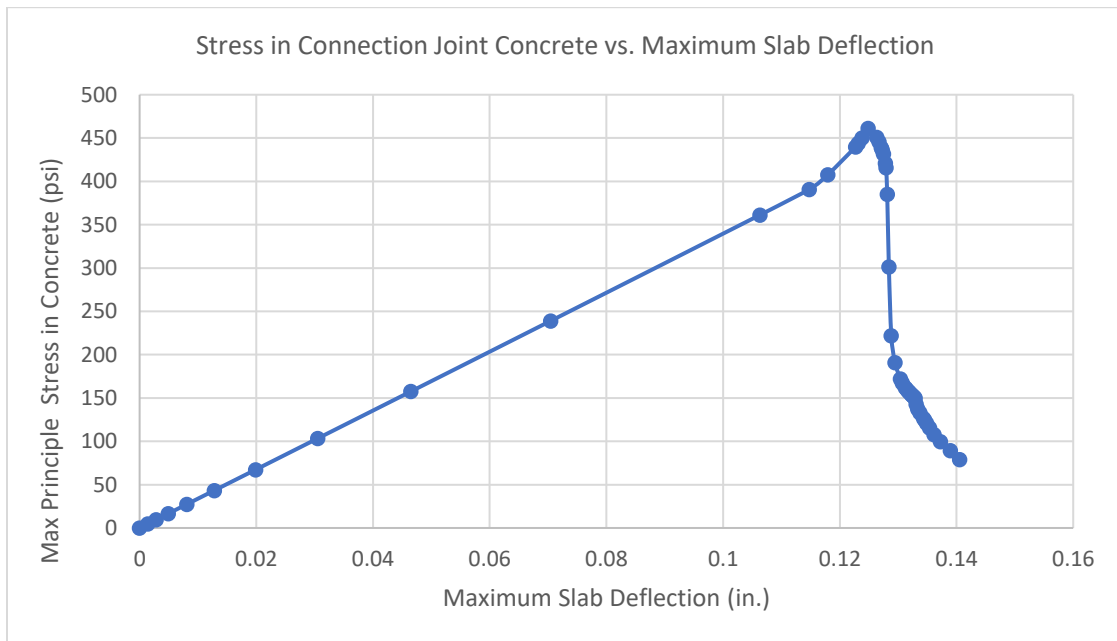


Figure 58: Tensile Stresses in Connection Joint (13-foot void)

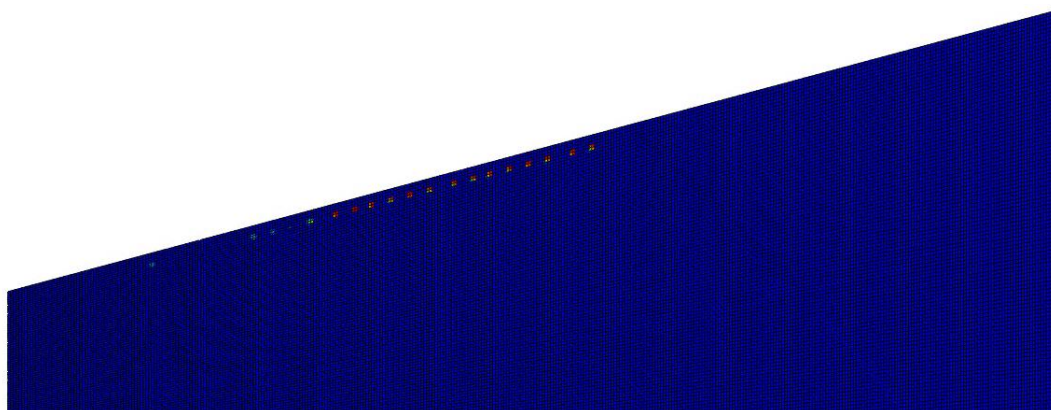


Figure 59: Locations of Damage-Based Failure in 16-Foot Void Model

It is important to note that the modeling techniques utilized for this model designate the dowels as embedded beam elements which cannot physically pull out of the surrounding concrete, which likely creates high areas of stress concentration in the connection joint. Although the FE models indicate cracking and concrete damage in these areas of stress concentration, this is necessarily indicative of failure in the actual field bridge. Thus, it is important to pay attention to the transverse forces present in that slab, as this is the area where approach slabs appear to crack most easily based on the field investigations presented in the literature review.

Between the base model and the model with the 5-foot void, tensile stresses in the area with the most vertical settlement remained around 157 psi. As with the stress increases observed in the connection joint, the tensile stresses mid-void begins to increase between the 5-foot and 8-foot void models, reaching a maximum value of 220 psi. This value increases again for the 10-foot model, reaching a maximum stress of 309 psi. For the 13-foot and 16-foot models, stresses continue to increase at the middle of the erosion void, reaching 394 psi and 424 psi, respectively.

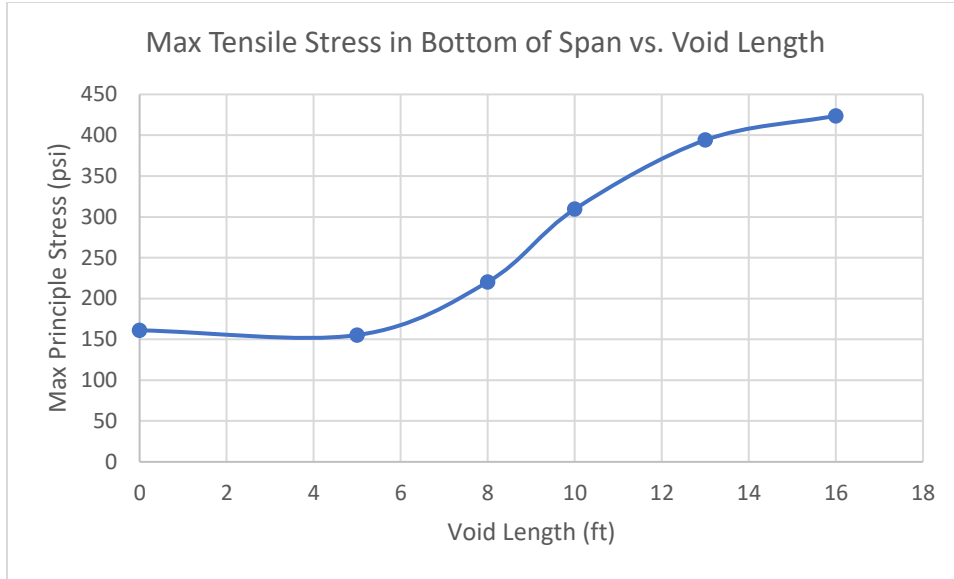


Figure 60: Max Tensile Stress in Bottom of Span vs. Void Length

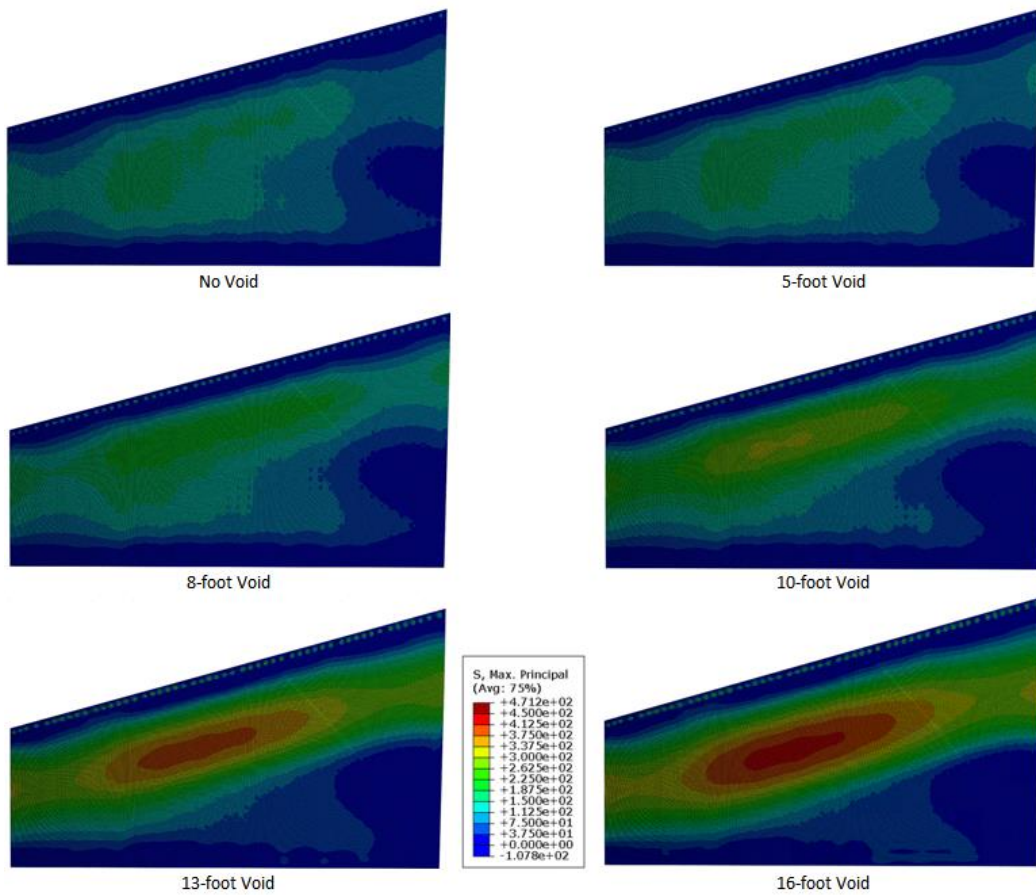


Figure 61: Maximum Principle Stress in Each Model

Due to the damage parameters used for these models, the 16-foot model failed to converge following the failure of the concrete in the connection joint. Thus, the model was not able to run sufficiently to determine at what point the concrete in the middle of the slab would begin to crack. Given the peak stress of 424 psi observed at mid-void in the 16-foot model, relatively close to the number at which the concrete in the connection joint failed, it is possible that the slab may be subject to transverse cracking should the voiding extend beyond the 16-foot length included in this study. However, it is worth noting that such an extreme example of voiding is rare and unlikely, as majority of the slabs investigated previously had voids of less than ten feet in length. Given the behavior of these models and the likelihood of such extreme voiding cases, it is anticipated that the Story County bridge approach slabs are adequately designed to span standard voiding conditions should they occur during service.

4.2 Washington County Finite Model

4.2.1 Purpose and Background

An important aspect to determining future design detail changes is the review and monitoring of previously-built structures. During the routine inspections performed each year on Iowa's bridges, it was noted that a specific bridge in Washington County, Iowa, was experiencing a particularly poor aging of each of its approach slabs. As this bridge, which consists of precast approach slabs tied to an integral abutment, fits the scope outlined for this project, it was identified as a useful subject for further inspection. As shown in the figure below, the approach slabs for this bridge experienced severe spalling directly above the tied connection dowels between the abutment and the approach slab.

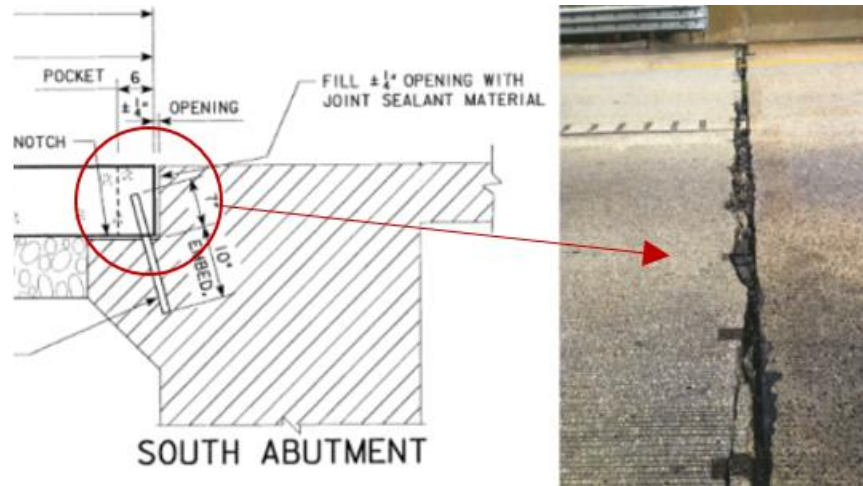


Figure 62: South Approach Slab Spalling Location

The information observed in the literature review indicates that this type of concrete failure at the connection point is possible due to excess settlement. As the slab settles, it begins to rotate around the corner of the abutment seat. It is theorized that this behavior creates tensile stresses within the embedded connection dowels as the dowels attempt to hold the two pieces of concrete together. In turn, this could possibly create areas of high tensile stress concentration, which may result in concrete failure and pull-out of the connection dowels from the concrete. It was determined that a finite element investigation into the impact of settlement on this failure area may provide insight into why this failure occurred.

4.2.2 Design Details

Bridge 606890, the subject of this study, is a pre-tensioned pre-stressed concrete beam bridge with a total span length of 180-foot-six-inches and a width of forty feet. The bridge was originally built in 1997 with integral abutments following IDOT Design 296. In 2012, the current tied approach slabs were installed following IDOT design 210. The approach slab itself features six precast slabs connected to one another via dowels, and the slab adjacent to the abutment is connected to the integral abutment via angled dowels. There is no sleeper slab present in this design, and the slab is intended to slide across the underlying subbase as the bridge expands and

contracts throughout the year. It is important to note that the design details utilized for this approach slab are not completely indicative of the standard design details used in most IDOT approach slabs. Compared to those used in the Story and Jasper models, these approach slabs use fewer connection dowels, a stronger (5 ksi) precast concrete, and the subbase consists of a 2 inch sand cushion, which may be subject to higher levels of settlement when compared to the standard modified subbase used for most approach slabs.

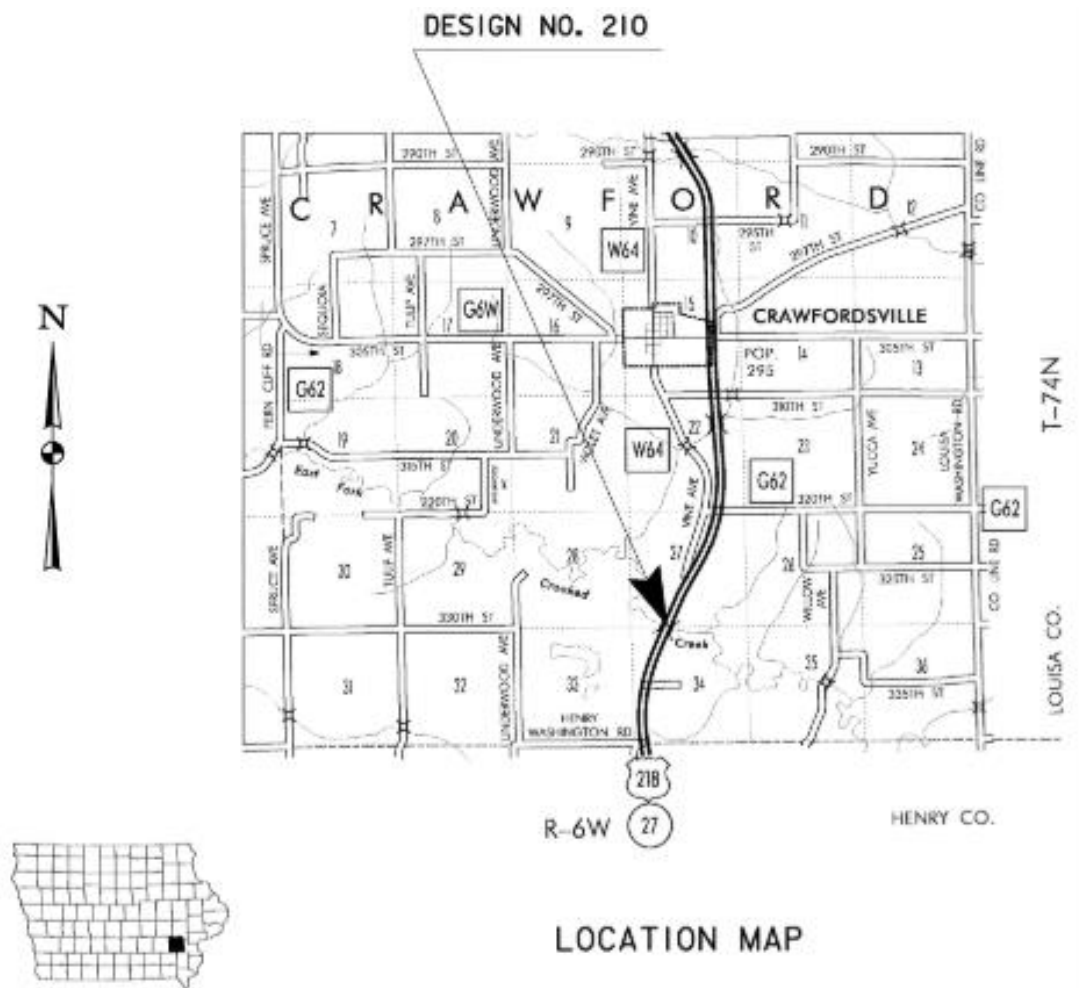


Figure 63: Bridge 606890 Location Map

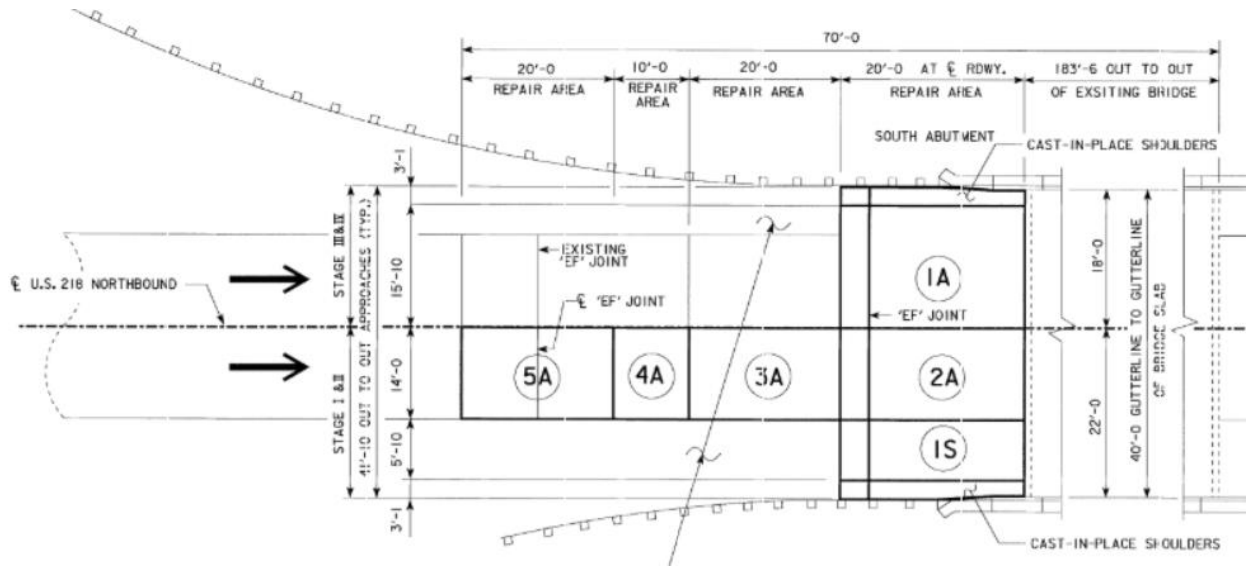


Figure 64: General Layout of Precast Panels

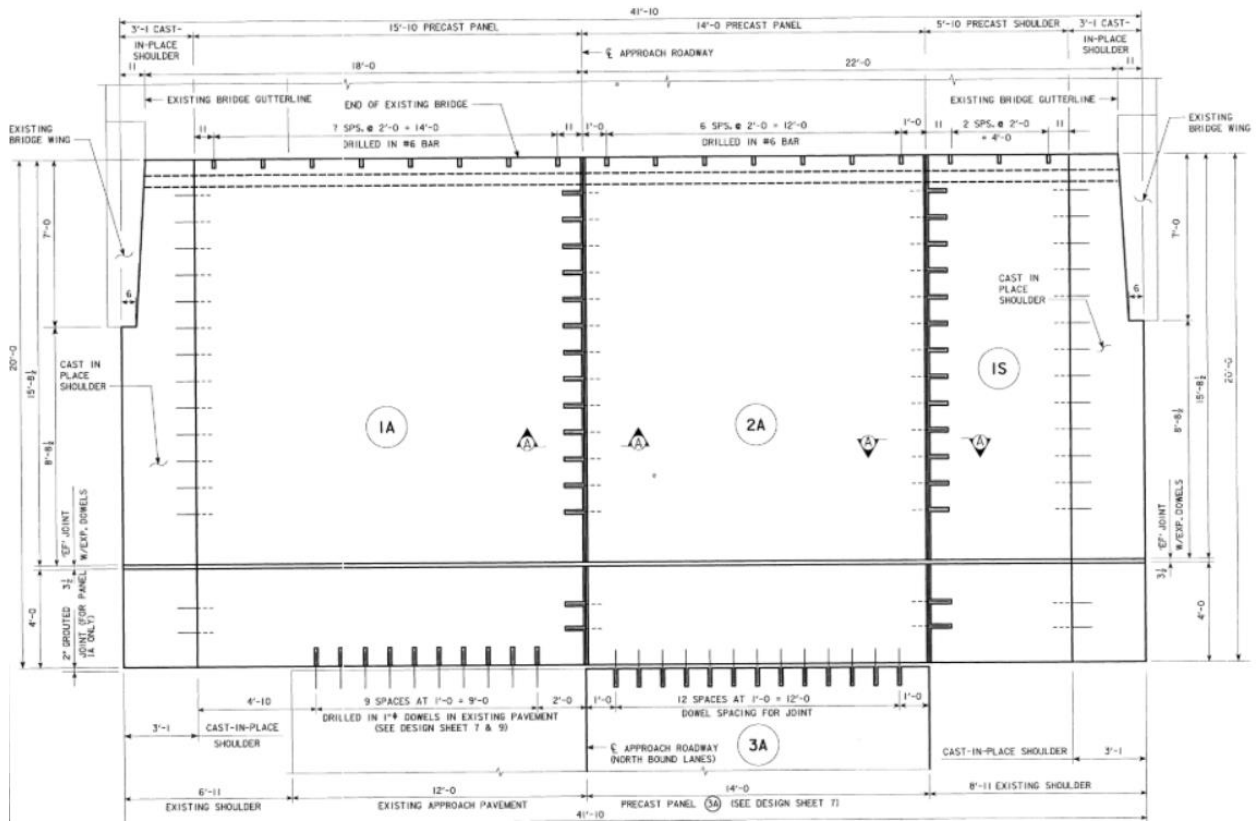


Figure 65: Layout of Precast Panels at Abutment

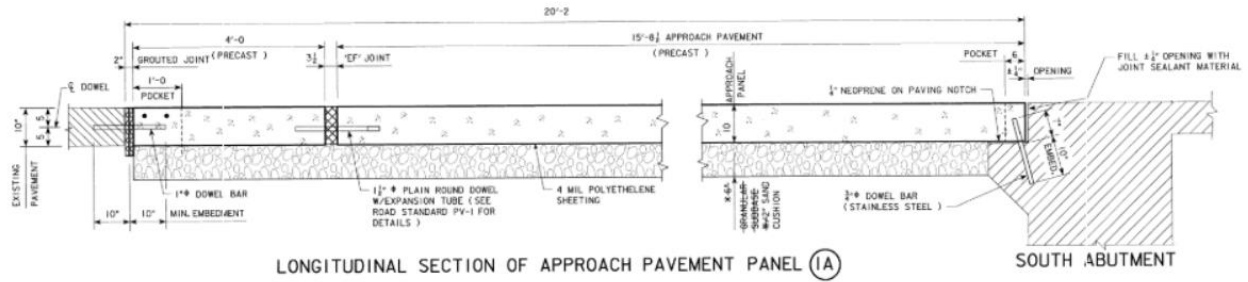


Figure 66: Longitudinal Section of Approach and Abutment

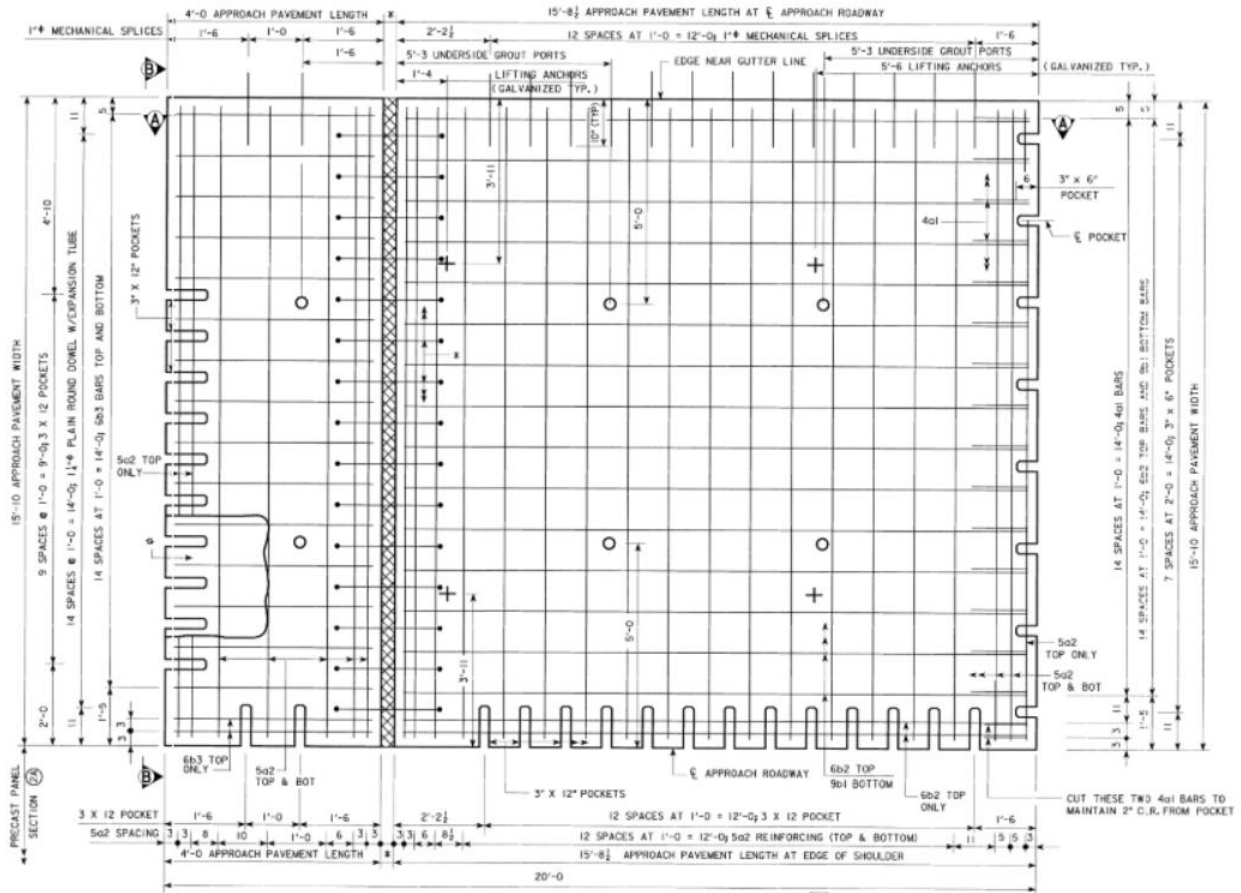


Figure 67: Rebar Layout for Panel 1A

The tied dowels consist of eighteen 3/4" stainless steel bars embedded at an angle into both the approach slab and the abutment paving notch, and the approach slab itself rests upon a two-inch sand cushion. The tied dowels are specified as having a seven-inch embedment into the approach slab and a ten-inch embedment into the abutment. The exact angle of the dowel itself

was not given in either this plan set or the IDOT design standard and was assumed based on the angle used in the Story County bridge. The required cover for the tied dowels is also not specified; it is assumed as 2 inches per the standard cover specified in the general notes of the plan set. The abutment consists of 3.5 ksi concrete, and the precast approach slab panels consist of 5 ksi concrete. All reinforcing steel for the bridge, abutment, and approach slab is indicated as 60 ksi steel. Connecting each of the precast panels is a set of 'EF' joints with 1-½" plain round dowels with an expansion tube.

4.2.3 Iowa DOT Field Investigation History

As noted earlier, new precast approach slab panels were tied into the integral abutment in 2012. Per Iowa DOT standards, bi-yearly inspections were performed and uploaded to the Iowa Department of Transportation's Structure Inventory and Inspection Management Systems (SIIMS) to monitor the bridge's performance. For this study, special attention was paid to the development of the approach slabs where the spalling in question has occurred.

The first record of the approach slab came in March of 2014, which states that the tied connection between the approach and abutment was "open" and "unsealed" in addition to the "spalling adjacent to deck" on the near (southern) approach pavement. It is stated that this near approach has been "mudpumped," likely to combat settling. It is also mentioned that the far (northern) abutment was also in poor condition, settling roughly 1" below the deck. It is clear from this initial inspection that both the near and far approach slabs were performing suboptimally, failing within their first two years of service.

The next round of inspections came in 2016 and saw the performance of the approach slabs continuing to decline. It is mentioned that both abutment openings were in poor condition and 100% open. While the near abutment remained unsealed, the far abutment had been filled with asphalt to combat the entrance of debris and water into the tied connection. In addition, the

far abutment had seal coal patches installed adjacent to the bridge. It is mentioned that the precast concrete in the near approach slab had “spalled all the way across adjacent to the deck joint.”

Two additional inspection reports were prepared in 2017 and 2018. These reports mention the same issues present in the 2016 edition but add that the near approach slab was filled with asphalt concrete in 2017.

Based on the above reports gathered from 2014-2018, both tied approach slabs began to fail within the first two years of service. Several attempts were made to mitigate these issues, namely the introduction of mudpumping to combat settlement and the inclusion of asphalt concrete to seal the joint openings left by the spalled concrete. While there are likely multiple reasons for these failures, the clear evidence of settlement and the concrete failure at the dowel connection identified excess settlement as a possible cause. It has been noted that majority of settlement in approach slabs occurs within the first year of service (White, 2007).

4.2.4 Finite Modeling Procedure

Following the correlations and precedents set by Iowa State University’s previous studies comparing field data to approach slab finite element models, a base finite element model for the tied approach slabs in bridge 606890 was originated as a part of this study. By following a similar set of finite element procedures and design considerations used in previous models, it is reasonable to assume that, should this model exhibit similar behavior and stress distributions to the previous studies, the values given in the output should be an accurate representation of this approach slab. The goal of this study is to simulate and investigate the effect of the approach slab’s settlement on the performance of the approach slab. Specifically, a key area of focus is at the joint connecting the approach slab to the abutment where clear signs of concrete failure occurred. To reduce analysis time, these models were limited to the approach slab, the subgrade

underneath, the tied dowels, the slab's reinforcing steel, and the upper section of the abutment. Keeping with previous studies performed by ISU, these models and their subsequent analyses were run in ABAQUS/CAE.

Instead of modeling the entire bridge, an effort that would drastically increase the runtime of the analysis, the base model for this approach slab consists of the approach slab, the uppermost part of the abutment, the longitudinal and transverse slab reinforcement, the sand cushion beneath the slab, and the tied dowels connecting the abutment and the approach slab. The sand cushion is modeled via a thin shear layer and a series of linear springs, as with the Jasper and Story models. The purpose of this model is to represent the approach slab, abutment, and connection as they were installed and currently operate in the field, and all approach slab elements were drawn with respect to the approach's plan set; the abutment dimensions were obtained from the bridge's original plan set.

To simplify the geometry of this model, approach slab segments 1A, 2A, 1S, and the two shoulder slabs were drawn as one uniform mass. Since the segments should function as a continuous slab following installation, this should give an accurate representation of the approach slab's geometry. In addition, the shape of the complete slab was approximated with all sides at right angles to allow for better meshing. Because the main concerns of this model are the concrete and tied dowels near the slab-abutment connection, the precast segments on the other side of the EF joint were ignored as majority of the critical stress in the model should be a result of the applied movement from the bridge deck. The final shape of the approach slab is 41'-10" wide and 15'-8½" long at the EF joint with a depth of 10 inches throughout the slab.

As noted above, the abutment geometry was drawn based on the original plan set from 1997. In an effort to simplify the model, the abutment geometry focused on the integral section

and the approach slab seat; the abutment was cut below these areas of study and replaced with a boundary condition to simulate the support its embedment in the soil would provide.

To fully represent the impact of the reinforcing steel, all reinforcement was drawn with wire-truss elements to allow for a more useful model of stress distribution throughout the slab. In addition, each of the 18 connection dowels have been modeled as a wire-beam element to allow the full transmission of forces between the integral abutment and the approach slab.

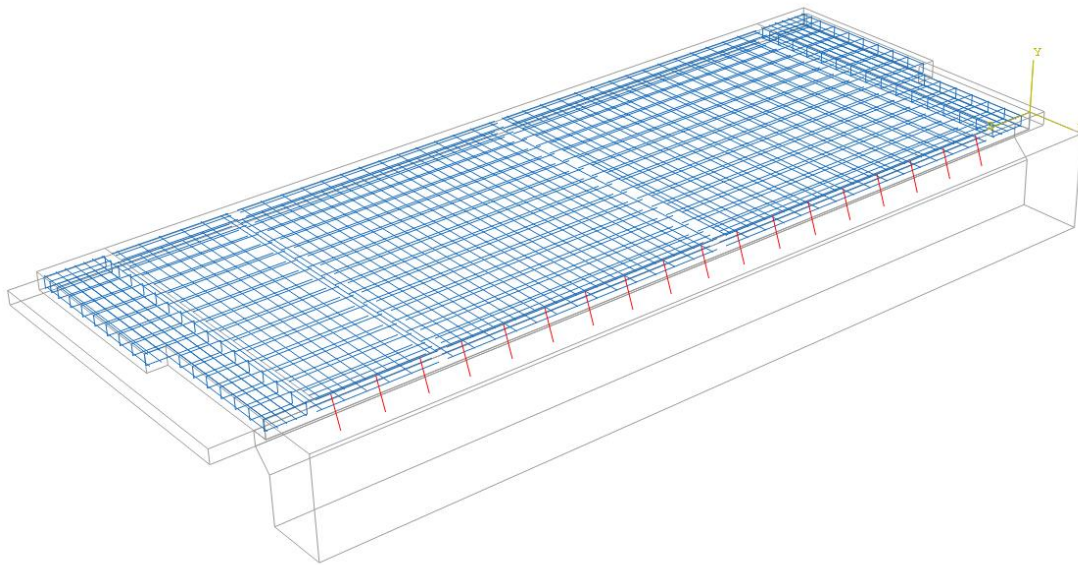


Figure 68: Washington Rebar and Connection Dowels

Per the 2012 approach slab plan set, the compressive strength for this concrete was set as 5000 psi and modeled with In addition, a Young's Modulus of 3605 ksi Poisson's ratio of 0.3 were used for linear elastic behavior and a density of 150 pcf was used for the slab concrete. Per the original plan set from 1997, concrete with a compressive strength of 3500 psi was used for the modeled abutment. Material properties for the sand were determined based on standard values used by the Iowa DOT and numbers found in other literature.

To further cut down on analysis runtime, each model part was meshed separately. In addition, this allowed for the areas of particular interest (the approach slab and the dowels) to be meshed finer than the rest of the model, creating a more accurate representation of the internal stresses and strains within these critical parts. The connection dowels and concrete slab were meshed on a 1-inch grid, the abutment on a 4-inch grid, and the sand layer on a 2-inch grid.

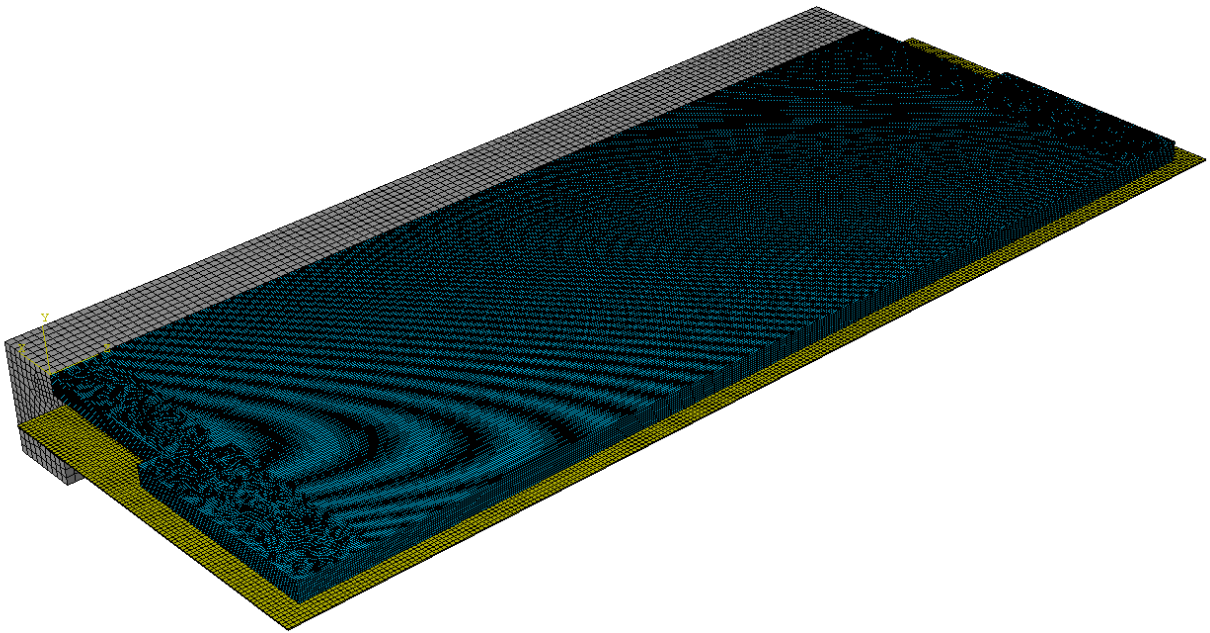


Figure 69: 606890 Model Meshing

Loading for this model consisted of gravity and the combination of the maximum amount of HL-93 load trucks that the approach slab would experience in the field. In this case, the maximum loading scenario for this approach slab would consist of two HL-93 trucks driving across the approach slab simultaneously. Each truck was modeled as two distributed strip loads of 36 kips each, totaling 72 kips for each truck. By evenly distributing these loads across the entire length of the slab, the analysis results will be more representative of a slab settling slowly

over time. Utilizing the same approach for the Jasper and Story models, a bed of linear springs was used to model the settlement of the slab as the loading condition was applied.

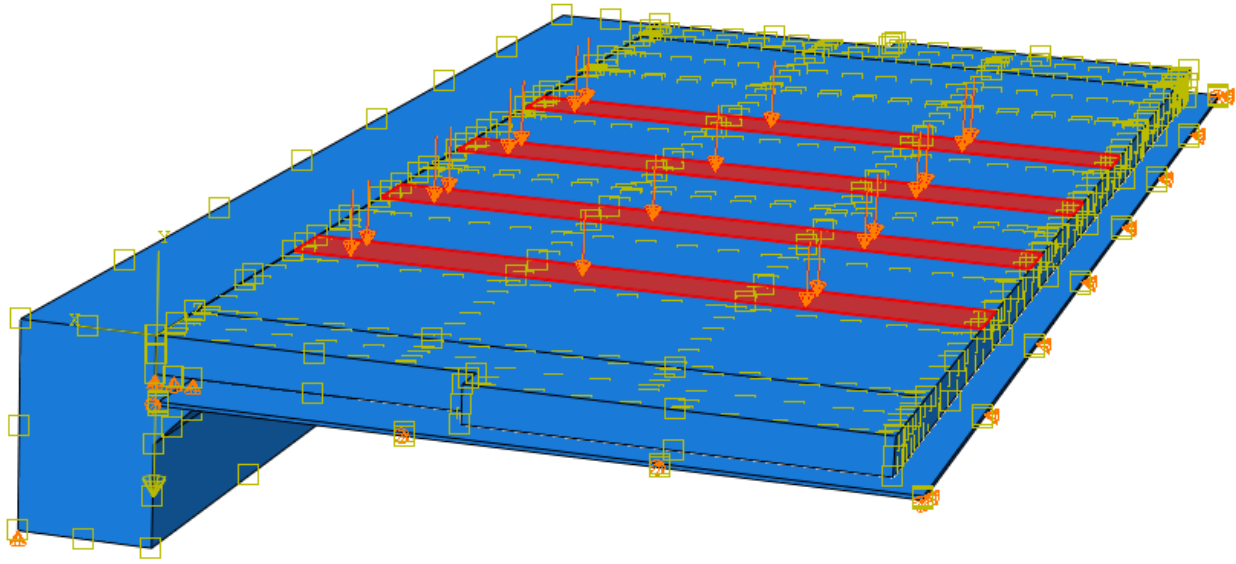


Figure 70: Washington County Loading Scenario

4.2.5 Finite Element Study and Results

As with the previous analyses, an initial baseline model was run to determine how the model would behave assuming appropriate soil stiffness and minimal settlement. Following the stiffness values used for the previous model, a modulus of subgrade reaction of 250 lb/ft^3 was used to calibrate the linear springs underneath the slab. This baseline model was also run utilizing ABAQUS's concrete damaged plasticity behavior to document any failures within the concrete.

As expected, this model displayed a similar behavior to the Jasper model. Because there is no sleeper slab to support the far end of the approach slab, forces within the connection joint start to increase as soon as the slab begins to settle. Although the complete vertical displacement

for this model only resulted in 0.014 inches at the far end of the slab, maximum concrete tensile stresses within the connection joint were recorded as 181 psi. Due to the fact that the concrete used in this approach slab is 5 ksi compared to the lower 4 ksi in the previous two models, it was expected that the Washington model will reach a higher tensile value prior to cracking or damage. Peak stresses of note elsewhere in the model occurred in the concrete along the top surface of the slab, likely as a result of the connection dowels attempting to restrict rotation of the slab at the abutment seat. However, the highest stress value reached was only 43 psi.

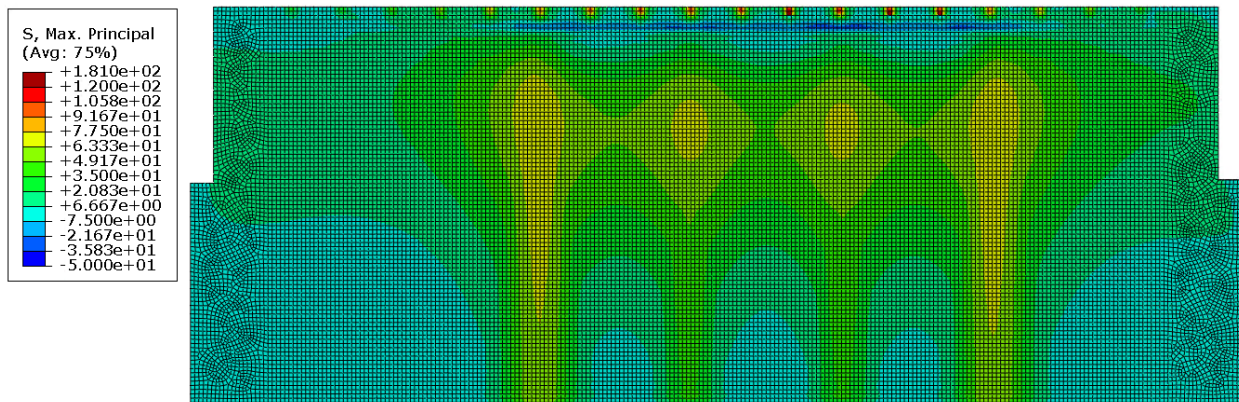


Figure 71: Stress Concentrations on Bottom of Slab

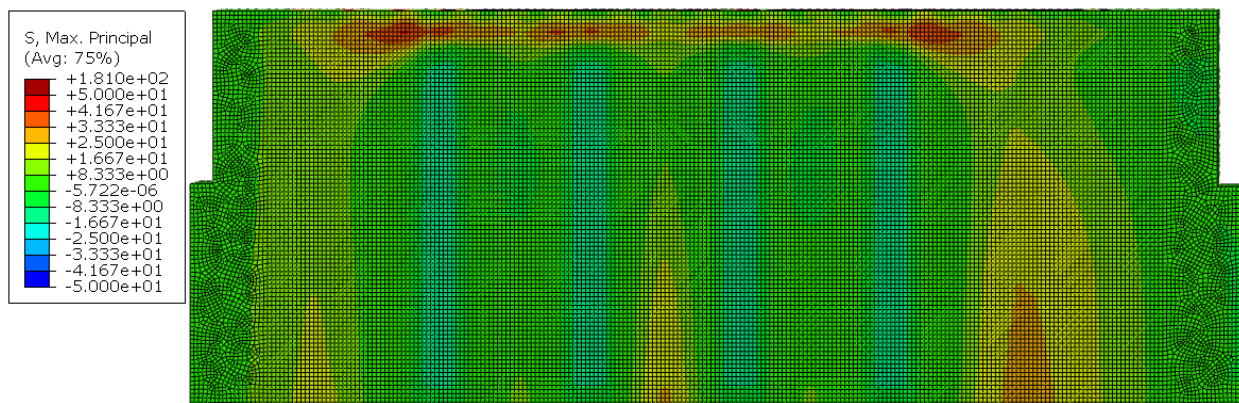


Figure 72: Areas of Tensile Stress on Top Surface of Approach Slab

Following the establishment of this base model, the stiffness value of the linear springs was reduced to simulate soil settlement in the model. However, as with the Jasper model, the stress concentrations at the connection dowels led to failure at a mere 0.052 inches of settlement with a peak tensile stress of 524 psi. These results imply that significant forces are created in the connection joint should any settlement of the slab occur. This comes as a stark contrast to the voiding scenario observed with the Story model, which is assumed to be supported on the far end by the sleeper slab. The stress concentrations and damage output provide by this FE model may provide some insight into the failure observed in the Washington County field approach slabs.

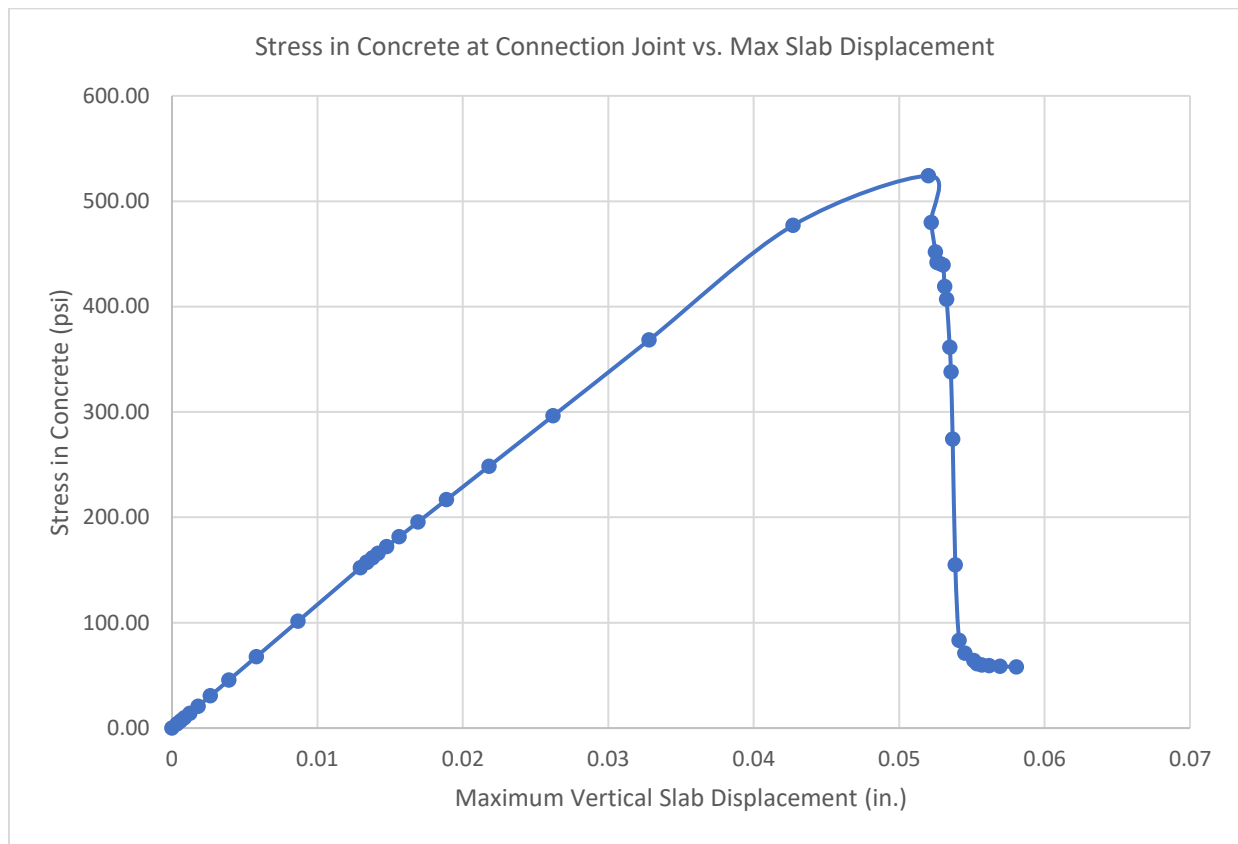


Figure 73: Concrete Failure in Washington Connection Joint

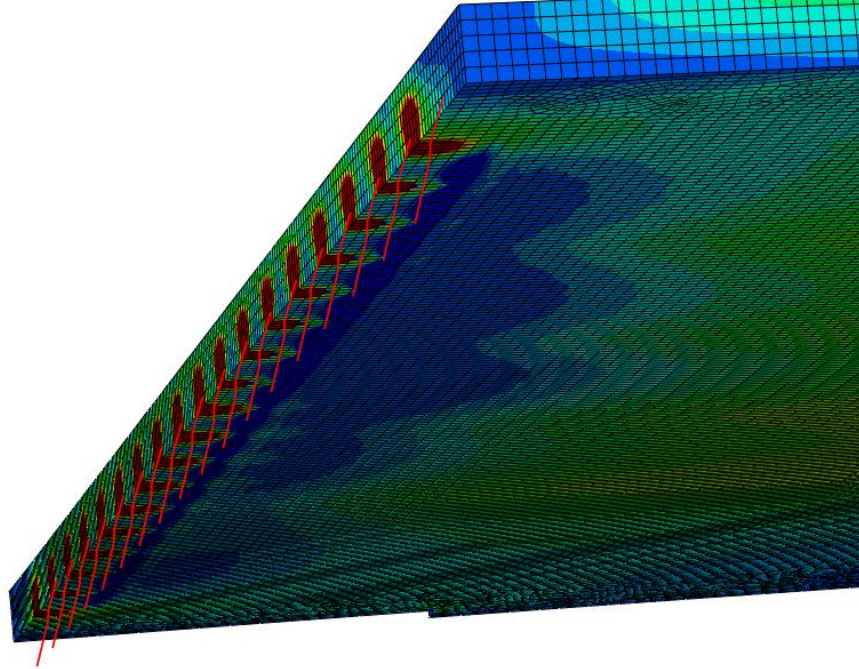


Figure 74: Stress Concentrations at Connection Joint

While credibility can be applied to this model given the similarity of the model failure to the failure exhibited in the field, it is important to consider how the stress distributions in the approach slab would have developed in other circumstances. It entirely possible that the stress concentrations displayed in the connection joint for the FE model are higher than those in the field slab. Unfortunately, the addition of damage parameters to the FE model creates an instability once several parts of the model begin to fail, and this leads to convergence issues. Because these convergence issues do not allow the model to continue applying load after these failures, one option is to change the model to assume the concrete in the slab is linear elastic. Doing so will allow the model to continue to run following the point where the previous model failed due to tensile cracking. By noting at what point different parts of the model reach appropriate levels of stress and strain to facilitate cracking, it is still possible to infer at what point this approach slab began to experience cracking at the connection joint.

After reformatting the model to assume a linear-elastic concrete, no other convergence issues were noted. The linear springs were calibrated with the applied load to provide a theoretical settlement of 1 inch to match the assumed settlement that the Washington approach slab underwent prior to being mudjacked back to its original height. Following the completion of the simulation, the far, unsupported end of the slab settled 0.96 inches. The maximum principle stresses occurred in the same areas as those in the original iteration of the model. Aside from the stress concentrations observed in the connection joint, one inch of settlement resulted in a concrete tensile stress of 475 psi in the area above the paving notch where the cracking was observed in the field specimen. The high amount of tensile stress in this area is likely a result of the connection dowels restricting rotation of the slab. As the slab settles on one side and the connection dowels prevent this rotation, the top of the slab is put in flexure and subject to stress concentrations.

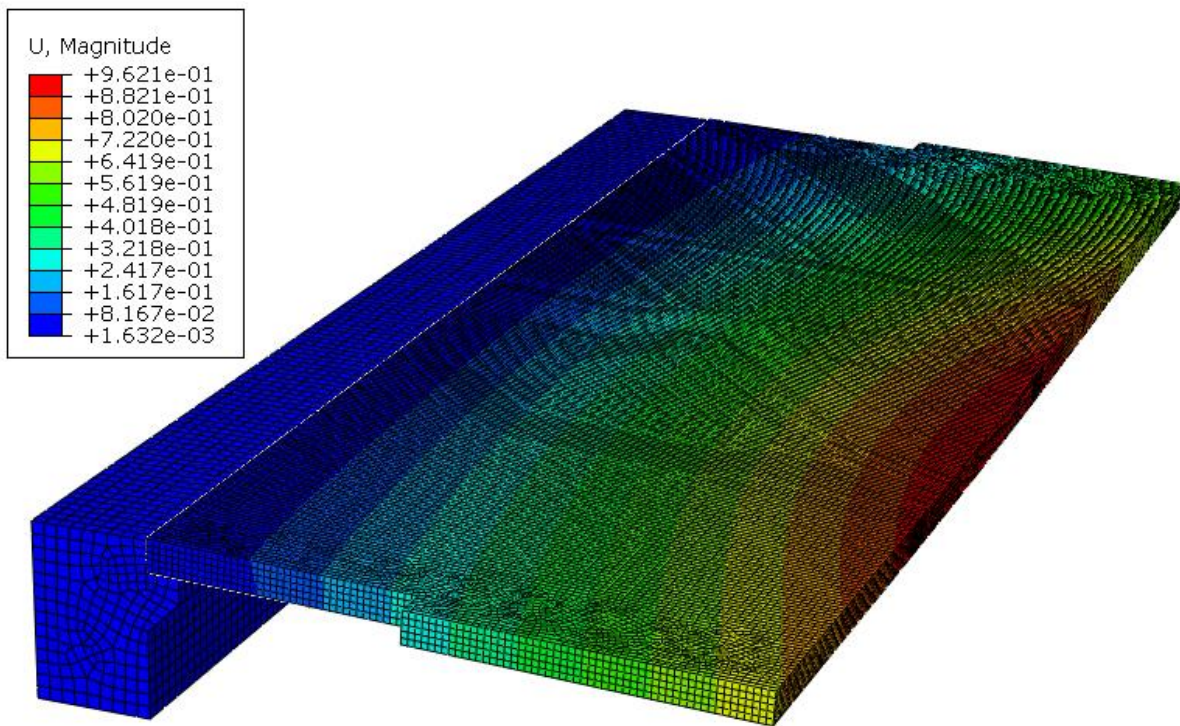


Figure 75: Washington Approach Slab Settlement

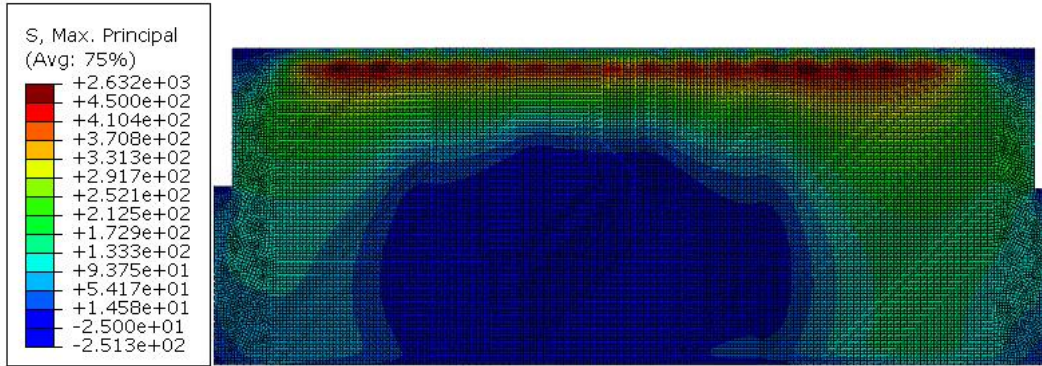


Figure 76: Max Principle Stresses in Washington Slab (Top)

Based on the results presented for the FE models of the Washington County approach slabs, it appears that excessive settlement played a role in the premature tensile cracking observed at the tied connection joint between the approach slab and the integral abutment. As the approach slab settled during its first year or two of service, the portion of the slab sitting on top the paving notch attempted to rotate and move upward from the face of the abutment seat. Due to the restraint placed on this rotation by the steel dowels embedded in the concrete of both the approach and the abutment, stress concentrations were formed in two areas. The first of these forces was the resultant of the embedded dowel pulling on the underside of the slab as it attempted to rotate upward. The results of the FE modeling indicate that the forces because of this behavior became evident quickly, which may provide evidence as to why this approach slab connection experienced such significant cracking so soon after its initial construction. The second set of forces, again resulting from the embedded dowels, did not become especially notable until the slab had settled a maximum of approximately one inch. Again, these forces appeared roughly in the same area as the spalled concrete in the field slab. As such, it is likely that the combination of excessive settlement and resistance provided by the connection dowels created high stress concentrations that resulted in the cracking concrete observed in the field slab.

CHAPTER 5. CONCLUSIONS AND RECOMMENDATIONS

5.1 Strip Seal Recommendations

The purpose of this study was to quantify and document the behavior of The D.S. Brown Company's A2R-400 and A2R-XTRA Strip Seal Expansion Devices installed with the SSA2 Railing. Given the nature of these devices and their importance in the protection of bridge substructure component, it is imperative that appropriate movement ranges be established for these strip seals to ensure that they reach their full design lifespan. As such, the following were the goals of this study:

- Verify the manufacturer's claims of total perpendicular movement for both the A2R-400 and A2R-XTRA strip seals at a zero-degree skew for both the straight sections and the upturned sections
- Provide experimentally obtained movement ranges for the A2R-400 strip seal for skew angles from 0°-60° considering both the straight and upturned sections
- Document the A2R-XTRA strip seal's performance and appropriate movement ranges for skew angles from 0°-60° for both the straight and upturned sections
- Determine whether or not the upturned termination sections presented a higher risk for failure and controlled the movement ranges for each strip seal
- Document and quantify any range restrictions on the A2R-400 due to foreign debris that may obstruct the strip seal in the field

From the laboratory tests run in this study, the manufacture's claims for a complete range of motion of 4 inches and 7 inches for the A2R-400 and A2R-XTRA, respectively, were appropriate for a zero-degree skew. In addition, these ranges were not impeded at any skew value for the A2R-400. However, the A2R-XTRA did exhibit a marked reduction at skew angles greater than 10-degrees and showed a consistent method of failure for both the straight and upturned sections.

Further, the upturned section of the A2R-XTRA also displayed a consistent issue when cycled through both extension and compression, as any failure in extension was exacerbated during closure. Thus, it is recommended that that the two tested expansion devices not be extended or contracted outside of the ranges provided in Tables 6 and 7. It is also likely that the use of this method of railing termination would result in a higher likelihood of failure for the A2R-XTRA, regardless of opening range, given its deficiencies when cycled.

In addition, a “real-world” scenario with debris present in the strip seal creates an increase in the amount of force required to close the joint completely. While this testing series displayed no clear signs of damage or puncture to the neoprene gland, and did not show any signs of failure, there is still the possibility that increased amounts of debris in the seal could be further pressed into the gland by passing vehicles. It is recommended that field joints stay monitored and regularly cleaned to prevent vehicular-based failure.

5.2 Moveable Abutment Approach Slab Recommendations

5.2.1 Literature Review and Slab Inventory Conclusions

Based on the observations and recommendations from previous research, several of the “bump” problems with moveable abutments stem from similar issues observed with more “traditional” abutment designs, namely soil settlement and erosion. Field instrumentation and investigations of older approach slabs indicate that the cyclical expansion and contraction of the moveable abutment create a higher likelihood of voiding directly adjacent to the abutment. By introducing this initial void, improper drainage and erosion of the designed subbase is likely. Field investigations performed in Iowa also highlight that a decent amount of approach slabs appear to be designed with sufficient structural stiffness to span these voids. However, as these conditions worsen and grow, many approach slabs will likely be subject to unnecessary cracking and additional drainage issues. It is still important to ensure that the initial soil conditions are

optimized to ensure proper stiffness to minimize settlement and voiding. Lastly, it is important to frequently monitor and maintain any observed field issues as they arise. Steps should be taken to patch void areas and mitigate further damage due to drainage and erosion.

Given the large number of unknowns that are present within approach slab design, it is also recommended that each slab be designed with an adequate amount of stiffness to span any potential voiding and erosion that may arise. Numerous studies, utilizing both field analysis and computer modeling, have shown that increasing slab thickness is the most effective way to increase structural rigidity and prevent slab deflection and transverse cracking should the underlying soil settle or form voids. In addition, results from previous studies suggest an increased concrete compressive strength and higher reinforcement ratio may provide additional rigidity and aid in overcoming settlement trenches.

The brief pilot inventory performed during this research series provided a set of criteria and guidelines that would help determine the performance of different IDOT approach slab designs. Additionally, the use of SIIMS and Google Maps was determined to be a decent method of investigating the general performance of approach slabs. However, the use of IRI data or roadway mapping technology, such as Roadview, is recommended for more accurate results regarding the surface roughness of approach slabs. It is also recommended that this study is continued and expanded to include a larger sample size before definitive conclusions can be drawn. A survey documenting approach slab performance correlated with different design parameters would provide useful information in determining where design improvements are needed.

5.2.2 Jasper and Story Model Conclusions

The Jasper County FE analysis focused on the impact of connection dowels on approach slab performance in the case of general slab settlement. Two variations of the same approach

slab model were created to simulate a settlement scenario under design loading. The first of these models, based on the actual field bridge located in Jasper County, Iowa, did not contain a tied approach connection at the abutment. In contrast, the “modified” version of this approach slab featured a series of steel connection dowels embedded within the concrete of both the approach and the abutment. Following the simulations run on each model, it was determined that the introduction of a tied approach-abutment condition creates stress concentrations in the approach slab concrete due to the restriction of the slab’s rotation due to settlement. Models run with damage parameters yielded significant convergence and instability issues due to the relatively early tensile failures observed in the concrete where the connection dowels were embedded. These tensile failures prevented the model from being run to completion to make an entirely accurate comparison between the two approach slab models. It is inferred that these stress concentrations are possibly due to the embedment condition applied in ABAQUS, and thus a linear-elastic concrete model was used to allow the simulation to continue. The results of this model indicate that, regardless of the magnitude of stress in the tied connection, there are certainly stress concentrations at this connection point that should be accounted for in design. The premature failure of the slab may also be since this approach slab was not originally designed to support a tied connection joint.

Following the results observed in the Jasper County FE analyses, a similar analysis was run a model the newly constructed approach slabs located in Story County, Iowa. Compared to the design detail of the Jasper slabs, the Story slabs were designed to accommodate the force transfer between the approach slab and the abutment via 53 connection dowels. In addition, this approach slab is supported by the addition of a sleeper slab to reduce overall rotation. Based on the findings of previous research performed by WJE in the state of Iowa, which found that an

appreciable number of approach slabs within the state suffer from voiding and erosion of the subbase, a series of FE models were generated to investigate how the Story approach slabs would accommodate these conditions. Voiding lengths of 5, 8, 10, 13, and 16 feet were used to gain insight into how the approach slab would fare when forced to span a variety of settlement trenches. This analysis revealed that the impact of the erosion void does not produce significant increases in tensile stress within the slab until the void length reaches approximately 6 feet. Following this point, the results of the investigation determined that the approach slab would possibly experience tensile cracking at the connection joint with a settlement void of 11 feet. It was also observed that transverse cracking would possibly begin to occur in the bottom of the slab for a 16-foot void. However, based on the standard lengths of voiding observed in the WJE reports, it is likely that the approach slab would be able to adequately span typically voiding conditions observed in the field.

5.2.3 Washington Investigation Conclusions

The purpose of this investigation was to examine the reasons behind the concrete failure at the tied approach slab connection joint for a moveable abutment bridge located in Washington County Iowa. A review of the Iowa DOT inspection records revealed that the approach slab suffered from spalling at the tied connection within its first two years of service. Other notes in these reports revealed that the slab itself likely suffered from a large amount of approach slab settlement, creating high levels of stress at the connection joint. Following the results observed with the Jasper and Story FE analyses, a finite model was originated to provide insight into how stresses within the approach slab may have developed as it settled following construction. As with the Jasper model, it was uncovered that the dowel ties between the approach slab and the abutment create areas of high tensile stress. In the case of the Washington approach slab, the cracking noted in the field slab matched the area where cracking occurred in the FE model. It is

believed that these stresses occur when the slab's rotation about the abutment is restricted by the connection dowels. Instability and convergence issues were again observed with this model due to the failure of the concrete at these stress concentrations, and the model was modified to gain insight into how the stresses within the slab would develop past this point. The model was run with one inch of settlement, and it was observed that the second place where tensile cracking would occur was in the top of the slab along the failure plane observed in the field slab.

5.2.4 Future Approach Slab Research

The research presented in the second half of this thesis deals with the effects of settlement on a dowel-tied connection between an approach slab and a moveable abutment. While there are several benefits to the use of this design for accommodating thermal movement, issues with their settlement persist. Field investigations referenced in this thesis point to the relative frequency with which these approach slabs experience problems with excessive voiding and erosion. For that reason, it is important that integrally-tied approach slabs be designed as sufficiently rigid to accommodate these settlement trenches. This thesis proposes Finite Element modeling as an efficient way to investigate the structural behavior of various approach slab configurations under different erosion and settlement conditions. However, it is also noted that FE modeling has some shortcomings when it comes to accurately modeling the interaction between the approach slab and the steel connection dowels. Areas of high stress concentration were observed and noted, and it is recommended that future research investigates whether failure of approach slabs at the connection joint is a common occurrence. Based on the observations from previous literature and the FE models used in this project, it is recommended that approach slabs be supported by a sleeper slab in addition to the abutment. As with the research performed by Krapf (2019), parametric analyses via FE modeling would be a useful way to investigate possible design modifications.

To gain a more accurate idea of the specific problems plaguing approach slabs with different design details, it is recommended that the statewide inventory of IDOT approach slabs is continued. This investigation will reveal which design details are at the highest risk of settlement, erosion, and cracking. Once these at-risk designs are identified, it is anticipated that future research opportunities will become clearer.

REFERENCES

- Abu-Farsakh, M., Chen, Q., Sharma, R., Zhang, X., 2008. *Large-scale model footing tests on geogrid reinforced foundation and marginal embankment soils*. Geotech. Test. J. ASTM 31 (No. 5), 413e423
- Aktan, H., & Attanayake, U. 2011. *High Skew Link Slab Bridge System with Deck Sliding over Backwall or Backwall Sliding over Abutments Part II. Research Report No. RC1563*. Michigan Department of Transportation Construction and Technology Division.
- Bashore, F. J., et al. *Determination of Allowable Movement Ratings for Various Proprietary Bridge Deck Expansion Joint Devices at Various Skew Angles*. Michigan Department of Transportation, 1984, www.michigan.gov/documents/mdot/RC-1245_415470_7.pdf.
- Briaud, J. L., James, R. W., and Hoffman, S. B. 1997. *Settlement of Bridge Approaches (The Bump at the End of the Bridge)*. NCHRP Synthesis 234. Washington, D.C: Transportation Research Board, National Research Council.
- Cai, C.S., Voyiadjis, G.Z., Shi, X., 2005. *Determination of Interaction between Bridge Concrete Approach Slab and Embankment Settlement. Final Report*. Louisiana Transportation Research Center (LTRC), Louisiana Department of Transportation and Development (LADOTD), Baton Rouge, LA, p. 150. Report No. FHWA/LA.05/ 403.
- Chee, M., LaFave, J.M., Fahnestock, L.A. 2018. *Assessment of Structural Concrete Approach Slab Cracking at Integral Abutment Bridges*. University of Illinois at Urbana-Champaign.
- Chen, Q., 2007. *An Experimental Study on Characteristics and Behavior of Reinforced Soil Foundation (Ph.D dissertation)*. Louisiana State University, Baton Rouge, USA.
- Chen, Q., & Abu-Farsakh, M. 2016. *Mitigating the bridge end bump problem: A case study of a new approach slab system with geosynthetic reinforced soil foundation*. Geotextiles and Geomembranes, 44(1), 39–50.
- ElBatanouny, M., Hawkins, K., Rende, N., Krauss, P. 2018. *Performance Evaluation of Recent Improvements of Bridge Abutments and Approach Backfill*. Wiss, Janney, Elstner Associates, Inc. Northbrook, IL.
- Greimann, L., Phares, B., Faris, A., and Bigelow, J. 2008 *Instrumentation and Monitoring of Integral Bridge Abutment-to-Approach Slab Connection*. CTRE Projects 05-197 and 05218, IHRB Projects TR-530 and TR-539, Iowa State University
- Krapf, D. 2019. *Increasing Service Life at Bridge Ends of Moveable Abutment Bridge*. Master's Thesis. Iowa State Department of Civil, Construction, and Environmental Engineering.

- Long, J. H., Olson, S. M., Stark, T. D., and Samara, E. A. 1998. *Differential Movement at Embankment-Bridge Structure Interface in Illinois*. Paper No. 98-1575. Washington, DC: Transportation Research Record.
- LRFD Bridge Design Manual 5.8.3: Expansion Joints*. Iowa Department of Transportation Office of Bridges and Structures. Ames, IA. <https://iowadot.gov/bridge/policy/05-08-03ExpJointLRFD.pdf>
- Mistry, V. C. 2005. *Integral Abutment and Jointless Bridges*. *Integral Abutment and Jointless Bridges (IAJB 2005)*, March 16-18, 2005, Baltimore, Maryland.
- Nadermann, A., Greimann, L., & Phares, B. 2010. *Instrumentation and Monitoring of Precast Bridge Approach Tied to an Integral Abutment Bridge in Bremer County*. Research Report No. InTrans Project 08-335. Iowa Department of Transportation Office of Bridge and Structures.
- Nassif, H., Abu-Amra, T., Shah, N. 2002. *Finite Element Modeling of Bridge Approach and Transition Slabs*. Center for Advanced Infrastructure & Transportation. Rutgers University.
- New Construction Expansion Joint Systems*. The D.S. Brown Company, July 2018, https://dsbrown.com/wp-content/uploads/2017/02/B_EJS_NewConstrucEJS_BRO00-5723_v59LR.pdf
- Oliva, M. G., & Rajek, G. 2011. *Toward Improving the Performance of Highway Bridge Approach Slabs*. Research Report No. CFIRE 03-10. Research and Innovative Technology Administration United States Department of Transportation.
- Phares, B. M., White, D., Bigelow, J., Berns, M., & Zhang, J. 2011. *Identification and Evaluation of Pavement-Bridge Interface Ride Quality Improvement and Corrective Strategies*. Research Report No. FHWA/OH-2011/1. Ohio Department of Transportation.
- Phares, B., & Dahlberg, J. 2015. *Performance and Design of Bridge Approach Panels in Wisconsin*. Research Report No. 0092-14-04. Wisconsin Department of Transportation Research & Library Unit.
- Rende, N., Donnelly, J. 2011. *Approach Slab Assessment – Full Testing Program Report*. WJE No. 2010.2389.2. Wiss, Janney, Elstner Associates, Inc. Northbrook, IL.
- Schaefer, V. R., Koch, J. C. 1992. *Void Development Under Bridge Approaches*. Report No. SD90-03. South Dakota Department of Transportation.
- Special Provision for Expansion Joint Device*. Michigan Department of Transportation. 24 June 2004, mdotcf.state.mi.us/public/dessssp/spss_source/03SP706A.pdf.

- Wahls, H.E. 1990. *NCHRP Synthesis 159: Design and Construction of Bridge Approaches*. Transportation Research Board. Washington, DC.
- White, D. J., Mekkawy, M. M., Sritharan, S., Sulieman, M. T. 2007. *Underlying Causes for Settlement of Bridge Approach Pavement Systems*. Journal of Performances of Constructed Facilities Vol. 21. No. 4: 273-282.
- White, D., Sritharan, S., Suleimann, M., Mohammed, M., and Chetlur, S. 2005. *Identification of the Best Practices for Design, Construction, and Repair of Bridge Approaches*. CTRE Project 02-118, Iowa DOT Project TR-481, Iowa State University
- WisDOT Bridge Manual, Chapter 28*. Wisconsin Department of Transportation. Madison, WI. July 2018. <https://wisconsin.gov/dtsdManuals/strct/manuals/bridge/ch28.pdf>
- Yasrobi, S. Y., Ng, K. W., Edgar, T. V., & Menghini, M. 2016. *Investigation of approach slab settlement for highway infrastructure*. Transportation Geotechnics, 6, 1–15.